VOL. 604 NO. 2 JULY 3, 1992

THIS ISSUE COMPLETES VOL. 604

JOURNAL OF CHROMATOGRAPHY

INCLUDING ELECTROPHORESIS AND OTHER SEPARATION METHODS

ELSEVIER

JOURNAL OF CHROMATOGRAPHY

INCLUDING ELECTROPHORESIS AND OTHER SEPARATION METHODS

Scope. The *Journal of Chromatography* publishes papers on all aspects of chromatography, electrophoresis and related methods. Contributions consist mainly of research papers dealing with chromatographic theory, instrumental development and their applications. The section *Biomedical Applications*, which is under separate editorship, deals with the following aspects: developments in and applications of chromatographic and electrophoretic techniques related to clinical diagnosis or alterations during medical treatment; screening and profiling of body fluids or tissues with special reference to metabolic disorders; results from basic medical research with direct consequences in clinical practice; drug level monitoring and pharmacokinetic studies; clinical toxicology; analytical studies in occupational medicine.

Submission of Papers. Manuscripts (in English; *four* copies are required) should be submitted to: Editorial Office of *Journal of Chromatography*, P.O. Box 681, 1000 AR Amsterdam, Netherlands, Telefax (+31-20) 5862 304, or to: The Editor of *Journal of Chromatography, Biomedical Applications*, P.O. Box 681, 1000 AR Amsterdam, Netherlands. Review articles are invited or proposed by letter to the Editors. An outline of the proposed review should first be forwarded to the Editors for preliminary discussion prior to preparation. Submission of an article is understood to imply that the article is original and unpublished and is not being considered for publication elsewhere. For copyright regulations, see below.

Publication. The *Journal of Chromatography* (incl. *Biomedical Applications*) has 39 volumes in 1992. The subscription prices for 1992 are:

J. Chromatogr. (incl. *Cum. Indexes, Vols. 551–600*) + *Biomed. Appl.* (Vols. 573–611):
Dfl. 7722.00 plus Dfl. 1209.00 (p.p.h.) (total *ca.* US$ 4880.25)

J. Chromatogr. (incl. *Cum. Indexes, Vols. 551–600*) only (Vols. 585–611):
Dfl. 6210.00 plus Dfl. 837.00 (p.p.h.) (total *ca.* US$ 3850.75)

Biomed. Appl. only (Vols. 573–584):
Dfl. 2760.00 plus Dfl. 372.00 (p.p.h.) (total *ca.* US$ 1711.50).

Subscription Orders. The Dutch guilder price is definitive. The US$ price is subject to exchange-rate fluctuations and is given as a guide. Subscriptions are accepted on a prepaid basis only, unless different terms have been previously agreed upon. Subscriptions orders can be entered only by calender year (Jan.–Dec.) and should be sent to Elsevier Science Publishers, Journal Department, P.O. Box 211, 1000 AE Amsterdam, Netherlands, Tel. (+31-20) 5803 642, Telefax (+31-20) 5803 598, or to your usual subscription agent. Postage and handling charges include surface delivery except to the following countries where air delivery via SAL (Surface Air Lift) mail is ensured: Argentina, Australia, Brazil, Canada, China, Hong Kong, India, Israel, Japan*, Malaysia, Mexico, New Zealand, Pakistan, Singapore, South Africa, South Korea, Taiwan, Thailand, USA. *For Japan air delivery (SAL) requires 25% additional charge of the normal postage and handling charge. For all other countries airmail rates are available upon request. Claims for missing issues must be made within three months of our publication (mailing) date, otherwise such claims cannot be honoured free of charge. Back volumes of the *Journal of Chromatography* (Vols. 1–572) are available at Dfl. 217.00 (plus postage). Customers in the USA and Canada wishing information on this and other Elsevier journals, please contact Journal Information Center, Elsevier Science Publishing Co. Inc., 655 Avenue of the Americas, New York, NY 10010, USA, Tel. (+1-212) 633 3750, Telefax (+1-212) 633 3990.

Abstracts/Contents Lists published in Analytical Abstracts, Biochemical Abstracts, Biological Abstracts, Chemical Abstracts, Chemical Titles, Chromatography Abstracts, Clinical Chemistry Lookout, Current Awareness in Biological Sciences (CABS), Current Contents/Life Sciences, Current Contents/Physical, Chemical & Earth Sciences, Deep-Sea Research/Part B: Oceanographic Literature Review, Excerpta Medica, Index Medicus, Mass Spectrometry Bulletin, PASCAL-CNRS, Pharmaceutical Abstracts, Referativnyi Zhurnal, Research Alert, Science Citation Index and Trends in Biotechnology.

US Mailing Notice. *Journal of Chromatography* (main section ISSN 0021-9673, *Biomedical Applications* section ISSN 0378-4347) is published (78 issues/year) by Elsevier Science Publishers (Sara Burgerhartstraat 25, P.O. Box 211, 1000 AE Amsterdam, Netherlands). Annual subscription price in the USA US$ 4880.25 (subject to change), including air speed delivery. Application to mail at second class postage rate is pending at Jamaica, NY 11431. **USA POSTMASTERS:** Send address changes to *Journal of Chromatography*, Publications Expediting, Inc., 200 Meacham Avenue, Elmont, NY 11003. Airfreight and mailing in the USA by Publication Expediting.

See inside back cover for Publication Schedule, Information for Authors and information on Advertisements.

0021-9673/92/$05.00

Printed in the Netherlands

VOL. 604, NO. 2 JOURNAL OF CHROMATOGRAPHY JULY 3, 1992

CONTENTS

(Abstracts/Contents Lists published in Analytical Abstracts, Biochemical Abstracts, Biological Abstracts, Chemical Abstracts, Chemical Titles, Chromatography Abstracts, Current Awareness in Biological Sciences (CABS), Current Contents/Life Sciences, Current Contents/Physical, Chemical & Earth Sciences, Deep-Sea Research/Part B: Oceanographic Literature Review, Excerpta Medica, Index Medicus, Mass Spectrometry Bulletin, PASCAL-CNRS, Referativnyi Zhurnal, Research Alert and Science Citation Index)

REGULAR PAPERS

Column Liquid Chromatography

Gas Chromatography

Supercritical Fluid Chromatography

Planar Chromatography

Electrophoresis

(Continued overleaf)

SHORT COMMUNICATIONS

Column Liquid Chromatography

Planar Chromatography

Journal of Chromatography, 604 (1992) 185–196
Elsevier Science Publishers B.V., Amsterdam

CHROM. 24 146

Separation of enantiomers using α-chymotrypsin-silica as a chiral stationary phase

I. Marle*, A. Karlsson** and C. Pettersson

Department of Analytical Pharmaceutical Chemistry, Uppsala University, Biomedical Center, Box 574, S-751 23 Uppsala (Sweden)

(First received November 29th, 1991; revised manuscript received February 24th, 1992)

ABSTRACT

Direct separations of enantiomeric acids and N-substituted amino acids using α-chymotrypsin adsorbed or covalently immobilized on silica as the chiral stationary phase are presented. Phosphate buffer was used as the mobile phase. α-Chymotrypsin covalently bound to an aldehyde-activated silica resulted in a stable phase as opposed to α-chymotrypsin adsorbed on silica. The covalently bound stationary phase maintained the chiral discrimination ability even after more than 4000 column volumes of mobile phase had passed through the column. An increase in the amount of α-chymotrypsin from 110 to 140 mg/g silica was found to affect the retention by a factor of two without significantly influencing the enantioselectivity. The effect of pH, ionic strength and charged modifiers was studied in order to find optimum conditions for chiral separations. The chiral resolution could be optimized by adjusting the pH and by addition of octanesulphonate to the mobile phase.

INTRODUCTION

The enantioselective discriminating properties of proteins and enzymes have been utilized in the development of chiral separation systems for use in liquid chromatography [1]. A large number of enantiomeric drugs have been resolved on chiral stationary phases based on immobilized bovine [2] and human serum albumin [3], α_1-acid glycoprotein [4], ovomucoid [5] and cellulase [6].

The endopeptidase α-chymotrypsin, known to catalyse the enantioselective hydrolysis of a broad range of amides and esters [7], was recently immobilized on a glutaraldehyde-activated hydrophilic polymer that had been chemically bound to silica. The resulting chiral stationary phase was used for the separation of enantiomeric amino acids and amino acid derivatives [8]. Wainer and co-workers studied the stereochemical recognition of enantiomeric free and derivatized amino acids [9] and enantiomeric dipeptides [10] on the immobilized α-chymotrypsin phase. They suggested that the interaction occurred both at the enzymatic active site of the α-chymotrypsin and at other hydrophobic sites on the enzyme.

α-Chymotrypsin immobilized on different kinds of solid phases was hydrolytically active and the resolution obtained of racemic amino acid esters or amides was actually a separation of L-amino acids and intact D-amino acid esters or amides [8,9,11].

In this paper, we report on different immobilization techniques used for the preparation of α-chymotrypsin silica phases, *i.e.*, adsorption and covalent immobilization via reactive epoxy, aldehyde and tresyl groups, and on their applicability as chiral stationary phases [12]. The purpose of this investigation was to evaluate enantioselectivity and chromatographic performance of the α-chymotrypsin silica phases and to study the effect of the mobile

Correspondence to: Dr. Curt Pettersson, Department of Analytical Pharmaceutical Chemistry, Biomedical Center, Uppsala University, P.O. Box 574, S-751 23 Uppsala, Sweden.

* Present address: Analytical Quality Control, Astra Pharmaceutical Production AB, S-151 85 Södertälje, Sweden.

** Present address: Analytical Chemistry, Astra Hässle AB, S-431 83 Mölndal, Sweden.

phase composition (pH, ionic strength and charged modifiers) on enantioselective retention.

EXPERIMENTAL

Apparatus

The pump used was a model 110 A (Altex Scientific, Berkeley, CA, USA) equipped with a pulse damper (Touzard et Matignon, Vitry, France). The injector was a Model 7125 (Rheodyne, Cotati, CA, USA) with a 20-μl loop. The detector was a SpectroMonitor D (LDC Analytical, Riviera Beach, FL, USA) with variable wavelength. The recorder was a Model BD 40 (Kipp & Zonen, Delft, Netherlands).

The separation columns were made of stainless steel with a polished inner surface, equipped with modified Swagelok connectors and stainless-steel frits (2-μm porosity) or stainless-steel sieve filters (2-μm porosity) supported by spreaders (HPLC Teknik, Robertsfors, Sweden).

The chromatographic systems were thermostated at 20.0 ± 0.1°C by a Type 02 PT 923 water-bath (Heto, Birkerød, Denmark).

The pH meter was a Model E 632 (Methrohm, Herisau, Switzerland).

Chemicals

LiChrospher Si 100 (10 μm, 100 Å), LiChrospher Si 300 (10 μm, 300 Å), LiChrosorb Si 100 (10 μm, 100 Å), LiChrosorb DIOL (5 μm, 100 Å), (*R*)- and (*S*)-N-(1-phenylethyl)phthalamic acid and periodic acid (pro analysi) were obtained from E. Merck (Darmstadt, Germany). LiChrosorb DIOL (10 μm, 100 Å) activated with 2,2,2-trifluoroethanesulphonyl chloride (tresyl chloride) was kindly supplied by L. Hansson of Hafslund Nycomed Innovation (Ideon, Malmö, Sweden). Bovine α-chymotrypsin (three times crystallized and lyophilized), D- and L-tryptophan, D- and L-N-Boc-phenylalanine (Boc = *tert.*-butoxycarbonyl), D-and L-N-CBZ-phenylalanine (CBZ = carbobenzoxy), DL- and L-N-acetyltryptophan, racemic warfarin and (*R*)- and (*S*)-1-phenylethanol were obtained from Sigma (St. Louis, MO, USA). (2*R*,3*R*)- and (2*S*,3*S*)-dibenzoyltartaric acid and (2*R*,3*R*)- and (2*S*,3*S*)-di-*p*-toluoyltartaric acid were purchased from Fluka (Buchs, Switzerland). Racemic 2-(4-chlorophenoxy)propionic acid and 3-glycidoxypropyltrimethoxysilane were obtained from Janssen Chimica (Beerse, Belgium). (*S*)-2-(4-Chlorophenoxy)propionic acid and racemic 2-(4-iodophenoxy)propionic acid were kindly supplied by the Department of Organic Pharmaceutical Chemistry, University of Uppsala, Sweden. Racemic ketoprofen was obtained from Kabi Pharmacia (Helsingborg, Sweden) and racemic ibuprofen from Astra Läkemedel (Södertälje, Sweden). (*R*)- and (*S*)-naproxen were supplied by Syntex Laboratories (Paolo Alto, CA, USA). (*R*)- and (*S*)-propranolol hydrochloride were supplied by Imperial Chemical Industries. Macclesfield, UK). (1*S*,2*R*)-Ephedrine hydrochloride were obtained from Serva (Heidelberg, Germany) and (1*R*,2*S*)-ephedrine hydrochloride from Academical Pharmacy (Uppsala, Sweden). N,N-Dimethyloctylamine (DMOA) was supplied by ICN Pharmaceuticals (Plainview, NY, USA) and sodium 1-octanesulphonate by Eastman Kodak (Rochester, NY, USA).

All other substances were of analytical-reagent grade and used without further purification.

The solute structures are given in Fig. 1.

Column preparation

The solid phases used for *in situ* immobilization of α-chymotrypsin (α-CHT) were packed by a slurry technique using chloroform (LiChrospher Si 100 and Si 300, LiChrosorb Si 100 and DIOL) or dichloromethane (tresyl chloride-activated LiChrosorb DIOL) as suspending medium and hexane as packing solvent. After packing the frits were exchanged for sieve filters to minimize the effects of protein denaturation [13] during the immobilization of the enzyme.

α-CHT covalently immobilized on silica in batch experiments (α-CHT-A and -B phases below) were packed at 200 bar using sodium phosphate buffer (pH 6.5, $I=0.1$) as suspending medium.

α-CHT adsorbed on silica

The LiChrospher Si 100, LiChrosorb Si 100 and LiChrospher Si 300 columns (150 × 4.6 mm I.D.) were equilibrated with sodium phosphate buffer ($I=0.1$). A mobile phase containing 2.00 g/l of α-CHT in the buffer was applied at 1 ml/min until the front boundary had reached the plateau. Depending on the experimental conditions (Table I) the breakthrough volume correspondend to 30–100 column volumes of α-CHT solution. Finally, the

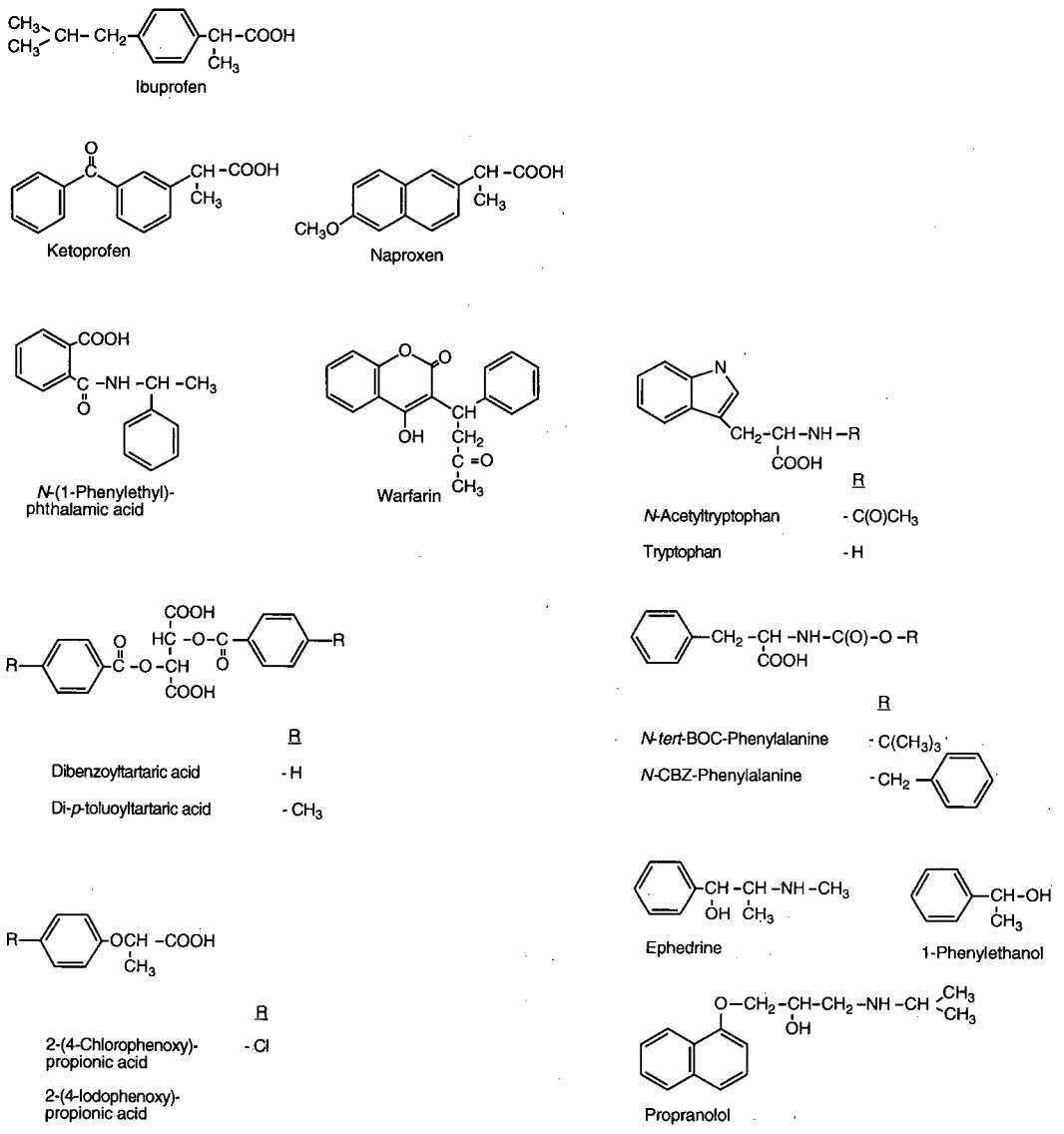

Fig. 1. Structures of solutes.

columns were equilibrated with sodium phosphate buffer (pH 5.3, $I = 0.1$).

The amount of α-CHT adsorbed was calculated by integration between Vm, obtained from the retention of sodium nitrate before the adsorption of α-CHT, and the breakthrough volume of α-CHT [14].

α-CHT-A: α-chymotrypsin immobilized on epoxide-activated silica

Monomeric epoxide-activated LiChrospher Si 100 was prepared according to Herman *et al.* [15]. The immobilization of α-CHT to epoxy-silica followed the description given by Hermansson [16]. The reaction scheme is given in Fig. 2a.

The amount of α-CHT immobilized on the silica of the α-CHT-A and -B phases was determined by

TABLE I

INFLUENCE OF PORE DIAMETER, SPECIFIC SURFACE AREA AND pH ON ADSORPTION OF α-CHT

Solid phase	Pore diameter (Å)	Specific surface area[a] (m^2/g)	pH	Amount of α-CHT adsorbed (mg/g)
LiChrospher Si 100	100	250	5.3	200
LiChrospher Si 100	100	250	7.4	300
LiChrosorb Si 100	100	300	7.4	220
LiChrospher Si 300	300	250	5.3	40
LiChrospher Si 300	300	250	7.4	130

[a] Ref. 25.

UV-spectrophotometry at 280 nm as the difference between the amount of α-CHT added to the reaction vessel and the amount of enzyme remaining in the supernatant after reaction and centrifugation.

The α-CHT-A phase was packed into a 100 × 3.0 mm I.D. column.

α-CHT-B: α-chymotrypsin immobilized on aldehyde-activated silica

LiChrosorb DIOL was oxidized to its aldehydic form by periodic acid [17]. A 4.0-g amount of LiChrosorb DIOL was suspended in 100 ml of water–methanol (4:1, v/v) and 2.0 g of periodic acid dissolved in 10 ml of the water–methanol mixture were added. The reaction mixture was stirred at room temperature for 48 h, then the aldehyde-activated silica was washed with an excess of water and dried.

α-CHT was immobilized on the aldehyde-activated silica mainly according to the method reported by Ohlson *et al.* [18]. A sample of 300 mg of α-CHT was dissolved in 15 ml of sodium carbonate buffer (pH 10, $I=0.2$) and 2 g of aldehyde-activated silica were added. The suspension was stirred at room temperature for 20 h. The α-CHT-silica was isolated by centrifugation and washed with water. The phase was finally mixed with suspending medium and stored in a refrigerator. The reaction scheme is given in Fig. 2b.

The α-CHT-B phase was packed into a 100 × 3.0 mm I.D. column.

α-CHT-C: in situ immobilization of α-chymotrypsin on aldehyde-activated silica

A column (150 × 4.6 mm I.D.) packed with LiChrosorb DIOL was equilibrated with water–methanol (4:1, v/v), 44 column volumes of 0.058 *M* periodic acid in the water–methanol mixture were pumped through the column and finally it was washed with 20 column volumes of sodium phosphate buffer (pH 6.3, $I=0.1$).

α-CHT was immobilized on the aldehyde-activated silica by applying a mobile phase consisting of 2.00 g/l of α-CHT in sodium carbonate buffer (pH 10, $I=0.1$) to the column at 1 ml/min until the front boundary had reached the plateau, corresponding to about 90 column volumes of α-CHT solution (Fig. 2b). The column was then washed with sodium phosphate buffer (pH 5.3, $I=0.1$) until a stable baseline was obtained.

The amount of α-CHT immobilized to the aldehyde-activated silica was determined as described above for α-CHT adsorbed on silica.

α-CHT-D: in situ immobilization of α-chymotrypsin on tresyl-activated silica

A column packed with tresyl-activated silica (150 × 3.0 mm I.D.) was equilibrated with coupling buffer, *i.e.*, sodium phosphate buffer (pH 7.1, $I=0.5$) containing 0.5 *M* NaCl [19]. A mobile phase containing 2.00 g/l of α-CHT in the coupling buffer was applied to the column at 1 ml/min until the breakthrough was complete, corresponding to 87 column volumes of α-CHT solution. The column was washed with 30 column volumes of coupling buffer and 30 column volumes of tris(hydroxymethyl)aminomethane (Tris)–HCl buffer (pH 8.0, $I=0.08$) to remove residual tresyl groups. It was finally equilibrated with sodium phosphate buffer (pH 5.3, $I=0.1$). The reaction scheme is given in Fig. 2c.

The amount of α-CHT immobilized on the tresyl-activated silica was determined by UV spectrophotometry at 282 nm. Eluate fractions were collected during the breakthrough and during the column washing. The amount of α-CHT immobilized was calculated as the difference between the amount of α-CHT that was introduced to the column and the amount found in the eluate fractions.

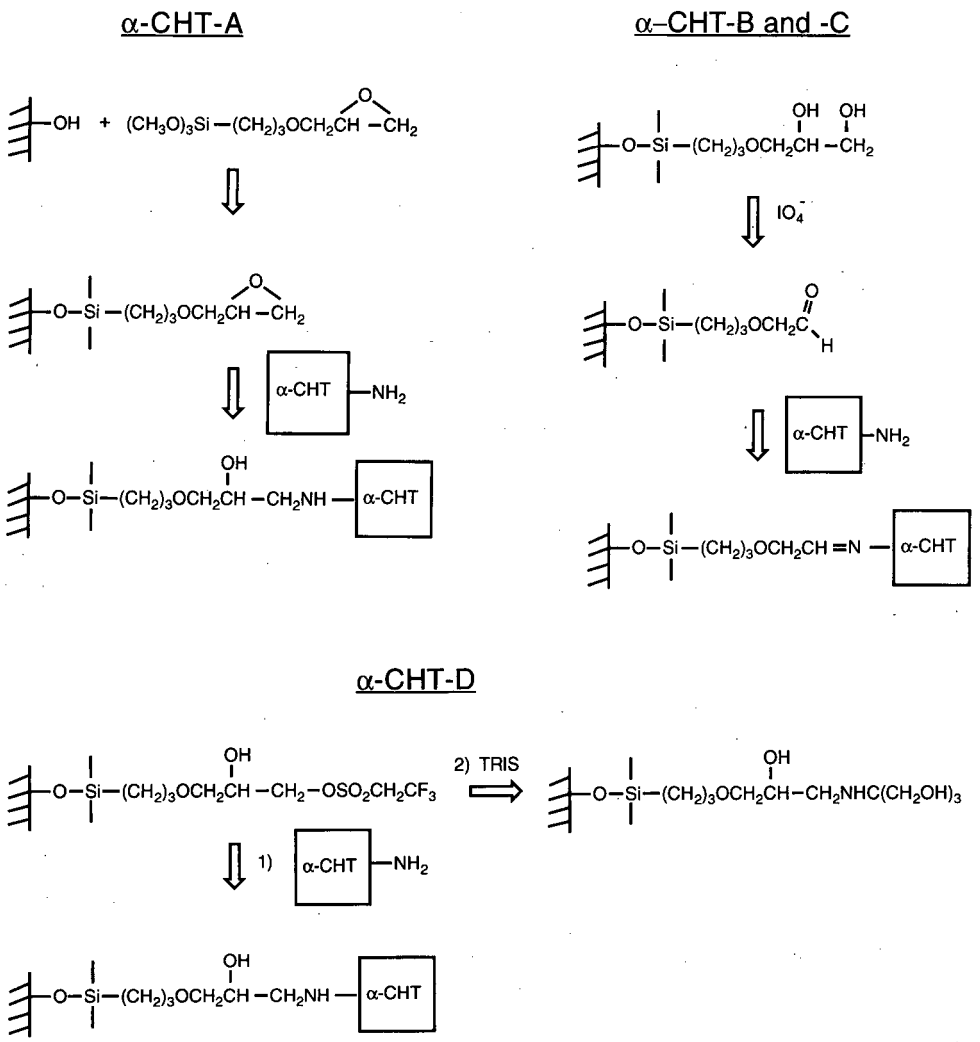

Fig. 2. Reaction schemes of the different methods for covalent immobilization of α-CHT on silica.

Chromatographic technique

The mobile phases were sodium phosphate buffers with an ionic strength of 0.1. The solutes were injected dissolved in the mobile phase at concentrations of about 0.1 m*M*. The flow-rate was 1 ml/min. V_0 was obtained by injection of sodium nitrate, which was assumed to be non-retained. The peak asymmetry factor, *asf*, was calculated as described previously [20].

RESULT AND DISCUSSION

α-Chymotrypsin adsorbed on silica phases

Different types of silicas were investigated in order to evaluate the chiral recognition and stability of α-CHT-coated silica phases (Table I). The amount α-CHT adsorbed on LiChrospher silica was affected by both the pore diameter of the solid phase and the mobile phase pH. Previously, maximum protein adsorption was observed at the isoelectric point of proteins, *i.e.*, bovine serum albumin on silica [21] and bovine serum albumin, lysozyme and α-CHT on porous glass [22]. It was not feasible

to study the adsorption of α-CHT at the isoelectric point, p*I* 8.1–8.3 [23], owing to the limited stability of silica at such a high pH [24]. However, in accordance with the observations for the adsorption of α-CHT on porous glass, it was found that a pH close to the p*I* favoured the adsorption of α-CHT on silica (Table I).

According to the manufacturer, LiChrospher Si 100 has the same specific surface area (250 m^2/g [25]) as LiChrospher Si 300 but a smaller mean pore diameter. A higher degree of exclusion of α-CHT (molecular size 50 × 40 × 40 Å [26]) from LiChrospher Si 100 than from LiChrospher Si 300 would have been expected. However, the LiChrospher Si 100 phase showed greater adsorption of the enzyme (Table I). A larger amount of isolated (free) silanol groups of the 100 Å silica than of the 300 Å silica [27,28] is probably the reason for the difference observed. Further, the adsorption of α-CHT on LiChrosorb Si 100 having a specific surface area of 300 m^2/g [25] was significantly lower than that on LiChrospher Si 100. However, the surface area accessible to α-CHT depends not only on the specific surface area but also of the pore structure, *i.e.*, pore size and pore distribution, which may be different for the two silica phases.

The α-CHT-coated silica phases gave enantioselective retention for various solutes, *e.g.*, naproxen (Fig. 3).

The coating of the silica with α-CHT was performed at pH 7.4, as this resulted in a sorbent with a high chiral capacity owing to the large amount of protein adsorbed (Table I). The chiral separation of naproxen ($\alpha = 1.68$) was effected when 120 column volumes (0.30 l) of the mobile phase, phosphate buffer (pH 5.3), had passed through the column.

Unfortunately, the leakage of α-CHT from the coated silica phases was relatively high. This is illustrated by the continuous decrease in the capacity factors on coated LiChrospher Si 100 shown in Fig. 4. Almost no enantioselectivity was observed when 1200 column volumes (3 l) of phosphate buffer pH 5.3 had passed through the column.

In conclusion, although chiral separations are possible on α-CHT-coated phases, they do not appear to be useful for quantitative analyses of enantiomers, owing to instability.

α-CHT covalently immobilized on silica

Immobilization technique and chromatographic performance. Three different silica phases with reactive epoxy (A), aldehyde (C) or tresyl (D) groups were used to immobilize α-CHT covalently (Table II). The highest stereoselectivities and shortest retention times were generally obtained when the α-CHT was immobilized on epoxy-silica, α-CHT-A. The high enantioselectivity was due to a higher loading of the enzyme on this phase. α-CHT covalently immobilized *in situ* on tresyl-activated silica resulted in increased retention and low stereoselectivity. Immobilization of α-CHT on aldehyde-(α-CHT-C) and tresyl-activated silica (α-CHT-D) gave about the same loading of the enzyme (Table II). However, the enantioselectivity of the α-CHT-C phase was higher than that of the α-CHT-D phase,

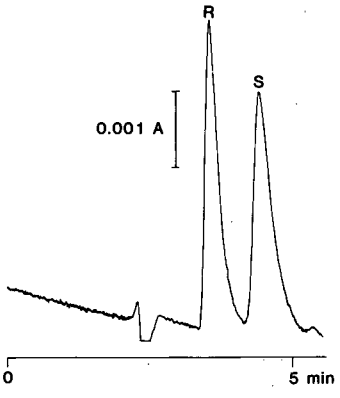

Fig. 3. Separation of (*R*,*S*)-naproxen. Solid phase: α-CHT adsorbed on LiChrospher SI 100 at pH 7.4. Mobile phase: phosphate buffer (pH 5.3).

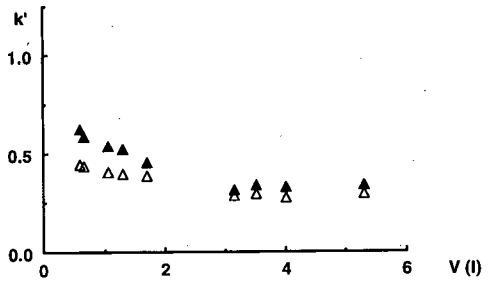

Fig. 4. Stability of an α-CHT-coated silica phase. Solid phase: α-CHT adsorbed on LiChrospher SI 100 at pH 5.3. Mobile phase: phosphate buffer (pH 5.3). Solutes: △ = (*R*)-naproxen; ▲ = (*S*)-naproxen.

TABLE II

ENANTIOSELECTIVE RETENTION OF α-CHT-SILICA PHASES

Mobile phase: Phosphate buffer (pH 5.3).

Solute	Parameter	A[a] (200 mg/g)[b]	C[a] (140 mg/g)[b]	D[a] (130 mg/g)[b]
N-(1-Phenylethyl)phthalamic acid	k'_2	0.89	1.3	1.8
	α	1.6	1.7	1.3
	asf	1.8	3.3	1.8
Naproxen	k'_2	2.7	10	16
	α	2.4	1.8	1.2
	asf	1.6	3.8	1.4
Warfarin	k'_2	2.5	11	61
	α	1.4	1.3	1.0
	asf	–	2.9	1.3
Di-*p*-toluoyltartaric acid	k'_2	1.7	4.4	1.7
	α	2.9	1.7	1.4
	asf	1.8	5.2	1.8

[a] For details, see Experimental.
[b] Amount of α-CHT immobilized.

whereas the retention using the α-CHT-C phase was generally lower than that using the α-CHT-D phase. The chromatographic performance of the α-CHT-A and -D phases was higher than that of the α-CHT-C phase, which gave strongly tailing peaks. In addition to the larger amount of α-CHT immobilized on the α-CHT-A phase than on the -C and -D phases, the different immobilization procedures and the different silica matrices used could also add to the discrepancies observed.

Although the chromatographic properties of the α-CHT-A phase were superior to those of the α-CHT-C phase, the latter chiral phase is to be preferred owing to its greater stability.

Stability and reproducibility. The stability of two batches of the α-CHT-C phase was investigated, columns 1 and 4 in Fig. 5. The retention times for the naproxen enantiomers decreased by about 10% on both columns but the stereoselectivity was unaffected even after 10 l (>4000 column volumes) of the mobile phase has passed through the columns. A small loss of α-CHT due to hydrolysis of the imino bond between the protein and the silica might be the reason for the slight decrease in retention. The uninfluenced enantioselectivity indicates that the solute retention is dominated by adsorption on α-CHT sites, *i.e.*, negligible adsorption on the matrix and the spacer. Using a highly adsorbing matrix, the enantioselectivity was shown to decrease with decreasing amount of chiral selector [29].

The α-CHT-C phases could be prepared with reproducible enantioselectivity (Fig. 5). Almost no

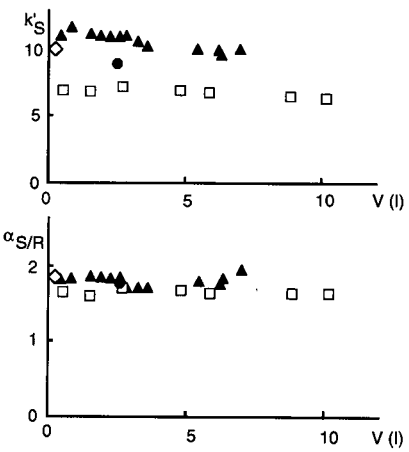

Fig. 5. Stability and reproducibility of solid phase α-CHT-C. Mobile phase: phosphate buffer (pH 5.3). Solutes: (*R*)- and (*S*)-Naproxen. ▲ = column 1 (140 mg α-CHT/g silica); ◇ = column 2 (130 mg/g); ● = column 3 (130 mg/g); □ = column 4 (110 mg/g).

differences in the enantioselectivity of naproxen were observed for the four columns investigated. The capacity factors were, as expected, dependent on the loading of the enzyme on the stationary phase. Increasing the amount of α-CHT from 110 to 140 mg/g of silica resulted in an increase in k' by a factor of two. This result may support the suggestion, given in a study using cyanogen bromide-activated Sepharose 4B as the matrix, that the last fraction of α-CHT is immobilized in a conformation other than the first one [30] and will result in a higher binding affinity for chiral solutes. The conformational change would be due either to a heterogeneity in the support material or to induced heterogeneity because of interactions of enzyme which attaches later to those protein molecules already established on the surface [30].

Solute structure and stereoselectivity

The α-CHT silica phases separated enantiomeric mono- and divalent acids, 1-phenylethanol, tryptophan and N-substituted amino acid derivatives, Tables III–V (for solute structures, see Fig. 1). All these solutes have an aromatic group in the vicinity of the asymmetric carbon atom, indicating that charge-transfer, hydrophobic and/or steric interactions may be important for chiral recognition on the α-CHT phase. The carboxylic acids were mainly ionized at the pH used (5.3 and 6.4) and may thus interact by electrostatic attraction with the α-CHT phase, as it has a positive net charge below pI 8.1–8.3 [23]. The high enantioselectivities obtained on α-CHT silica allowed the resolution of various enantiomers, despite the low column efficiency (Figs. 6–9). The small separation factors obtained for the enantiomers of propranolol and ephedrine indicate that the α-CHT silica phases are less suitable for separating enantiomeric amino alcohols.

Regulation of retention and enantioselectivity by the mobile phase composition

pH and ionic strength. The influence of pH on enantioselective retention is presented in Table V. On increasing the pH a decrease in retention of the carboxylic acids and an increase in retention for the amines was observed. This might be due to a change in hydrophobic and/or electrostatic interactions. However, native α-CHT can exist in at least two conformational states, one enzymatically active and the other inactive, and the fraction of α-CHT present in the active conformation increases from 45% to 85% when the pH is increased from 3 to 7 (I=0.1) [31,32].

Covalent immobilization of α-CHT on silica, Sepharose or synthetic polymer most often changes the physical properties of the free enzyme resulting in, for example, a decrease in the specific activity, a displacement of the pH of maximum hydrolytic activity, an increase in the thermal stability and decreased autolysis [33–37]. It seems reasonable to assume that the fraction of immobilized α-CHT being hydrolytically active will undergo similar conformational changes as the native enzyme on pH

TABLE III

SOLUTE STRUCTURE AND ENANTIOSELECTIVITY WITH α-CHT-C SOLID PHASE

Mobile phase: phosphate buffer (pH 5.3).

Solute	Column[a]	k'_2	α
2-(4-Iodophenoxy) propionic acid	1	1.26	1.16
Di-*p*-toluoyl tartaric acid	2	4.43	1.67
N-(1-Phenylethyl) phthalamic acid	2	1.31	1.7
Warfarin	2	10.8	1.31
1-Phenylethanol	1	0.72	1.2

[a] See caption to Fig. 5.

TABLE IV

SOLUTE STRUCTURE AND ENANTIOSELECTIVITY WITH α-CHT-B[a] SOLID PHASE

Mobile phase: phosphate buffer (pH 6.4)

Solute	k'_2	α
Tryptophan	0.77	1.4
N-Acetyltryptophan	2.71	1.92
N-CBZ-phenylalanine	5.25	1.62
N-Boc-phenylalanine	2.42	2.6
Ketoprofen	2.43	1.0
Ibuprofen	1.4	1.0
Naproxen	6.22	1.54

[a] 130 mg α-CHT/g silica.

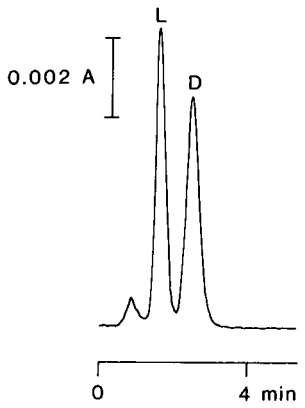

Fig. 6. Separation of DL-N-acetyltryptophan. Solid phase: α-CHT-B. Mobile phase: phosphate buffer (pH 6.4).

changes. The increase in retention at pH 5.3 for the uncharged 1-phenylethanol and the weak acid warfarin ($pK_a = 5.0$ [38]) indicated a modification of the retaining properties of the α-CHT silica phase by pH. Further, the change in enatioselectivity at pH 5.3 for several solutes also supports the proposal of conformational changes.

Ionic strength variations in the range 0.01–1.0 influence the binding properties and the enzymatic activity of native α-CHT [31]. The effect of the ionic strength in the range 0.025–0.1 on the enatioselective retention of some solutes on α-CHT silica is given in Table VI. Propranolol gave stereoselective retention on the α-CHT silica phase only at low buffer ion concentrations, whereas the enantiomers

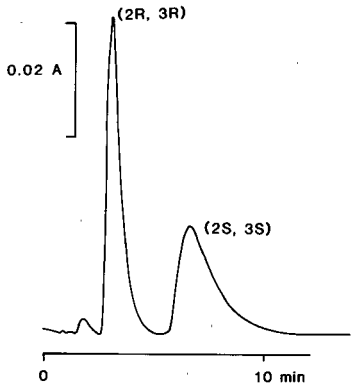

Fig. 7. Separation of (2*R*,3*R*;2*S*,3*S*)-di-*p*-toluoyltartaric acid. Solid phase: α-CHT-A. Mobile phase: phosphate buffer (pH 3.8).

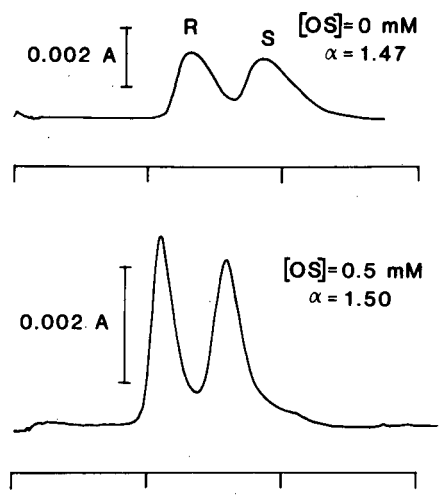

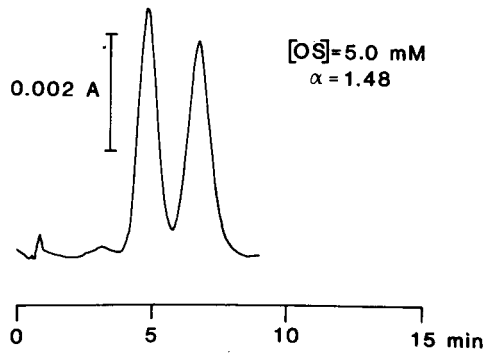

Fig. 8. Influence of octanesulphonate (OS) on enantioselective resolution. Solid phase: α-CHT-B. Mobile phase: OS in phosphate buffer (pH 5.0). Solute: (*R*,*S*)-naproxen.

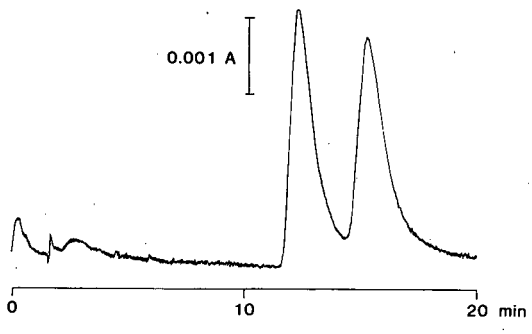

Fig. 9. Separation of the enantiomers of warfarin. Solid phase: α-CHT-C (110 mg α-CHT/g silica). Mobile phase: phosphate buffer (pH 5.4).

TABLE V

INFLUENCE OF pH ON ENANTIOSELECTIVE RETENTION

Solid phase: α-CHT-A. Mobile phase: phosphate buffer.

Solute	pH 3.85		pH 5.28		pH 6.40	
	k'_2	α	k'_2	α	k'_2	α
2-(4-Chlorophenoxy) propionic acid	0.50	1.0	0.28	1.0	0.18	1.0
Di-benzoyl tartaric acid	2.54	2.05	0.46	2.3	0.23	2.1
Di-*p*-toluoyl tartaric acid	9.13	2.85	1.71	3.0	0.81	2.2
Naproxen	4.15	2.13	2.72	2.45	1.61	2.5
N-(1-Phenylethyl) phthalamic acid	1.30	1.3	0.89	1.6	0.58	1.6
Warfarin	1.97	1.37	2.51	1.38	1.5	1.0
N-CBZ-phenylalanine	3.37	1.36	–	–	2.06	1.98
N-Boc-phenylalanine	1.7	2.0	1.58	2.4	1.14	2.4
N-Acetyltryptophan	1.5	1.4	1.58	1.7	1.28	1.9
Tryptophan	0.17	1.4	0.37	1.7	0.45	1.5
1-Phenylethanol	0.29	1.0	0.41	1.1	0.40	1.1
Propranolol	1.12	1.04	3.9	1.0	5.3	1.0
Ephedrine	0.28	1.1	1.4	1.1	1.6	1.1

of naproxen and di-*p*-toluoyltartaric acid were separated at both low and high buffer ion concentrations.

Charged modifiers. Addition of organic cations and anions to the mobile phase has been used to regulate retention and stereoselectivity on protein chiral stationary phases, *e.g.*, immobilized α_1-acid glycoprotein [4] and albumin [39].

Octanesulphonate (OS) in the mobile phase decreased the retention times of (*R*)- and (*S*)-naproxen but had almost no effect on the enantioselectivity when α-CHT-silica was used as the stationary phase (Fig. 8). OS improved the column efficiency and the peak symmetry and thus increased the chiral resolution.

Chiral separations using a cationic modifier, dimethyloctylamine (DMOA), in the mobile phase were also investigated (Table VII). The capacity factors for the enantiomeric acids were not affected by the DMOA, indicating a negligible retention of the acids as ion pairs with DMOA. Interestingly, contrary to the improved enantioselectivity of chiral carboxylic acids using α_1-acid glycoprotein-silica as stationary phase [4], DMOA had no effect on

TABLE VI

INFLUENCE OF IONIC STRENGTH (*I*) ON ENANTIOSELECTIVE RETENTION

Solid phase: α-CHT-A. Mobile phase: phosphate buffer (pH 5.3).

Solute	I = 0.025		I = 0.050		I = 0.10	
	k'_2	α	k'_2	α	k'_2	α
Naproxen	1.68	2.2	1.92	2.2	2.20	2.3
Di-*p*-toluoyl tartaric acid	1.21	4.3	1.28	4.0	1.49	3.2
Propranolol	11.4	1.1	7.95	1.0	5.4	1.0

TABLE VII

INFLUENCE OF DIMETHYLOCTYLAMINE (DMOA) ON ENANTIOSELECTIVE RETENTION

Solid phase: α-CHT-A. Mobile phase: DMOA in phosphate buffer (pH 5.4).

Solute	DMOA (m*M*)								
	0			0.20			2.0		
	k'_2	α	*asf*	k'_2	α	*asf*	k'_2	α	*asf*
Naproxen	1.99	2.2	1.6	2.04	2.3	1.6	2.03	2.2	1.7
Di-*p*-toluoyl tartaric acid	1.30	3.3	1.6	1.30	3.5	1.8	1.58	3.3	1.6
N-(1-Phenylethyl) phthalamic acid	–	–	–	0.65	1.7	1.7	0.58	1.9	1.7
N-Boc-phenylalanine	–	–	–	1.02	2.3	2.1	1.35	3.3	1.8
N-CBZ-phenylalanine	–	–	–	2.08	1.11	1.8	2.14	1.57	1.9
Tryptophan	–	–	–	0.26	1.4	1.9	0.22	1.9	1.6
Propranolol	4.98	1.0	1.8	2.87	1.0	2.4	1.75	1.0	1.9

the enantioselectivity for the anionic solutes naproxen, di-*p*-toluoyltartaric acid and N-(1-phenylethyl)phthalamic acid (Table VII). However, the significant changes in the enantioselectivity for the amino acid derivatives when DMOA was present in the mobile phase suggested that DMOA may interact with the immobilized enzyme, giving rise to altered binding properties. The decrease in the retention of propranolol with increasing concentration of DMOA might be due to a competition by propranolol enantiomers and DMOA for the same adsorption sites on the stationary phase.

ACKNOWLEDGEMENTS

We are grateful to Professor D. Westerlund and Dr. R. Isaksson for valuable comments on the manuscript. This project was supported by the Swedish Natural Science Research Council (project No. K-Ku 1972-102). Research grants from the Swedish Academy of Pharmaceutical Sciences and the I.F. Foundation for Pharmaceutical Research are gratefully acknowledged.

REFERENCES

1 I. W. Wainer, in W. J. Lough (Editor), *Chiral Liquid Chromatography*, Blackie, Glasgow and London, 1989, Ch. 7.
2 S. Allenmark, *J. Liq. Chromatogr.*, 9 (1986) 425–442.
3 E. Domenici, C. Bertucci, P. Salvadori, G. Felix, I. Cahagne, S. Motellier and I. W. Wainer, *Chromatographia*, 29 (1990) 170–176.
4 J. Hermansson and G. Schill, in P. R. Brown and R. A. Hartwick (Editors), *High Performance Liquid Chromatography (Chemicals Analysis*, Vol. 98) Wiley, New York, 1989, Ch. 8.
5 T. Miwa, T. Miyakawa, M. Kayano and Y. Miyake, *J. Chromatogr.*, 408 (1987) 316–322.
6 P. Erlandsson, I. Marle, L. Hansson, R. Isaksson, C. Pettersson and G. Pettersson, *J. Am. Chem. Soc.*, 112 (1990) 4573–4574.
7 J. B. Jones and J. F. Beck, *Tech. Chem. (N.Y.)*, 10 (1976) 133–191.
8 I. W. Wainer, P. Jadaud, G. R. Schonbaum, S. V. Kadodkar and M. P. Henry, *Chromatographia*, 25 (1988) 903–907.
9 P. Jadaud, S. Thelohan, G. R. Schonbaum and I. W. Wainer, *Chirality*, 1 (1989) 38–44.
10 P. Jadaud and I. W. Wainer, *J. Chromatogr.*, 476 (1989) 165–174.
11 J. Kalbe, H. Höcker and H. Berndt, *Chromatographia*, 28 (1989) 193–196.
12 I. Marle and C. Pettersson, presented at the *13th International Symposium on Column Liquid Chromatography, Stockholm, June 25–30, 1989.*
13 N. Daoud, T. Arvidsson and K.-G. Wahlund, *J. Chromatogr.*, 385 (1987) 311–322.
14 J. R. Conder and C. L. Young, *Physicochemical Measurement by Gas Chromatography*, Wiley, Chichester, 1979, pp. 354–356.
15 D. P. Herman, L. R. Field and S. Abbott, *J. Chromatogr. Sci.*, 19 (1981) 470–476.
16 J. Hermansson, *J. Chromatogr.*, 269 (1983) 71–80.
17 E. L. Jackson, in R. Adams, W. E. Bachmann, L. F. Fieser, J. R. Johnson and H. R. Snyder (Editors), *Organic Reactions*, Vol. 2, Wiley, New York, 1944, Ch. 8.

18 S. Ohlson, L. Hansson, P.-O. Larsson and K. Mosbach; *FEBS Lett.*, 93 (1978) 5–9.
19 L. Hansson, Hafslund Nycomed Innovation, Ideon, Malmö, personal communication.
20 I. Marle, P. Erlandsson, L. Hansson, R. Isaksson, C. Pettersson and G. Pettersson, *J. Chromatogr.*, 586 (1991) 233–248.
21 P. Erlandsson, L. Hansson and R. Isaksson, *J. Chromatogr.*, 370 (1986) 475–483.
22 T. Mizutani, *J. Liq. Chromatogr.*, 8 (1985) 925–983.
23 P. Desnuelle, in P. D. Boyer, H. Lardy and K. Myrbäck (Editors), *The Enzymes*, Vol. 4, Academic Press, New York, 1960, Ch. 5.
24 K. K. Unger, *Porous Silica*, Elsevier, Amsterdam, 1979, p. 14.
25 *Product Information on HPLC Sorbents*, E. Merck, Darmstadt, 1982.
26 A. V. Levashov, Y. L. Khmelnitsky, N. L. Klyachko, V. Y. Chernyak and K. Martinek, *Anal. Biochem.*, 118 (1981) 42–46.
27 K. K. Unger, R. Janzen, G. Jilge, K. D. Lork and B. Anspach, in C. Horváth (Editor), *High Performance Liquid Chromatography —Advances and Perspectives*, Vol. 5, Academic Press, New York, 1988, Ch. 1.
28 J. Köhler, D. B. Chase, R. D. Farlee, A. J. Vega and J. J. Kirkland, *J. Chromatogr.*, 352 (1986) 275–305.
29 C. Pettersson, E. Heldin and H. W. Stuurman, *J. Chromatogr. Sci.*, 28 (1990) 413–420.
30 D. S. Clark and J. E. Bailey, *Biotechnol. Bioeng.*, 26 (1984) 1090–1097.
31 A. R. Fersht and Y. Requena, *J. Mol. Biol.*, 60 (1971) 279–290.
32 J. D. Stoesz and R. W. Lumry, *Biochemistry*, 17 (1978) 3693–3699.
33 L. Goldstein, *Biochim. Biophys. Acta*, 315 (1973) 1–17.
34 A.-C. Koch-Schmidt and K. Mosbach, *Biochemistry*, 16 (1977)) 2105–2109.
35 D. Wu and R. R. Walters, *J. Chromatogr.*, 458 (1988) 169–174.
36 C. I. Mekras, M. H. George and J. A. Barrie, *Int. J. Biol. Macromol.*, 11 (1989) 113–118.
37 H.-L. Wu, D. A. Lace and M. L. Bender, *Proc. Natl. Acad. Sci. U.S.A.*, 78 (1981) 4118–4119.
38 A. C. Moffat, J. V. Jackson, M. S. Moss and B. Widdop (Editors), *Clarke's Isolation and Identification of Drugs*, Pharmaceutical Press, London, 2nd Ed., 1986.
39 S. Andersson and S. Allenmark, *J. Liq. Chromatogr.*, 12 (1989) 345–357.

Journal of Chromatography, 604 (1992) 197–201
Elsevier Science Publishers B.V., Amsterdam

CHROM. 24 155

High-performance liquid chromatographic determination of the enantiomeric excess of 1,3-glyceryl diethers obtained by stereoselective catalytic reduction

Marco Pallavicini and Luigi Villa

Istituto di Chimica Farmaceutica e Tossicologica, Università di Milano, Viale Abruzzi 42, 20133 Milan (Italy)

Edoardo Cesarotti

Dipartimento di Chimica Inorganica e Metallorganica, Università di Milano, Centro CNR, Via Venezian 21, 20133 Milan (Italy)

(First received February 12th, 1992; revised manuscript received March 5th, 1992)

ABSTRACT

The degree of stereodifferentiation in the catalytic enantioselective reduction of some prochiral diethers of 1,3-dihydroxy-2-propanone was determined by high-performance liquid chromatography using the cellulose tris(3,5-dimethylphenylcarbamate) derivative Chiralcel OD as the chiral stationary phase. The method was validated and the analytical results evaluated with respect to the rotation values of the reduction products and those reported previously for the same intermediates prepared from chiral starting materials.

INTRODUCTION

An asymmetric synthesis of 1,3-glyceryl diethers (Fig. 1) by stereoselectively reducing the corresponding ketones has been reported [1]. The glyceryl ethers, useful building blocks for synthesizing the enantiomers of several biologically active compounds such as phospholipids, platelet activating factor (PAF) and β-blockers, are usually prepared from chiral starting materials (D-mannitol, L-serine, ascorbic and tartaric acids).

Alternative approaches are based on the stereoselective chemical [2] or biological [3] reduction of prochiral ketones or the enzymatic differentiation of the two enantiotopic oxymethylenic groups in prochiral 1,3-glyceryl diesters obtained from 1,3-dihydroxypropanone [4,5].

The comparative evaluation of the degree of enantioselectivity achieved with these different approaches is limited, however, by the heterogeneity of the procedures used to determine the enantiomeric composition of the products.

This is usually determined: (a) by comparing the optical rotations with those reported for the same substances in optically pure forms [2,4,6–9]; (b) by derivatization using an enantiomerically pure reagent and analysing the diastereomeric composition by chromatography or NMR spectroscopy [2–5, 10–12]; and (c) by NMR analysis in the presence of an optically active shift reagent [6,13].

All these methods are limited in terms of accuracy, precision and feasibility. Determining the optical purity with the reported optical rotations re-

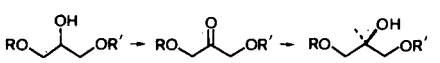

Fig. 1. Synthesis of 1,3-glyceryl diethers.

Correspondence to: Dr. M. Pallavicini, Istituto di Chimica Farmaceutica e Tossicologica, Università di Milano, Viale Abruzzi 42, 20133 Milan, Italy.

0021-9673/92/$05.00

quires definite, high values of optical rotation as terms of reference. The second method is unsuitable for routine use and requires that the derivatization is quantitative with respect to the substrate and that the derivatizing agent is enantiomerically pure [14]. With the third procedure, high enantiomeric excesses cannot be determined with a satisfactory degree of precision [6].

Initially the degree of differentiation in the catalytic reduction was evaluated by comparing the optical rotation values of the hydrogenation products with those reported previously [6]. These compounds are usually prepared from 1,2-di-O-isopropylidene-*sn*-glycerol [11] and used as intermediates in the synthesis of optically pure PAF [6]. Later, however, considering the low values of the optical rotations and the limitations of the procedures, a high-performance liquid chromatographic method on a chiral stationary phase was used to determine the enantiomeric excesses. This technique allows the rapid, precise and direct determination of the enantiomeric excess. In this respect, cellulose trisphenylcarbamates adsorbed on silica gel have proved to be chiral stationary phases suitable for the resolution of many racemic compounds. Secondary alcohols with aromatic rings, such as 1,3-glyceryl diethers **1–3** (Fig. 2), can interact with the polar carbamate groups via hydrogen bonding and with the phenyl groups via π–π interaction. The resulting diastereomeric complexes have comparatively different stabilities. Among those commercially available, one of the most effective is cellulose tris(3,5-dimethylphenylcarbamate) adsorbed on silica gel [15].

This paper describes the validated conditions used to resolve the enantiomeric components of three different 1,3-glyceryl diethers and discusses the results achieved by this procedure and by simply comparing polarimetric data.

EXPERIMENTAL

Apparatus and materials

High-performance liquid chromatography (HPLC) was carried out on a Chiralcel OD column (250 × 4.6 mm I.D.) from Daicel using a Waters 510 pump and a Pye Unicam Pu 4025 UV detector (analytical wavelength 254 nm). Chromatographic data were collected and processed on a Waters 740 data module. HPLC-grade solvents were purchased from Merck (Darmstadt, Germany).

Optical rotations were measured in a 1-dm cell of 1 ml capacity using a Perkin-Elmer 241 polarimeter.

Methods

The racemic compounds 1-O-benzyl-3-O-trityl glycerol (**1**), 1-O-octadecyl-3-O-trityl glycerol (**2**) and 1-O-benzyl-3-O-octadecyl glycerol (**3**) (Fig. 2), synthesized from 1,2-di-O-isopropylidene glycerol by the methods of Hirth and Barner [6], were oxidized to the ketones with pyridinium chlorochromate in dichloromethane and then stereoselectively reduced to the corresponding alcohols. The complexes utilized for the reduction were [(*S*)-(−)] and [(*R*)-(+)-2,2′-bis(diphenylphosphino)-1,1′-binaphthyl]ruthenium(II) chloride dimers, triethylamine solvate, $\{Ru_2Cl_4[(S)\text{-BINAP}]_2\}N(C_2H_5)_3$ and $\{Ru_2Cl_4[(R)\text{-BINAP}]_2\}N(C_2H_5)_3$, prepared according to previously published methods [16].

In addition, the optically pure *S*- isomers of compounds **1** and **2** were obtained from 1,2-di-O-isopropylidene-*sn*-glycerol by the same method used for the preparation of the racemic forms.

The optical rotations of the hydrogenation products and of the *S* forms of compounds **1** and **2** were measured under the same conditions using the methods of Hirth and Barner [6].

The enantiomeric composition was determined by HPLC on a chiral stationary phase under the following conditions: compounds **2** and **3**, hexane–isopropanol (99.4:0.6, v/v), flow-rate 1 ml/min;

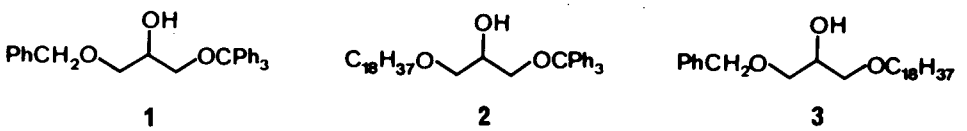

1 2 3

Fig. 2. 1,3-Glyceryl diethers prepared from 1,2-di-O-isopropylidene glycerol.

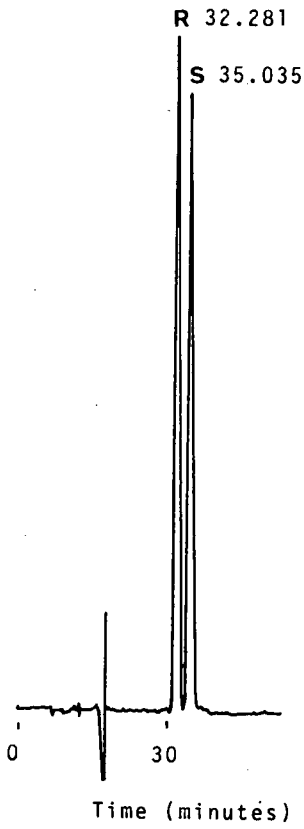

Fig. 3. Resolution of racemic 1-O-benzyl-3-O-trityl glycerol on the Chiralcel OD column. For the elution conditions, see under Experimental.

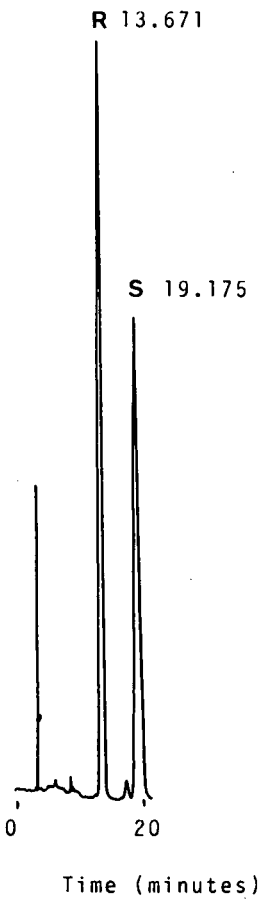

Fig. 4. Resolution of racemic 1-O-octadecyl-3-O-trityl glycerol on the Chiralcel OD column. For the elution conditions, see under Experimental.

compound **1**, hexane–ethanol–water (90.63:9.06:0.3, v/v/v), flow-rate 0.2 ml/min.

To achieve the resolution of compound **1** it was necessary to replace isopropanol with ethanol, to add water and to drastically reduce the flow-rate.

Figs. 3–7 show the chromatograms of the racemic compounds **1–3** and the *S* forms of compounds **1** and **2**.

Table I gives the optical rotations of the hydrogenation products, the optical purities of the same compounds calculated from the reference values and the corresponding enantiomeric excesses determined by HPLC.

RESULTS AND DISCUSSION

The enantiomeric excesses determined by HPLC only agree with the optical purities calculated from the optical rotations for compound **1**, whereas they are significantly different for compounds **2** and **3**.

When the stereodifferentiation of a reaction is high, as for the catalytic reduction to compounds **1** and **2**, the amount of stereocontrol must be determined with the greatest precision possible. This is less essential for compound **3**, as it was obtained with a low degree of enantioselectivity, usually less than 30% enantiomeric excess.

To confirm these results, optically pure (*S*)-**1** and (*S*)-**2** were prepared from 1,2-di-O-isopropylidene-*sn*-glycerol. A comparison of the chromatograms of optically pure (*S*)-**1** and (*S*)-**2** with those of racemic mixtures (see Figs. 6 and 7) clearly indicates that 1,2-di-O-isopropylidene-*sn*-glycerol provides optically pure compounds (*S*)-**1** and (*S*)-**2**, as the minor

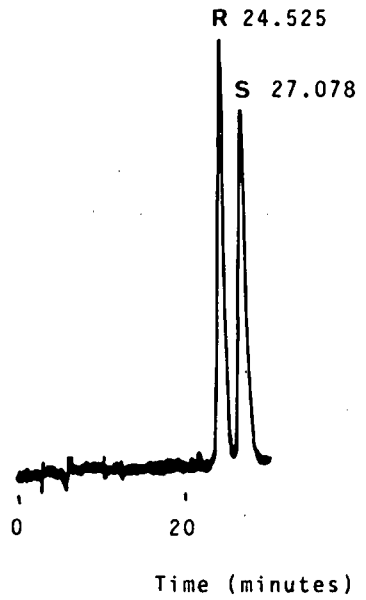

Fig. 5. Resolution of racemic 1-O-benzyl-3-O-octadecyl glycerol on the Chiralcel OD column. For the elution conditions, see under Experimental.

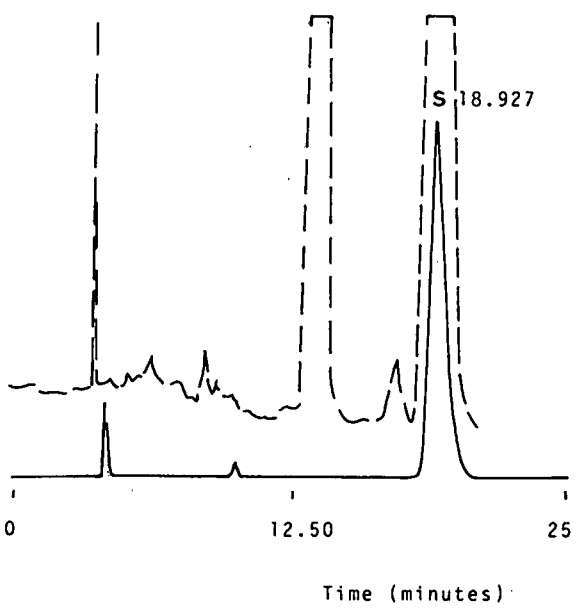

Fig. 7. Chromatogram of (*S*)-1-O-octadecyl-3-O-trityl glycerol (1-O-trityl-3-O-octadecyl-*sn*-glycerol) obtained with the Chiralcel OD column, superimposed over the chromatogram of the racemic mixture shown in Fig. 4 (broken line). For the elution conditions, see under Experimental.

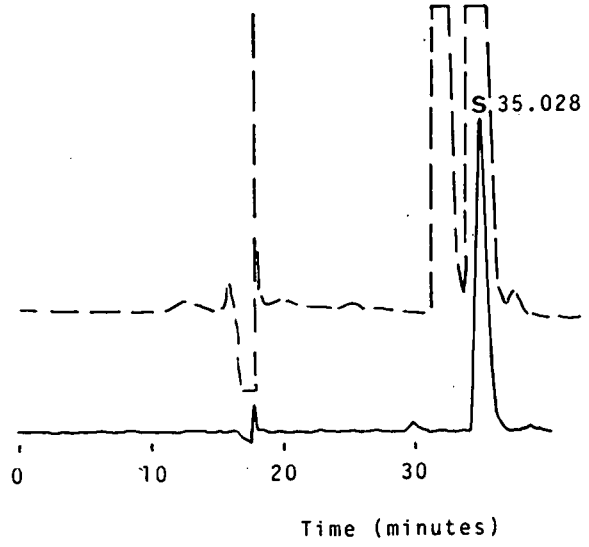

Fig. 6. Chromatogram of (*S*)-1-O-benzyl-3-O-trityl glycerol (1-O-trityl-3-O-benzyl-*sn*-glycerol) obtained with the Chiralcel OD column, superimposed over the chromatogram of the racemic mixture shown in Fig. 3 (broken line). For the elution conditions, see under Experimental.

TABLE I

OPTICAL ROTATIONS, OPTICAL PURITIES CALCULATED FROM REFERENCE VALUES AND ENANTIOMERIC EXCESSES DETERMINED BY HPLC OF THE 1,3-GLYCERYL DIETHERS OBTAINED BY ENANTIOSELECTIVE HYDROGENATION

c = Concentration.

Compound	$[\alpha]_D^{20}$	Optical purity (%)[a]	Enantiomeric excess (HPLC) (%)
(*R*)-**1**	+5.59 (c=5, benzene)	87.8	87.3
(*S*)-**1**	−5.54	87.0	86.0
(*R*)-**2**	+4.70 (c=5, benzene)	98.3	88.5
(*S*)-**2**	−4.59	96.0	86.1
(*R*)-**3**	+0.60 (c=10, benzene)	36.8	26.9
(*S*)-**3**	−0.48	30.1	20.6

[a] Reference optical rotation values [6]: −6.37 [(*S*)-**1**], −4.78 [(*S*)-**2**], + 1.63 [(*R*)-**3**].

R enantiomer is undetectable. The corresponding optical rotations are −6.50 and −5.31, respectively. The optical purity of stereoselectively hydrogenated products **1** and **2**, calculated with reference to these values agree with the enantiomeric excess values determined by HPLC. This proves that the relationship between the enantiomeric excess and the optical rotation for compounds **1** and **2** is linear. To determine the corresponding correlation coefficients (r), in addition to the two samples of compounds **1** and **2** obtained by catalytic hydrogenation and from optically active 1,2-di-O-isopropylidene glycerol, two samples of the compounds were prepared at different enantiomeric excesses by mixing the appropriate amounts of the enantiomerically pure *S* compounds with the racemic mixtures. The linear relationships found between the optical rotations and the corresponding enantiomeric excess values determined by HPLC gave $r = 0.99979$ and $r = 0.99795$ for compounds **1** and **2**, respectively.

The HPLC method based on the chiral stationary phase Chiralcel OD achieved the aim of developing a rapid, sensitive and precise procedure to determine the enantiomeric excess of these substrates. This is shown by the following method performances: linearity: $r = 0.99992$ (**1**), 0.99985 (**2**), 0.99944 (**3**); precision: determinations on six samples of the three racemic compounds at different concentrations showed a mean area first peak/area second peak ratio of 0.9896 (coefficient of variation 1.61%) for compound **1**, 1.0108 (1.86%) for compound **2** and 1.0016 (1.56%) for compound **3**; sensitivity: the method is sensitive to the injection on-column of about 20 ng of compound **1**, 0.2 μg of compound **2** and 1 μg of compound **3**. The calculated k' values gave separation factors of 1.15, 1.46 and 1.14 for compounds **1**, **2** and **3**, respectively.

The evaluation of the degree of stereodifferentiation based on the comparison of the polarimetric data implies increasing the reference rotation value of compounds **1** and **2** to 6.50 (0.05) and 5.31 (0.05), respectively.

REFERENCES

1 E. Cesarotti, A. Mauri, M. Pallavicini and L. Villa, *Tetrahedron Lett.*, 32 (1991) 4381.
2 H. Suemune, A. Akashi and K. Sakai, *Chem. Pharm. Bull.*, 33 (1985) 1055.
3 F. Aragozzini, E. Marconi, D. Potenza and C. Scolastico, *Synthesis*, (1989) 225.
4 H. Suemune, Y. Mizuhara, H. Akita and K. Sakai, *Chem. Pharm. Bull.*, 34 (1986) 3440.
5 D. Breitgoff, K. Laumen and M. P. Schneider, *J. Chem. Soc., Chem. Commun.*, (1986) 1523.
6 G. Hirth and R. Barner, *Helv. Chim. Acta*, 65 (1982) 1059.
7 M. E. Jung and T. Shaw, *J. Am. Chem. Soc.*, 102 (1980) 6304.
8 M. Ohno, K. Fujita, H. Nakai, S. Kobayashi, K. Inoue and S. Nojima, *Chem. Pharm. Bull.*, 33 (1985) 572.
9 A. H. Al-Hakim, A. H. Haines and C. Morley, *Synthesis*, (1985) 207.
10 P. E. Sonnet, E. G. Piotrowski and R. T. Boswell, *J. Chromatogr.*, 436 (1988) 205.
11 G. Hirth and W. Walther, *Helv. Chim. Acta*, 68 (1985) 1863.
12 V. Kerscher and W. Kreiser, *Tetrahedron Lett.*, 28 (1987) 531.
13 A. B. Mikkilineni, P. Kumar and E. Abushanab, *J. Org. Chem.*, 53 (1988) 6005.
14 J. A. Dale, D. L. Dull and H. S. Mosher, *J. Org. Chem.*, 34 (1969) 2543.
15 Y. Okamoto, M. Kawashima and K. Hatada, *J. Chromatogr.*, 363 (1986) 173.
16 T. Ikariya, Y. Ishii, H. Kawano, T. Arai, M. Saburi, S. Yoshikawa and S. Akutagawa, *J. Chem. Soc. Chem. Commun.*, (1985) 922.

Journal of Chromatography, 604 (1992) 203–211
Elsevier Science Publishers B.V., Amsterdam

CHROM. 24 163

Reversed-phase liquid chromatography using monoalkylammonium compounds in the mobile phase

Effects of monoalkylammonium chain length on the efficiency, selectivity and separation of xanthine and uric acid derivatives

E. Naline, C. Palette-Pays, J. Moreau, C. Advenier and M. Pays

Département de Biochimie et de Pharmacologie, Hôpital André Mignot, 177 Rue de Versailles, F-78157 Le Chesnay (France)

(First received December 12th, 1991; revised manuscript received February 25th, 1992)

ABSTRACT

A systematic analysis of the influence of several chromatographic parameters on the adsorption of monoalkylammonium modifiers on a chemically bonded phase in reversed-phase high performance liquid chromatography is presented. The most important variables are the alkyl chain length, the concentration of the monoalkylammonium modifiers and the acetonitrile content in the mobile phase. The results can be applied to the separation and structure determination of xanthine and uric acid derivatives and to the study of retention mechanisms.

INTRODUCTION

The chromatographic performance on chemically bonded-phase high-performance liquid chromatographic (HPLC) columns of solutes containing amine functional groups, such as xanthine and uric acid derivatives, is often poor. The chromatography of these derivatives can be improved by adding a modifying agent to the mobile phase [1]. Optimization of the retention and selectivity of these derivatives has been carried out by an appropriate combination of the composition and pH of the mobile phase and by adding a suitable alkylamine modifier, changing the chromatographic mode [reversed-phase (RP) HPLC] into reversed-phase ion-pair partition [2].

The use of octadecylsilyl (ODS) phases dynamically modified by adding ion-pairing reagents, such as dioctylammonium [3], dimethyloctylammonium [4], hexylammonium [5,6], dibutylammonium [7], tetrabutylammonium [8,9], cetyltrimethylammonium [10–12] and decylammonium ion [13,14], to the eluent leads to a better chromatographic behaviour and helps to resolve problems associated with retention, column efficiency and peak symmetry [15,16]. The theoretical dependence of the capacity factors (k') on the concentration of the ion-pair reagent, on the pH values of the mobile phase and on the pK_a values of the solutes has been discussed by several workers [11,17–21]. A practical equation based on the electrostatic model of reversed-phase ion-pair chromatography (RP-IPC) describes the relationship between the capacity factor of ionic

Correspondence to: Dr. E. Naline, Département de Biochimie et de Pharmacologie, Hôpital André Mignot, 177 Rue de Versailles, F-78157 Le Chesnay, France.

0021-9673/92/$05.00

solutes and the eluent concentration of the modifier [9,22–24]. However, no exhaustive study on the conditions of use of monoalkylammonium ions has yet been reported [3,25–27].

The purpose of this study was to investigate the adsorption of different monoalkylammonium ions on the ODS surface and to determine their influence on the chromatographic behaviour of uric acid and xanthine derivatives.

EXPERIMENTAL

Apparatus

Chromatography was performed on a Varian 5000 instrument equipped with a stainless-steel Ultrasphere IP (5 μm) column (15 cm × 0.4 cm I.D.) (Beckman Instruments, Berkeley, CA, USA). UV detection was performed with a Spectroflow 773 spectrophotometer (Kratos Analytical Instruments, Westwood, NJ, USA) set at 280 nm. A CR-3A peak integrator (Shimadzu, Kyoto, Japan) was used and automatic injections of 20 μl were performed with a Model 231 injector (Gilson Medical Electronics, Middleton, WI, USA). The flow-rate was 2 ml/min. For the breakthrough curves, a Shodex RI SE-11 differential refractometer (Showa Denko, Tokyo, Japan) was used.

Chemicals

Doubly distilled water was used throughout.

Theophylline (1,3-dimethylxanthine, 1,3-DMX), dyphylline and caffeine (1,3,7-trimethylxanthine, 1,3,7-TMX) were obtained from Sigma (St. Louis, MO, USA), 3-methylxanthine (3-MX), 7-methylxanthine (7-MX), 1-methylxanthine (1-MX), 1,7-dimethylxanthine (1,7-DMX), 1-methyluric acid (1-MU), 3-methyluric acid (3-MU), 7-methyluric acid (7-MU), 9-methyluric acid (9-MU), 1,7-dimethyluric acid (1,7-DMU), 3,7-dimethyluric acid (3,7-DMU), 1,3-dimethyluric acid (1,3-DMU), 1,9-dimethyluric acid (1,9-DMU), methylamine · HCl, ethylamine · HCl, *n*-propylamine, *n*-butylamine, *n*-pentylamine, *n*-hexylamine, *n*-heptylamine, *n*-octylamine, *n*-nonylamine, *n*-decylamine, *n*-undecylamine, *n*-dodecylamine, *n*-tetradecylamine, *n*-hexadecylamine and *n*-octadecylamine from Fluka (Buchs, Switzerland) and acetonitrile from Merck (Darmstadt, Germany).

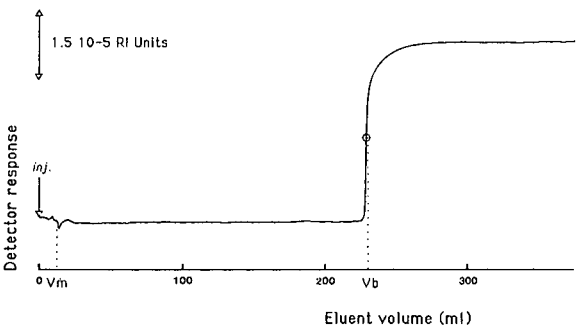

Fig. 1. Breakthrough curve of decylammonium ion using a differential refractometer (range ×8). Eluent, acetonitrile–85 m*M* acetate buffer (pH 4.0) (2:98, v/v); decylammonium ion, 0.75 m*M*; temperature, 25°C; flow-rate, 2 ml min^{-1}. V_b is the breakthrough volume.

Column loading and equilibration

The amounts of *n*-alkylammonium ions adsorbed by the stationary phase from the standard eluent were determined by the breakthrough method [19, 28–30] (Fig. 1). Before breakthrough volume measurement, the HPLC columns were washed successively with acetonitrile and the degassed mobile phase (standard eluent) prepared with 85 m*M* sodium acetate buffer (pH 4.0)–acetonitrile (98:2, v/v).

The standard eluent containing 0.75 m*M* *n*-alkylamine was used for the adsorption diagrams and the standard eluent containing *n*-decylamine (0.38–3.75 m*M*) was used for the isotherm adsorption.

The breakthrough volume, V_b, was measured from the moment of changing the standard eluent to the mid-point of the eluted front. The *n*-alkylammonium ion concentration in the stationary phase (C_{st}, μmol g^{-1}) was calculated using the equation

$$C_{st} = \frac{(V_b - V_0)C_m}{W_{st}} = \frac{Q_{ads}}{W_{st}}$$

where C_m (mmol l^{-1}) is the concentration of pairing ions in the mobile phase, V_b is the breakthrough volume, V_0 is the void volume of the chromatographic system, W_{st} (g^{-1}) is the packing within the column and Q_{ads} is the amount of pairing ion adsorbed in the stationary phase [19,25].

RESULTS AND DISCUSSION

Effect of alkyl chain length on n-alkylamine adsorption

After running a mobile phase containing 0.75 m*M* of the alkylammonium ion, the amounts of alkylamines containing 1–16 carbon atoms adsorbed were determined. The structures of the alkylamines used were $CH_3(CH_2)_{n-1}NH_2$ ($1 \leqslant n \leqslant 16$). The scope of the study was determined by the solubility characteristics of the alkylammonium ions in the mobile phase. Amines containing 18 carbon atoms or more could not be used as they were not soluble under our experimental conditions.

Several workers have observed linear relationships between log C_{st} and the number of carbon atoms in the alkyl chain of the modifier for homologous series [25]. Alkylammonium ions adsorption can be expressed by

$$\log C_{st} = an + b$$

where n is the number of carbon atoms in the alkyl chain of the modifier and a and b are constants for a given set of experiments.

Fig. 2 shows the exponential variation of alkylammonium ion concentration in the stationary phase (C_{st}) *versus* n. Primary monoalkylamines containing 1–4 carbon atoms are not fixed on the column; the corresponding ammonium cations are too hydrophilic. For alkylammonium ions containing 5–10 carbon atoms, the amount of alkylammonium ions adsorbed in the stationary phase (Q_{ads}) increases with increasing length of the alkyl chain, and the fixation is linear. If we use the adsorption isotherm referred to by Ståhlberg [23], we deduce from the slope in Fig. 2 that the increase in adsorption energy per CH_2 group is 1.9 kJ mol^{-1} [31]. This value is lower than that obtained for the adsorption of this kind of ion between water and oil (2.88–2.97 kJ mol^{-1} [32,33]) and the reason is probably the presence of acetonitrile in the mobile phase [34].

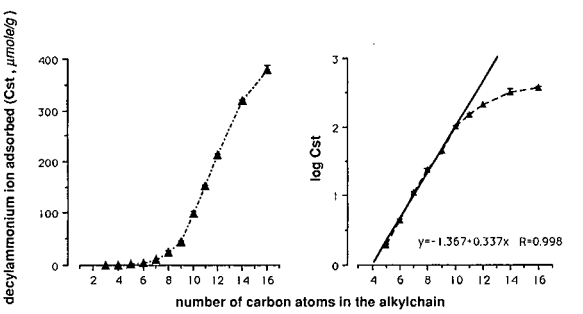

Fig. 2. Adsorption of alkylammonium ion by a 15-cm Ultrasphere IP (5 µm) column as a function of the number of carbon atoms in the alkyl chain in the mobile phase [acetonitrile–85 m*M* acetate buffer (pH 4.0) (2:98, v/v); alkylammonium ion, 0.75 m*M*]. Temperature, 25°C; flow-rate, 2 ml min^{-1}.

However, when $n > 10$ the variations are irregular. In this instance, the lower efficacy of the fixation can be explained by the electrostatic theory of ion-pair chromatography [23,24]. A surface potential exists whenever there is an excess of charged species of one type of sign over species of the opposite sign on the surface. The non-linearity of the adsorption isotherm of n-alkylammonium ions is due in turn to repulsion from the electrical double layer created and to the decrease in available surface area [23,35].

Table I shows the percentage occupation of the octadecyl site; the stationary phase used (Ultrasphere IP) contains 11.7% of carbon, which is equivalent to 541 µmol of octadecyl chains per gram of stationary phase. Under the experimental conditions chosen ($5 < n < 10$), the percentage occupation of the octadecyl sites is limited (<20%). Then, neutral derivatives undergo a dual mechanism of retention owing to the hydrophobic interactions

TABLE I

OCCUPATION OF THE STATIONARY PHASE FOR A CONCENTRATION OF 0.75 m*M* OF ALKYLAMMONIUM ION IN THE MOBILE PHASE

Alkyl chain length, n	Occupation of octadecyl sites (%)
6	0.8
7	2
8	4
9	8
10	18.5
11	28
12	39
14	59
16	71.2

with the stationary and mobile phases, while negatively charged species are retained by an ion-pair mechanism [1,7,22,23,34–36].

Under our experimental conditions (pH 4.0, 2% acetonitrile), the choice of the decylammonium ion permits the separation of the puric derivatives. The decylammonium ion is then characterized by a regular fixation with a percentage occupation of the octadecyl sites that is sufficiently low to determine an appropriate modulation for the retention of derivatives. This modifier adsorption decreases the k' of uncharged species and increases that of anionic species.

Adsorption isotherm; effect of decylammonium concentration in mobile phase

Ståhlberg [23] developed an electrostatic retention model for RP-IPC. The phenomenon of adsorption at the bonded phase–eluent interface involves an electrical double layer, creating an electrostatic surface potential [25,33,34,37]. This adsorption of the modifier can be described by a Langmuir equilibrium in which allowance is made for the electrical contributions to the adsorption energy, and also by a Freundlich isotherm [34]. In a number of instances (cetyltrimethylammonium ion [37], tetralkylammonium ion [25], alkylbenzyldimethylammonium ion [38] and hexylammonium ion [6]), adsorption of long-chain amines was well fitted by the following empirical relationship:

$$C_{st} = \alpha(C_m)\beta \quad \text{or} \quad \log C_{st} = \alpha' + \beta \log C_m$$

where α, α' and β are constants for a given set of experiments.

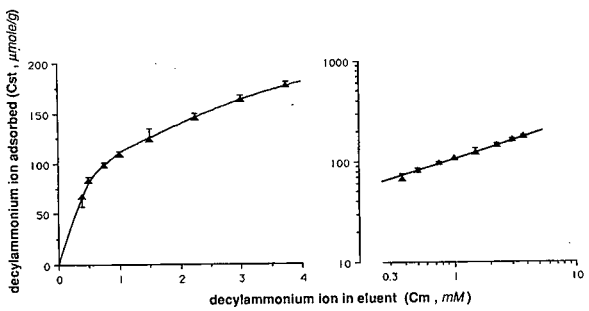

Fig. 3. Adsorption isotherms of decylammonium ion on a 15-cm Ultrasphere IP (5 μm) column from standard eluent [acetonitrile–85 mM acetate buffer (pH 4.0) 2:98, v/v)]. Temperature, 25°C; flow-rate 2 ml min^{-1}.

Fig. 3 shows that the adsorption isotherm of decylammonium ion from the standard eluent on to the ODS phase is fitted by the Freundlich equation over an aqueous concentration range of 0.38–3.75 mM at pH 4.0. Under these conditions the variation of log C_{st} is linear and increases with increasing concentration of decylammonium ions in the mobile phase. The experimental isotherm is described by the equation

$$\log C_{st} = 2.026 + 0.398 \log C_m \quad (R = 0.985)$$

Influence of acetonitrile content in mobile phase

Under our experimental conditions with slightly soluble alkylammonium ions (decylamine concentration in the mobile phase less than 1 mM) and an acetonitrile content varying from 0.25 to 4%, it was possible to establish a regular fixation without losing column efficiency.

It is known that retention values in RP-IPC are dependent on the concentration of organic solvent in the mobile phase [39–42]. The dependence of retention values on the concentration of the ion-pair reagent has been discussed by several workers [11,17–21,25,40–42]. Acetonitrile decreases the surface concentration of the adsorbed ion-pairing reagent [41]. Fig. 4 shows that the fixation of decylammonium ions decreases when the acetonitrile content increases. This adsorption can be expressed by the equation [25,41]

$$\log[C^+]_{st} = X - Y[\mathrm{ACN}]$$

where X and Y are constants for a given set of experiments and [ACN] is the acetonitrile content in the mobile phase.

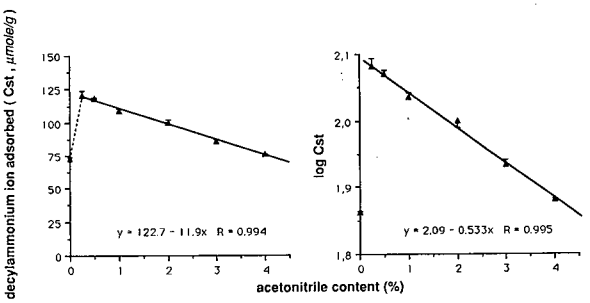

Fig. 4. Adsorption of decylammonium ion by a 15-cm Ultrasphere IP (5 μm) column as a function of acetonitrile content in the mobile phase [acetonitrile–85 mM acetate buffer (pH 4.0); alkylammonium ion, 0.75 mM]. Temperature, 25°C; flow-rate 2 ml min^{-1}.

Regarding the chromatographic behaviour of xanthine and uric acid derivatives, for a volume fraction of acetonitrile higher than 4%, it has been observed that the elution is very rapid and that the theophylline metabolites are not separated [14]. At concentrations lower that 0.25%, the mechanism of separation in RP-IPC is altered.

Under our experimental conditions, the presence of acetonitrile in the mobile phase reduces the free energy of the modifier adsorption usually found for this kind of ion [9,23,31–34,41,42]. The addition of acetonitrile modifies the dielectric constant, the viscosity and the superficial tension at the bonded phase–eluent interface. The substantial lowering of the superficial tensions, even at the supposedly low percentages of acetonitrile, favours the accessibility of the alkylammonium chains to the octadecylsiloxane sites [39].

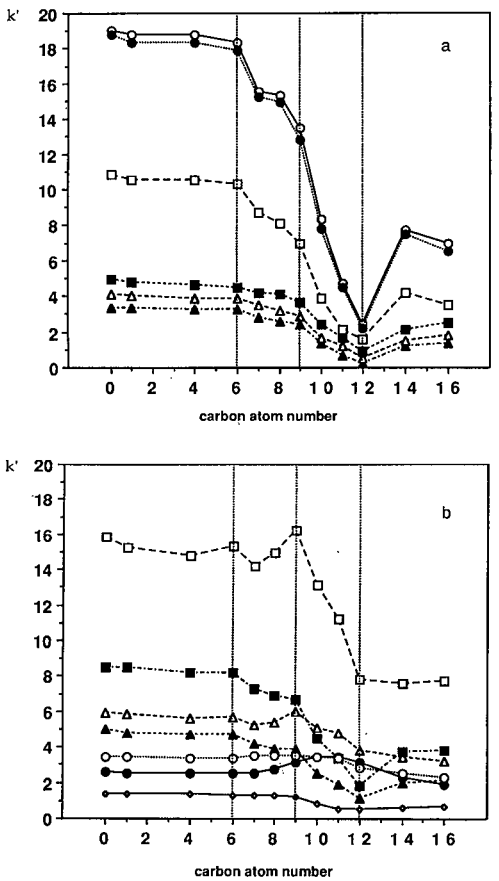

Fig. 5. Effect of alkyl chain length on the retention of (a) xanthine derivatives and (b) uric acid derivatives. (a) ○ = 1,3-DMX; ● = 1,7-DMX; □ = 3,7-DMX; ▲ = 7-MX; △ = 3-MX; ■ = 1-MX. (b) ▲ = 3,7-DMU; △ = 1,9-DMU; ■ = 1,3-DMU; □ = 1,7-DMU; ◇ = 3-MU; ● = 7-MU; ○ = 1-MU.

Chromatographic results and retention mechanisms

Alkylammonium ions have been applied to the separation of puric acid derivatives. Decylamine, in particular, has been used to separate theopylline metabolites [14]. Solute retention has been reported to vary with the chain length of the pairing ion [18,25,43,44]. The variations of the capacity factors (k') of uric acid and xanthine derivatives with the size of the alkyl chains are shown in Fig. 5. These variations divide the alkylammonium ions into four groups.

Group 1 is composed of alkylammonium ions which have an alkyl chain containing six carbon atoms or less. These ions reduce by less than 6% the k' values, expressed as relative values compared with the k' values determined in a mobile phase devoid of alkylamine. Such variations are negligible, being within the limits of experimental errors. This absence of variation confirms that alkylammonium ions with short chains have no effect on separation mechanisms. These constituents are entirely in the mobile phase, and in our experiments they had no effect on apolar, polar or ionic solutes; in particular, no ion pairing was observed.

Group 2 consists of alkylammonium ions which have an alkyl chain containing six to nine carbon atoms; these divide the derivatives of xanthine and

TABLE II

pK_a VALUES OF PURINE DERIVATIVES [45,46]

Derivative	pK_a	Derivative	pK_a
7,9-DMU	5.05	9-MX	6.12
9-MU	5.10	1,3-DMU	6.22
1,9-DMU	5.18	1-MX	7.90
1,7,9-TMU	5.28	7-MX	8.42
7-MU	5.45	3-MX	8.45
1-MU	5.48	1,7-DMX	8.65
1,7-DMU	5.93	1,3-DMX	8.68
1,9-DMX	5.99	3,9-DMU	8.91
1,3,7-TMU	6.01	1,3,9-TMU	9.39
3-MU	6.02	3,7,9-TMU	9.42
3,7-DMU	6.04	3,7-DMX	10.00
		3,9-DMX	10.14

uric acid into two categories: derivatives whose k' values decrease from 17% to 34% are the derivatives of xanthic and dimethyluric acids with methyl substituents in position 3 [N(3)–CH_3] and with a pK_a above 6 (Table II, Figs. 6 and 7); and derivatives whose k' values increase from 5% to 26% are the derivatives of uric acid with a pK_a below 6, corresponding to the N(3)–H-related acidic character expressed by C(2)–O^- (Table II, Figs. 6 and 7).

In group 2, when significant amounts of alkylammonium ions are adsorbed on the ODS surface, compounds without acidic character (non-ionic solutes such as xanthine derivatives and uric derivatives with $pK_a > 6$) are chromatographed according to a reversed-phase partition mechanism. The acidic compounds (7-MU, 1-MU and 1,9-DMU with $pK_a < 6$) are separated by reversed-phase ion-pair partition or by an intermediate mechanism.

Group 3 ($10 \leqslant n \leqslant 12$) is characterized by a decrease in all k' values which is minor (8–25%) for uric acid derivatives with $pK_a < 6$, despite an increase in cationic charge density in the stationary phase. On the other hand, the marked fall (>40%) observed with all the other derivatives can be attributed to the overcrowding resulting from an increase in the amount of *n*-alkylammonium ions adsorbed by the stationary phase, which limits the "reversed-phase partition phenomena". The adsorption of the pairing ion causes a decrease in the available hydrophobic surface area [43,44].

In group 4, which includes the very long-chain alkylammoniums ($n > 12$), a major increase in k' values was observed for xanthine derivatives and uncharged uric acid solutes (relative variation above 172%), whereas the k' values of anionic uric acid derivatives (7-MU, 1-MU and 1,9-DMU) decreased down to C_{16}. With xanthic derivatives and uncharged derivatives 3-MU, 1,3-DMU and 3,7-DMU, the effect of reduced accessibility to apolar sites was maximum for $n = 12$. For anionic uric derivatives ($pK_a < 6$), a decrease in k' beginning with $n = 11$ was confirmed for group 4 with $14 \leqslant n \leqslant 16$, whereas in this group the uncharged xanthic and uric solutes had increased or erratic retentions.

The results obtained orient the choice of the modifier towards a 9–10-carbon chain length, at the junction of groups 2 and 3 as defined above.

General comments on the structure of the xanthine and uric acid derivatives

The general structure and anionic forms of xanthine derivatives are shown in Fig. 6 and those of uric acid derivatives in Fig. 7. The similarity of behaviour in each class, demonstrated in Fig. 5, makes it possible to compare the behaviours of various solutes.

The 7-MU and 1-MU solutes (anionic uric derivatives) with $pK_a < 6$) have a particular behaviour with k' values that are maximum for $n = 10$ and minimum for $n = 16$ (Fig. 5b). The increase in retention resulting from ion pairing is significant with 7-MU and smaller with 1-MU. This result can be ascribed to the structural behaviour. With both solutes, the anionic form responsible for the pairing is C(2)–O^- (Fig. 7) [46]. The regular ion pairing observed with 7-MU is limited with 1-MU by steric hindrance due to the methyl group in position 1, which limits the accessibility of the solute to the cationic sites of the stationary phase.

The chromatographic behaviour of the 3-MU solute is identical with that of the monomethylxanthic derivatives and is characterized by a decrease in k' values for $n = 12$ (Fig. 5b). At pH 4.0, this solute ($pK_a = 6.02$) is in the uncharged lactam form (2,4,6-trioxo), with a pyrimidinic structure that is closer to the monomethylxanthines at this pH (Fig. 7). With 3-MU, the first ionic dissociation is in the N(7)–H position corresponding to the C(8)–O^- structure showing an electronic charge distribution that is different from that of the 7-MU and 1-MU derivatives [first ionic dissociation in the N(3)–H position corresponding to the C(2)–O^- structure] [46,47]. At pH 4.0, the ionic dissociation of 3-MU is negligible, but apart from its peculiar polarizability the maximum conjugation of hydration sites explains why this solute has a greater polarity than the other monomethyluric derivatives. The order of elution is 3-MU > 7-MU > 1-MU.

These 1-MX, 3-MX and 7-MX monomethylxanthines (Fig. 5) are characterized by a V-shaped variation of k' values, falling for $n = 12$, then rising until $n = 16$. These solutes with pK_a around 8 (Table II) are non-ionic at pH 4.0 and highly sensitive to the decrease in the number of apolar sites of the charged ODS. The order of elution is 7-MX > 3-MX > 1-MX. This results in solvation interactions (less with 1-MX, which limits the hydration site conjuga-

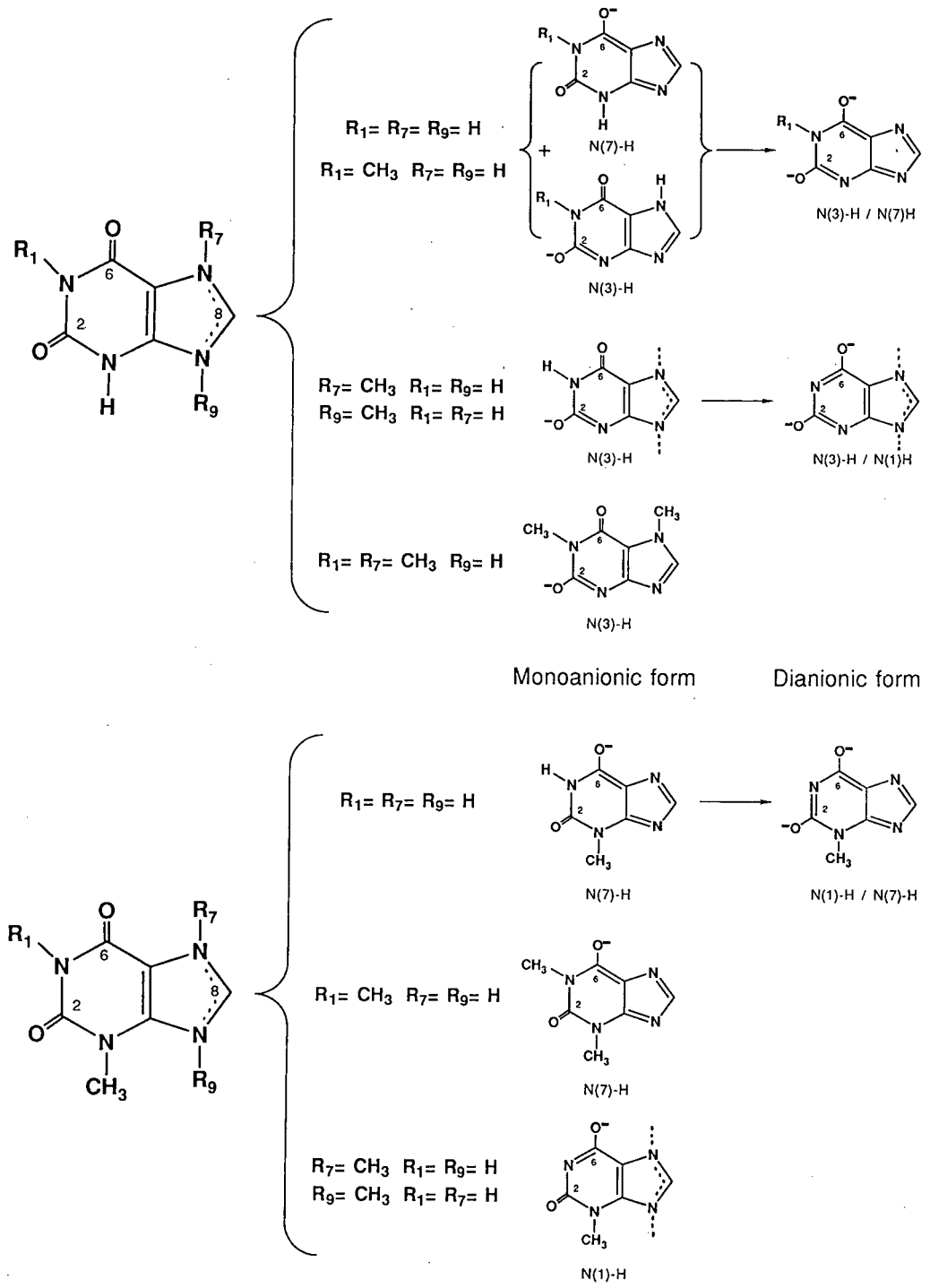

Fig. 6. General structures and ionic forms of xanthine derivatives.

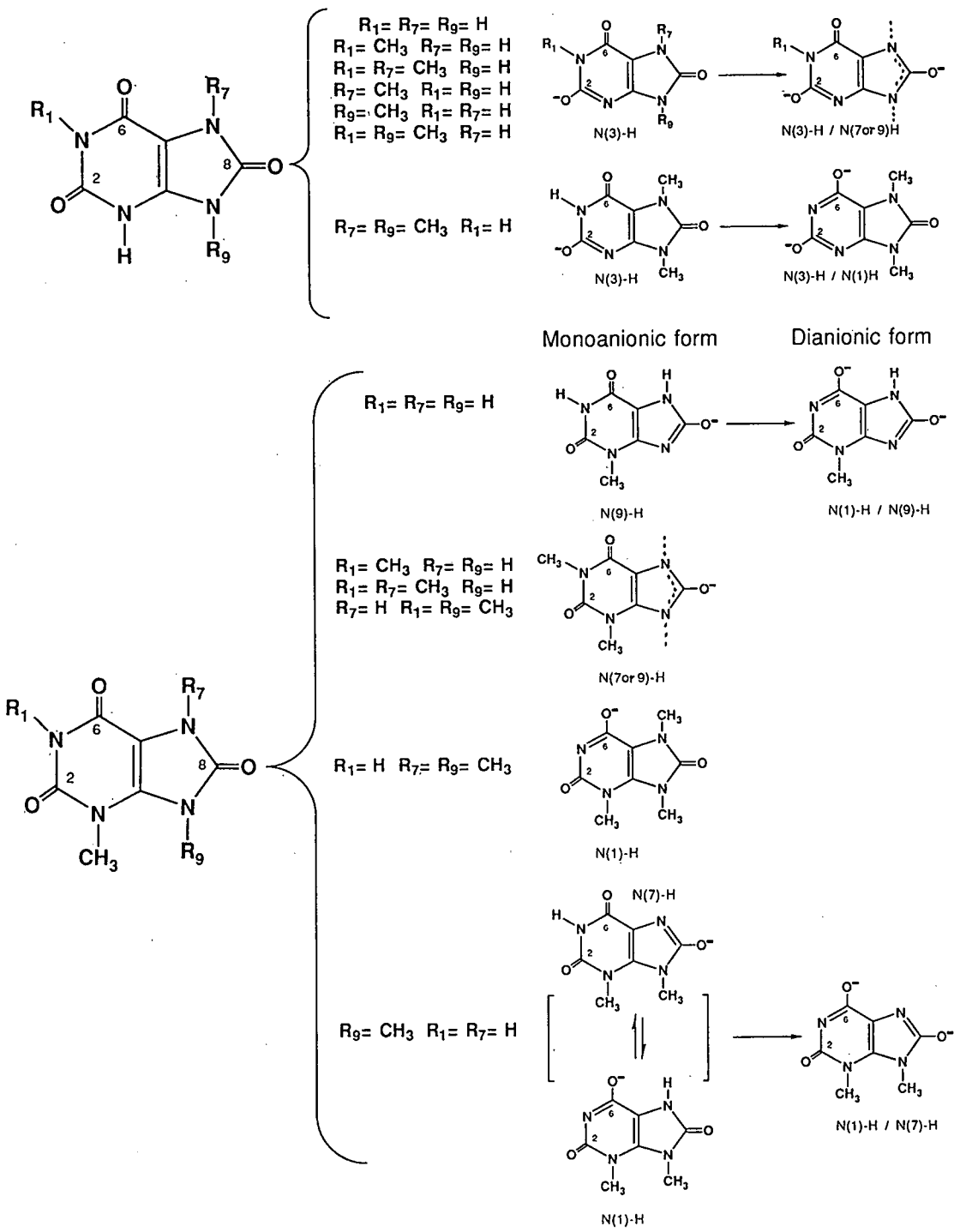

Fig. 7. General structures and anionic forms of mono- and dimethyluric acid derivatives.

tion) and in differences in cyclic anisotropy: a methyl substitution on N(7) of the xanthine derivatives ensures an increase in charge on C(8), which is greater than that resulting from methylation on N(3) or N(1) [N(3)-CH_3 > N(1)-CH_3 effect) [47,48].

The chromatographic behaviour of dimethylxanthines is similar to that of monomethylxanthines (decrease in k' values for $n = 12$) (Fig. 5a), with a more pronounced and hydrophobic character for 1,7-DMX and 1,3-DMX.

Dimethyluric derivatives with $pK_a > 6$ [those with a substitution on N(3) such as 3,7-DMU and 1,3-DMU] show k' variations that are similar to those of xanthine derivatives, thus confirming their low polar character under the experimental conditions (Fig. 5a and b).

The most acidic dimethyluric derivatives [with substitution on the N(9) or N(7) position, such as 1,9-DMU and 1,7-DMU (Fig. 5b], have an intermediate behaviour without any significant change in k' values until $n = 10$, then a fall for $n = 12$ and a constant value for $n > 12$.

REFERENCES

1 J. S. Kiel, S. L. Morgan and R. K. Abramson, *J. Chromatogr.*, 320 (1985) 313.
2 S. H. Hansen, P. Helboe and M. Thomsen, *J. Chromatogr.*, 544 (1991) 53.
3 J. H. Knox and J. Jurand, *J. Chromatogr.*, 149 (1978) 297.
4 A. Sokolowski and K. G. Wahlund, *J. Chromatogr.*, 189 (1980) 299.
5 R. M. Smith, T. G. Hurdley, R. Gill and A. C. Moffat, *J. Chromatogr.*, 351 (1986) 259.
6 J. L. M. Van de Venne and J. L. H. M. Hendrikx, *J. Chromatogr.*, 167 (1978) 1.
7 B. Dimitrova and O. Budevsky, *J. Chromatogr.*, 409 (1987) 81.
8 Y. V. Tikhonov, A. M. Pimenov, S. A. Uzhevko and R. T. Toguzov, *J. Chromatogr.*, 520 (1990) 419.
9 J. Ståhlberg and I. Hägglund, *Anal. Chem.*, 60 (1988) 1958.
10 M. L. Bieganowska, A. Petruczynik and M. Gadzikowska, *J. Chromatogr.*, 520 (1990) 403.
11 S. H. Hansen and P. Helboe, *J. Chromatogr.*, 285 (1984) 53.
12 V. D. Shatz, O. V. Sahartova and I. Kalvins, *J. Chromatogr.*, 521 (1990) 19.
13 J. Fekete, P. Del Castilho and J. C. Kraak, *J. Chromatogr.*, 204 (1981) 319.
14 E. Naline, B. Flouvat, C. Advenier and M. Pays, *J. Chromatogr.*, 419 (1987) 177.
15 B. A. Bidlingmeyer, *J. Chromatogr. Sci.*, 18 (1980) 525.
16 R. Gloor and E. L. Johnson, *J. Chromatogr. Sci.*, 15 (1977) 413.
17 Cs. Horváth, W. Melander and I. Molnar, *Anal. Chem.*, 49 (1977) 142.
18 Cs. Horváth, W. Melander, I. Molnar and P. Molnar, *Anal. Chem.*, 49 (1977) 2295.
19 J. H. Knox and R. A. Hartwick, *J. Chromatogr.*, 204 (1981) 3.
20 A. Bartha, Gy. Vigh, H. A. H. Billiet and L. de Galan, *Chromatographia*, 20 (1985) 587.
21 H. A. H. Billiet, J. Vuik, J. K. Strasters and L. de Galan, *J. Chromatogr.*, 384 (1987) 153.
22 A. Bartha and J. Ståhlberg, *J. Chromatogr.*, 535 (1990) 181.
23 J. Ståhlberg, *J. Chromatogr.*, 356 (1986) 231.
24 J. Ståhlberg and A. Bartha, *J. Chromatogr.*, 456 (1988) 253.
25 M. E. Del Rey and L. E. Vera-Avila, *J. Liq. Chromatogr.*, 10 (1987) 2911.
26 J. S. Kiel, S. L. Morgan and R. K. Abramson, *J. Chromatogr.*, 320 (1985) 313.
27 R. Gill, S. P. Alexander and A. C. Moffat, *J. Chromatogr.*, 247 (1982) 39.
28 J. F. K. Hubert and R. G. Gerritse, *J. Chromatogr.*, 58 (1971) 137.
29 C. P. Terweij-Groen, S. Heemstra and J. C. Kraak, *J. Chromatogr.*, 161 (1978) 69.
30 S. H. Hansen, P. Helboe, M. Thomsen and U. Lund, *J. Chromatogr.*, 210 (1981) 453.
31 T. Wakamatsu and D. W. Fuerstenau, in W. J. Webber and E. Matijevic (Editors), *Adsorption from Aqueous Solutions (Advances in Chemistry Series*, No. 79), American Chemical Society, Washington, DC, 1968, pp. 161–171.
32 D. A. Haydon and F. H. Taylor, *Philos. Trans. R. Soc. London, Ser. A*, 252 (1960) 225.
33 J. T. Davies and E. K. Rideal, *Interfacial Phenomena*, Academic Press, New York, 1961, Ch. 4.
34 R. S. Deelder and J. H. M. Van den Berg, *J. Chromatogr.*, 218 (1981) 327.
35 A. Bartha, Gy. Vigh and Z. Varga-Puchony, *J. Chromatogr.*, 499 (1990) 423.
36 W. Melander and Cs. Horváth, in M. T. W. Hearn (Editor), *Ion-Pair Chromatography (Chromatographic Science Series*, Vol. 31), Marcel Dekker, New York, 1985, p. 27.
37 J. H. Knox and G. R. Laird, *J. Chromatogr.*, 122 (1976) 17.
38 E. Tomlinson, C. M. Riley and T. M. Jefferies, *J. Chromatogr.*, 173 (1979) 89.
39 Cs. Horváth and W. Melander, *J. Chromatogr. Sci.*, 15 (1977) 393.
40 E. Tomlinson and C. M. Riley, in M. T. W. Hearn (Editor), *Ion-Pair Chromatography (Chromatographic Science Series*, Vol. 31), Marcel Dekker, New York, 1985, pp. 101–111.
41 A. Bartha, Gy. Vigh and J. Ståhlberg, *J. Chromatogr.*, 506 (1990) 85.
42 A. Bartha, Gy. Vigh and J. Ståhlberg, *J. Chromatogr.*, 485 (1989) 403.
43 C. T. Hung and R. B. Taylor, *J. Chromatogr.*, 202 (1980) 333.
44 C. T. Hung and R. B. Taylor, *J. Chromatogr.*, 209 (1981) 175.
45 A. R. Katritzky and J. M. Lagowski, in A. R. Katritzky (Editor), *Physical Methods in Heterocyclic Chemistry*, Vol. 1, Academic Press, New York, 1963, p. 99.
46 W. Pfleiderer, *Justus Liebigs Ann. Chem.*, (1974) 2030.
47 E. Naline, Thèse pour l'Obtention du Grade de Docteur d'Etat es-Sciences Pharmaceutiques, Université de Caen, Caen, 1987.
48 A. P. Mazurek, *J. Chem. Soc.*, (1980) 1293.

Journal of Chromatography, 604 (1992) 213–218
Elsevier Science Publishers B.V., Amsterdam

CHROM. 24 174

Determination of trace amounts of alcohols in sodium alkyl sulphate mixtures using high-performance liquid chromatography and surface tension measurements

G. Czichocki

Max-Planck-Institut für Kolloid- und Grenzflächenforschung, Rudower Chaussee 5, O-1199 Berlin (Germany)

P. Müller

Zentrum für Selektive Organische Synthese, Rudower Chaussee 5, O-1199 Berlin (Germany)

D. Vollhardt

Max-Planck-Institut für Kolloid- und Grenzflächenforschung, Rudower Chaussee 5, O-1199 Berlin (Germany)

M. Krüger

Gesellschaft für Lebensmittelforschung mbH, Landgrafenstrasse 16, W-1000 Berlin 30 (Germany)

(First received November 7th, 1991; revised manuscript received March 10th, 1992)

ABSTRACT

A method was developed for the simultaneous trace analysis of C_8, C_{10} and C_{12} alkanols in sodium alkyl sulphate mixtures. The alkanols determined after derivatization with aromatic isocyanates, RNCO (R = phenyl, 1-naphthyl, 2-anthryl). In the preferred method, microbore high-performance liquid chromatography was applied with acetonitrile–water as eluent after derivatization with 1-naphthyl isocyanate at 333 K using an RP-18 5-μm reversed-phase column. The peaks were monitored at 222 nm.

INTRODUCTION

The contamination of surfactants with highly surface-active impurities is a general problem in the interpretation of measurements in surface and colloid chemistry. Sodium alkyl sulphates (SAS) as commonly used model surfactants frequently contain trace amounts of impurities which change their surface properties fundamentally. In earlier papers we described the kinds of impurities in SAS. It has been demonstrated that long-chain alcohols have the strongest effect on the surface and, therefore, the greatest influence on the adsorption isotherms of SAS because of their high surface activity [1]. The determination of residual alcohols and procedures for their removal are prerequisites for exact surface-chemical investigations.

The conversion of alcohols into urethanes with aromatic isocyanates has been examined for its applicability in high-performance liquid chromatography (HPLC) [2–4]. A method for the determination of trace amounts of dodecanol in sodium dodecyl sulphate has been reported [5].

In this paper, results of the derivatization proce-

Correspondence to: Dr. Gunther Czichocki, Max-Planck-Institut für Kolloid- und Grenzflächenforschung, Rudower Chaussee 5, O-1199 Berlin, Germany.

0021-9673/92/$05.00

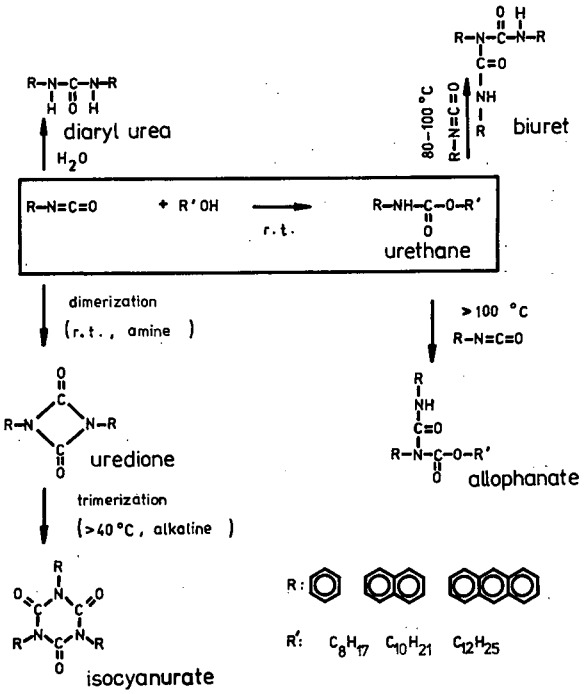

Fig. 1. Derivatization reaction of alcohols with aromatic isocyanates.

dure for phenyl-, 1-naphthyl- and 2-anthrylurethanes are presented. For the simultaneous determination of alcohols in SAS mixtures an improved sensitivity of urethane detection was ascertained by comparing the detection limits of appropriate derivatives using UV detection. In addition, for comparison purposes the influence of alcohols on the surface properties of SAS was studied using surface-tension measurements.

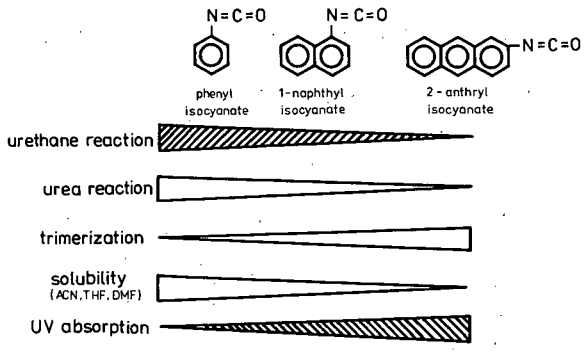

Fig. 2. Effect of coefficients of the derivatization reaction.

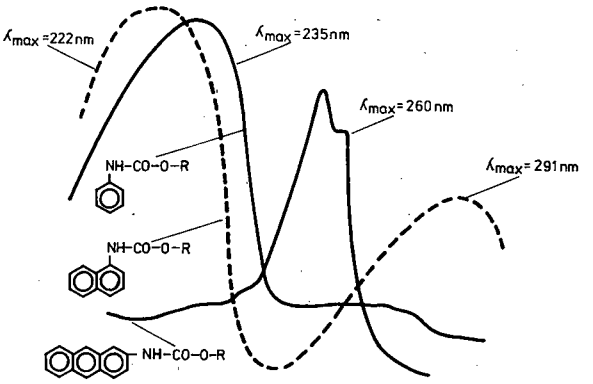

Fig. 3. UV spectra of dodecyl-phenyl-, -naphtyl- and -anthryl-urethane in acetonitrile.

EXPERIMENTAL

HPLC method

The determination of alkanols in SAS was carried out at trace levels (alkanol content 10^{-1}–10^{-3} mol%). For the derivatization of long-chain alcohols with aromatic isocyanates it is important that, on the one hand, the derivatization reaction meets all requirements (fast reaction, complete reaction, relatively few by-products) and, on the other, the detection limit of the derivative is as high as possible. The reaction conditions must be exactly controlled because of various reaction possibilities of isocyanates with alcohols and with themselves (Fig. 1).

The reaction rate of urethane formation decreases from phenyl to anthryl isocyanate and the UV absorption increases in the same direction, which means the sensitivity becomes higher (Fig. 2). From the reaction scheme it also appears that the reaction should be carried out at low temperature and with a short reaction time.

Fig. 3 shows the main maxima for the three urethanes of alkyl chain length C_{12}. The sensitivity limit is shifted depending on the wavelength of UV detection. Considering all these factors (Figs. 1–3), the derivatization reaction for the trace determination of alcohols in SAS was performed with 1-naphthyl isocyanate at room temperature for 30 min and the absorbance was monitored at 222 nm. This method yields excellent results within the derivatizations described. The molar ratio of 1-naphthyl isocyanate to alcohol amounts to 300:1–30 000:1 for 0.1–0.001% alcohol in the SAS, respectively.

Surface tension measurements

Surface tension was measured with an improved ring method as described elsewhere [1]. Special purity of the main component is required in order to characterize trace amounts of highly surface-active alcohols in SAS.

Apparatus

Investigations were carried out on a Hewlett-Packard HP 1090 M liquid chromatograph equipped with a diode-array detector and a ChemStation HP 9000, 300 data system. Microbore columns (100 × 2.1 mm I.D.) packed with 5-μm RP-18 made in the laboratory from silica gel Si 100 and 5-μm Hypersil ODS (Merck, Darmstadt, Germany) were used for chromatographic separations. A 2- or 2.5-μl volume of each sample was injected using an automatic sampler.

Reagents

The eluent was acetonitrile–water. The acetonitrile used was suitable for UV spectrophotometry (Schwedt, Germany).

Liquid chromatography

Derivatized samples (2 or 2.5 μl) were injected into the chromatographic system with an automatic sampler system. Chromatographic separations were carried out at 333 K. The flow-rate was 0.35 or 1 ml min^{-1}, respectively, using gradient elution for optimum separation of urethanes from by-products. The column was washed with acetonitrile and equilibrated after each separation. Standards (O-alkylnaphthylurethanes dissolved in dimethylformamide) were injected for calibration prior to each series of measurements.

TABLE I

MOLAR ABSORPTIVITIES, ε, AND CALIBRATION COEFFICIENTS, *A* (AMOUNT/AREA), OF ALKYLNAPHTHYLURETHANES AT 222 nm

Alkyl chain length	ε (l mol^{-1} cm^{-1})	*A* (mg)
C_8	55 359	$5.3 \cdot 10^{-8}$
C_{10}	54 859	$5.9 \cdot 10^{-8}$
C_{12}	47 779	$6.1 \cdot 10^{-8}$

RESULTS AND DISCUSSION

The absorption maximum of alkylnaphthylurethanes in the UV region at 222 nm was preferred for detection in HPLC (using acetonitrile–water) because of its high molar absorptivity (Table I). The maximum at 200 nm is unsuitable because of solvent absorption in this range and the intensity of the maximum at 290 nm is lower than that at 222 nm.

The absorption maximum of alkylnapthylurethanes at 222 nm is slightly shifted by a change in R. Fig. 4 shows the linearity of the calibration graphs over the concentration range employed. The most suitable concentration range of the alcohols for the determination was 0.001–0.1 mg/ml. Optimum conditions for the determination procedure (amount of naphthyl isocyanate, presence of sodium dodecyl sulphate, method of preparation) selected in a pre-

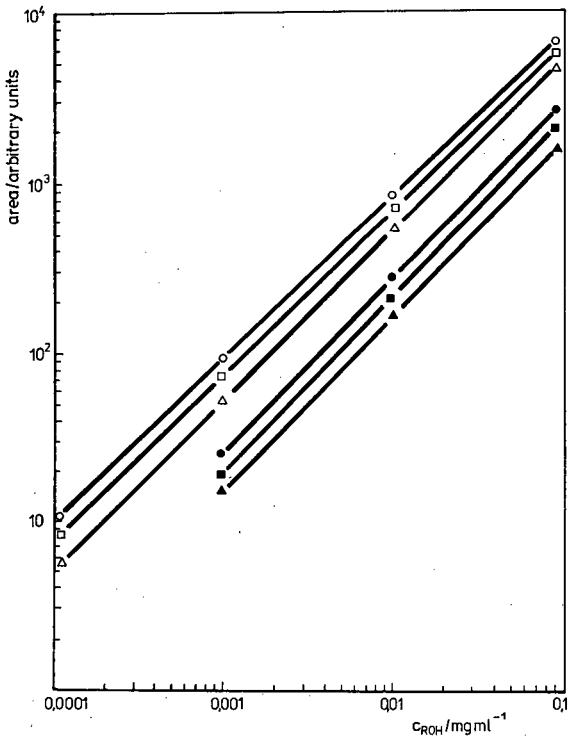

Fig. 4. Calibration with standard urethanes with alkyl chain lengths of (○) C_8, (□) C_{10} and (△) C_{12} and calibration after derivatization in the presence of SAS with alkyl chain lengths of (●) C_8, (■) C_{10} and (▲) C_{12}.

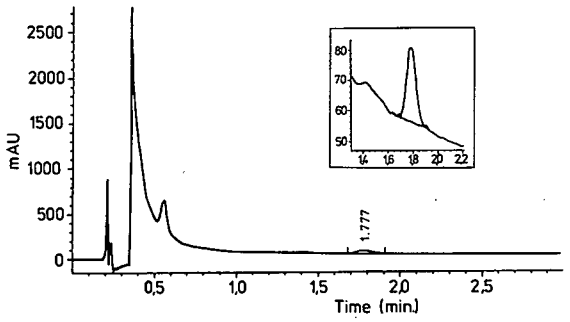

Fig. 5. Chromatogram of dodecylnaphthylurethane from the residual dodecanol (0.01%) in sodium dodecyl sulphate, Column, 5-μm RP-18 (100 × 2.1 mm I.D.). Eluent, A = water, B = acetonitrile; gradient, 0–2.5 min from 78% to 80% B, 2.5–3.75 min from 80% to 100% B, 3.75–6.25 min 100% B, 6.25–6.50 min from 100% to 78% B. Post time, 4.00 min; flow-rate, 1.0 ml min^{-1}; injection volume, 2.5 μl.

vious study [5] were used for calibration and determination. The efficiency of the derivatization process without medium effects was found to be >95% quantitative. The accompanying compounds in the sample caused variations in the adsorption behaviour of the sample solution. Alkylnaphthylurethanes with various carbon numbers in the alkyl chain appear to be adjacent to one another. Good reliability and reproducibility were achieved by using microbore columns and a computer for processing chromatograms. The retention volumes were found to be reproducible.

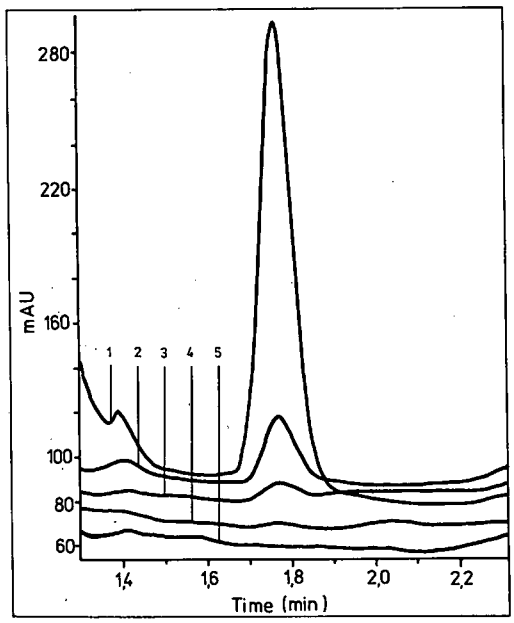

Fig. 6. Integrated peaks of dodecylnaphthylurethanes from dodecanol in sodium dodecyl sulphates of different quality from various producers (1–4) and laboratory-made (5). Column and detection as in Fig. 5. Dodecanol content: 1 = $6.5 \cdot 10^{-2}$; 2 = $1.1 \cdot 10^{-2}$; 3 = $2 \cdot 10^{-3}$; 4 = $1 \cdot 10^{-3}$; 5 = $< 10^{-3}$%.

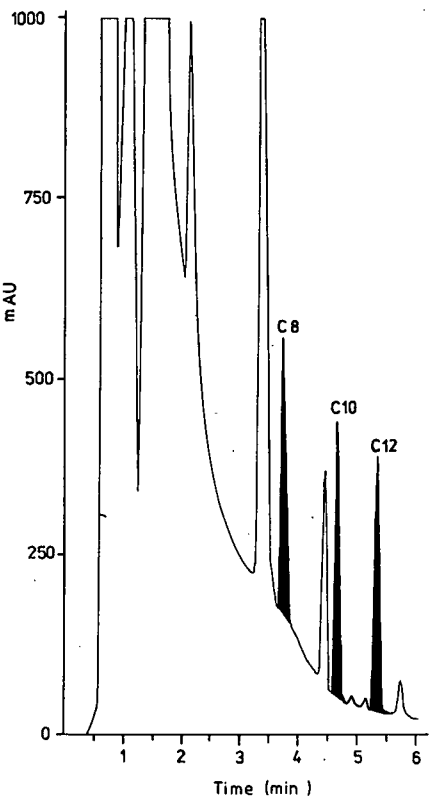

Fig. 7. Separation of alkylnaphthylurethanes of the chain lengths C_8, C_{10} and C_{12} from the mixture of SAS after alcohol derivatization. Column, 5-μm RP-18 (100 × 2.1 mm I.D.). Eluent, A = water, B = acetonitrile; gradient, 0–1 min 55% B, 1–4.5 min from 66% to 100% B, 4.5–5 min, 100% B, 5–6 min, from 100% to 66%. Post time, 2.75 min; flow-rate, 0.35 ml min^{-1}; injection volume, 2.0 μl.

Figs. 5 and 6 show chromatograms and integrated peaks of dodecylnaphthylurethane from residual alcohol in sodium dodecyl sulphates from various commercial producers as well as a laboratory-made product with different dodecanol contents. The lowest impurity content (dodecanol) was found in the laboratory-made product (Fig. 6, curve 5). Fig. 7 shows a chromatogram for the separation of C_8,

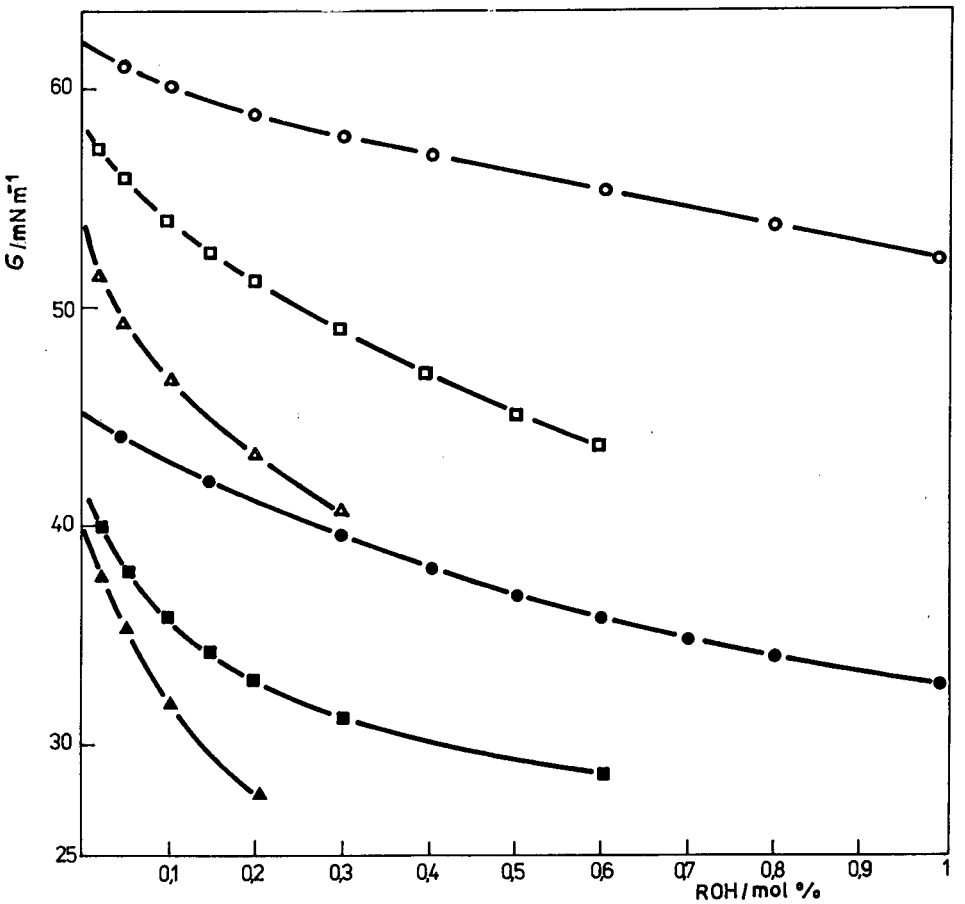

Fig. 8. Depression of the surface tension decreased by alcohols in aqueous solutions of SAS with alkyl chain lengths of C_8, C_{10} and C_{12}. ○ = 0.03, ● = 0.1 *M* sodium octyl sulphate; □ = 0.01, ■ = 0.03 *M* sodium decyl sulphate, △ = 0.003, ▲ = 0.007 *M* sodium dodecyl sulphate.

C_{10} and C_{12} urethanes in a mixture of corresponding SAS.

For comparison, the effect of defined amounts of alcohols on SAS of the same chain length was systematically investigated using surface tension (σ) measurements. The calibration graphs for the alcohol content of sodium octyl, decyl and dodecyl sulphate were measured for selected SAS concentrations near or below the critical micelle concentration. The surface tension changes of an optimally purified SAS solution due to increasing amounts of alcohol of the same alkyl chain length are shown in Fig. 8. In the region between 0.01 and 1 mol% of alcohol the surface tension changes continuously with increasing alcohol ratio, but there is no straight line for σ *vs.* log $c_{alcohol}$ ($\sigma = \sigma_{SAS+alcohol}$) or for σ *vs.* $c_{alcohol}$. Corresponding to the dependence of the surface activity on the alkyl chain length, the sensitivity increases with increasing chain length of the alcohol. Note the concentration differences of sodium octyl, decyl and dodecyl sulphate in Fig. 8.

In conclusion an HPLC method has been introduced for the determination of trace amounts of alcohols into surface-active sodium alkyl sulphates. The procedure is based on the conversion of alcohols into urethanes. The sensitivity of the HPLC method is high, the detection limit being about 10^{-3}%. Compared with surface-tension measurements, the main advantage of the HPLC method is its selectivity to alcohols of different chain lengths. Other trace surface-active compounds do not interfere in the determination of alcohols by HPLC. The

sensitivity of the HPLC method increases slightly with decreasing alkyl chain length of the alcohols, whereas that of the surface-tension measurement increases strongly with increasing alkyl chain length. In this connection the two methods are complementary.

REFERENCES

1 G. Czichocki, D. Vollhardt and H. Seibt, *Tenside Detergents*, 18 (1981) 320.
2 B. Björkquist and H. Toivonen, *J. Chromatogr.*, 153 (1978) 265.
3 R. Wintersteiger and G. Wenniger-Weinzierl, *J. Chromatogr.*, 237 (1982) 399.
4 R. Wintersteiger, *J. Liq. Chromatogr.*, 5 (1982) 897.
5 G. Czichocki, H. Much and D. Vollhardt, *J. Chromatogr.*, 280 (1983) 109.

Journal of Chromatography, 604 (1992) 219–224
Elsevier Science Publishers B.V., Amsterdam

CHROM. 24 186

Differential elution from a Sephadex G-15 column of sodium and phosphate ions of sodium phosphate with sodium or potassium phosphate buffer

Toshihiko Okada

First Department of Biochemistry, Kanazawa Medical University, Uchinada, Ishikawa 920-02 (Japan)

Minoru Miyakoshi and Masao Inoue

Central Research Laboratory, Kanazawa Medical University, Uchinada, Ishikawa 920-02 (Japan)

Mayumi Miyanabe, Yasuko Ueno and Yasuko Nakabayashi

Central Clinical Laboratory, Kanazawa Medical University Hospital, Uchinada, Ishikawa 920-02 (Japan)

(First received July 8th, 1991; revised manuscript received March 10th, 1992)

ABSTRACT

When a sample solution containing sodium-22-labelled sodium chloride and carrier-free phosphorus-32-labelled phosphoric acid was eluted from a Sephadex G-15 column with either 0.025 *M* sodium or potassium phosphate buffer (pH 7.0), the labelled phosphate ion was eluted earlier than the sodium-22. The presence of cold 0.72 *M* sodium chloride with the sodium-22-labelled sodium chloride in the sample did not affect the elution sequence. When 1 *M* monosodium phosphate was eluted with distilled water from fresh and phosphate-treated Sephadex columns, the sodium and phosphate ions were eluted together in approximately the same fractions in both instances. From these observations, it is concluded that sodium ion repeatedly exchanges its partner phosphate ion with that in the eluent during its elution from Sephadex.

INTRODUCTION

When inorganic compounds are eluted from Sephadex, they sometimes do not obey the rule of steric exclusion but are affected by various side-effects (such as solute–gel matrix interactions and solute–solute interactions) which alter the elution volumes predicted from the sizes of the hydrated ions [1].

In previous work [2], we studied the elution of sodium or potassium chloride from a Sephadex G-15 column with 0.025 *M* sodium or potassium phosphate buffer (pH 7.0). The elution profile of the ions showed that the sample cation was accompanied by the phosphate ion from the eluent and was eluted in early fractions, whereas the chloride ion from the sample was accompanied by the cation of the eluent and was eluted in late fractions.

The following mechanism for the ion-exchange reaction was assumed: the phosphate ion from the eluent was eluted more rapidly than the chloride ion from the sample, so a cation-exchange reaction occurred between the sample and the eluent until all the cations of the ion pair from the sample had been replaced by cations from the eluent. The cation (from the sample)–phosphate ion pair thus formed

Correspondence to: Dr. T. Okada, First Department of Biochemistry, Kanazawa Medical University, Uchinada, Ishikawa 920-02, Japan.

0021-9673/92/$05.00

was eluted earlier than the cation (from the eluent)–chloride ion pair.

In this study, we examined whether the cation and phosphate ion of the cation (from the sample)–phosphate ion pair were eluted together or separated during the elution. For this, a mixture of sodium-22-labelled sodium chloride and phosphorus-32-labelled phosphoric acid in sodium or potassium phosphate buffer was eluted with the same buffer and the elution profiles of the sodium-22 and phosphorus-32 were examined.

EXPERIMENTAL

Chemicals

Sodium chloride (NaCl), monosodium phosphate ($NaH_2PO_4 \cdot 2H_2O$), disodium phosphate ($Na_2HPO_4 \cdot 12H_2O$), monopotassium phosphate (KH_2PO_4) and dipotassium phosphate (K_2HPO_4) were of analytical-reagent grade from Wako (Osaka, Japan). Blue dextran 2000, a product of Pharmacia (Uppsala, Sweden), was purchased from Seikagaku Kogyo (Tokyo, Osaka, Japan). Sodium-22-labelled sodium chloride ($^{22}NaCl$, 61.60 mCi/mg, 99% pure) was obtained from New England Nuclear (Boston, MA, USA). Carrier-free phosphorus-32-labelled phosphoric acid in 0.08 *M* hydrochloric acid solution ($H_3{}^{32}PO_4$), produced by the Japan Atomic Energy Research Institute, was obtained from Japan Radioisotope Association (Tokyo, Japan).

Eluents and samples

The eluents were 0.025 *M* sodium and potassium phosphate buffers (pH 7.0) and distilled water.

The sample salts were 0.03 μCi of $^{22}NaCl$ and 0.03 μCi of $H_3{}^{32}PO_4$ dissolved in 0.6 ml of phosphate buffer, the eluent. In some experiments, the sample was added to cold 0.72 *M* NaCl solution. Monosodium phosphate solution (1 *M*) was also used.

Procedure

Sephadex G-15 (Pharmacia) (dry particle diameter 40–120 μm) was packed according to a standard procedure in a glass column (Excel type SE-1000, 1 m × 19 mm I.D.; bed height 90 cm, porous polystyrene support). A peristaltic pump (LKB) (gear ratio 3:250) was connected between the eluent reservoir and the top of the column to maintain a constant flow-rate (12 ml/h).

Previous experiments [3] showed that phosphate ion (P^-) was bound on the gel tightly and did not exchange with the P^- in the eluent under the conditions used in these experiments. Therefore, to prevent adsorption of the phosphorus-32-labelled phosphate ion ($^{32}P^-$) on the gel, we pre-equilibrated the gel with phosphate buffer (the eluent) and dissolved carrier-free $H_3{}^{32}PO_4$ (the sample salt) in the eluent.

A sample of 0.6 ml of solution was applied to the top of the column. The eluate was collected in 10-min fractions with an LKB 7000 Ultrorac fraction collector. All columns were operated at 4°C.

Two sample–eluent systems, $^{22}NaCl \cdot H_3{}^{32}PO_4$–sodium phosphate buffer and $^{22}NaCl \cdot H_3{}^{32}PO_4$–potassium phosphate buffer, were employed. In each system, the sample in 0.72 *M* NaCl was also used. In one experiment, 1 *M* monosodium phosphate was eluted with distilled water.

Determination of ions

The amounts of sodium ion (Na^+) and potassium ion (K^+) were determined with a Corning Model 480 flame photometer (Corning Medical, Sudbury, UK) and chloride ion (Cl^-) was measured in a Corning Model 925 chloride analyser. Phosphate ion (P^-) was determined by the method of Fiske and Subbarow [4]. Sodium-22 ($^{22}Na^+$) was counted in a Model JDC-751 Auto well gamma system (Aloka, Tokyo, Japan), and phosphorus-32-labelled phosphate ion ($^{32}P^-$) in a Model LSC-900 liquid scintillation counter (Aloka). The Auto well gamma system counts $^{32}P^-$ about 1.2% as efficiently as the liquid scintillation counter, and the liquid scintillation counter counts $^{22}Na^+$ about 5% as efficiently as the Auto well gamma system. Hence the small $^{32}P^-$ peak appearing within the $^{22}Na^+$ fractions might actually result from counting $^{22}Na^+$ by liquid scintillation.

RESULTS

Elution with sodium phosphate buffer

When a sample containing $^{22}NaCl$ and $H_3{}^{32}PO_4$ was eluted with sodium phosphate buffer ($^{22}NaCl \cdot H_3{}^{32}PO_4$–sodium phosphate buffer system), the elution profiles showed that the peak fraction of the

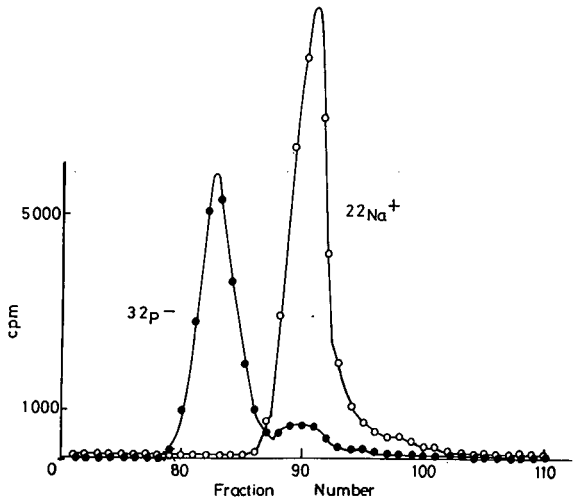

Fig. 1. Elution profiles of $^{22}Na^+$ and $^{32}P^-$ from a sample solution of $^{22}NaCl$ and $H_3{}^{32}PO_4$. Eluent: sodium phosphate buffer.

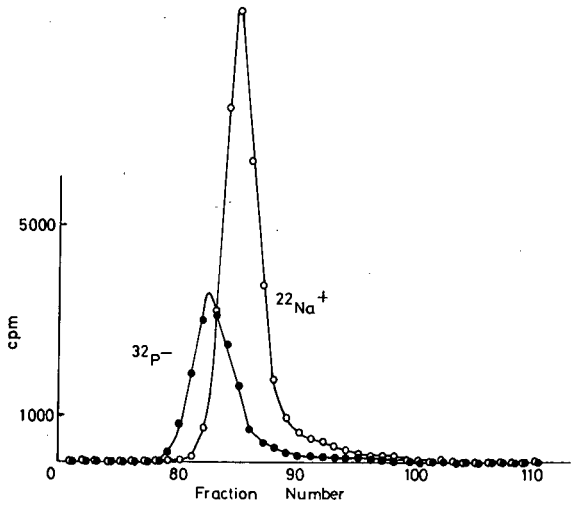

Fig. 3. Elution profiles of $^{22}Na^+$ and $^{32}P^-$ from the same sample as in Fig. 1 eluted with potassium phosphate buffer.

$^{32}P^-$ was No. 83 or seven fractions earlier than that of $^{22}Na^+$ (Fig. 1). The small $^{32}P^-$ peak within the $^{22}Na^+$ fractions may not have been due to $^{32}P^-$ but to $^{22}Na^+$ counted in the liquid scintillation counter, as described under Experimental.

When the same sample in 0.72 *M* NaCl was eluted with sodium phosphate buffer, the $^{22}Na^+$ spread because of the high concentration of cold NaCl. The peak fraction of the $^{32}P^-$ was No. 80, which was ten fractions earlier than that of $^{22}Na^+$ (Fig. 2).

Elution with potassium phosphate buffer

When a sample containing $^{22}NaCl$ and $H_3{}^{32}PO_4$ was eluted with potassium phosphate buffer ($^{22}NaCl \cdot H_3{}^{32}PO_4$–potassium phosphate buffer system), the elution profiles showed that the peak fraction of the $^{32}P^-$ was No. 83, or two fractions earlier than that of $^{22}Na^+$ (Fig. 3).

When the same sample in 0.72 *M* NaCl was eluted with potassium phosphate buffer, the $^{22}Na^+$ spread. Again the peak fraction of the $^{32}P^-$ was No. 83, which was earlier than that of $^{22}Na^+$ (Fig. 4).

Elution with distilled water

First, 1 *M* monosodium phosphate was eluted with distilled water from a fresh Sephadex G-15 column, and then from a phosphate-treated column, to

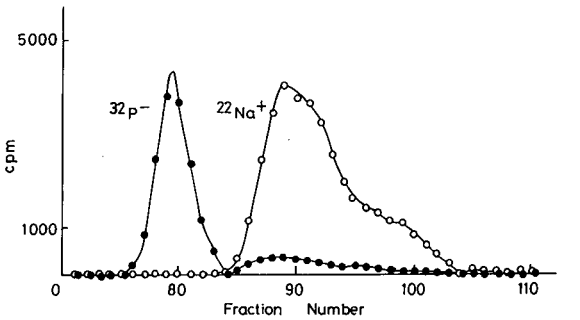

Fig. 2. Elution profiles of $^{22}Na^+$ and $^{32}P^-$ from the same sample as in Fig. 1 but in cold 0.72 *M* NaCl. Eluent: sodium phosphate buffer.

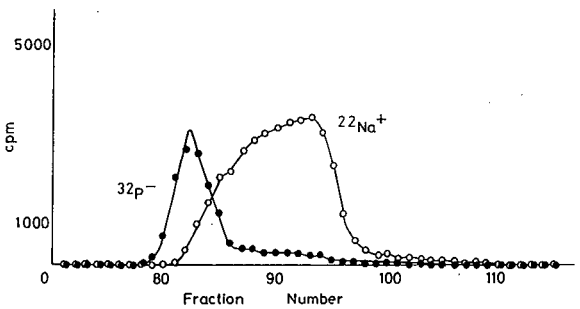

Fig. 4. Elution profiles of $^{22}Na^+$ and $^{32}P^-$ from the same sample as in Fig. 1 but in cold 0.72 *M* NaCl eluted with potassium phosphate buffer.

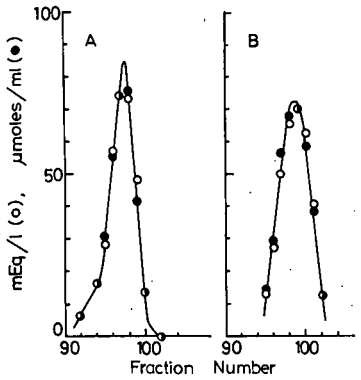

Fig. 5. Elution profiles of Na^+ (○) and P^- (●) from 1 *M* monosodium phosphate solution eluted with distilled water from (A) a fresh Sephadex G-15 column and (B) a phosphate-treated column. mEq = milliequivalent.

determine whether Na^+ and P^- from sodium phosphate in the sample were eluted together or separately. The two ions were eluted together in approximately the same fractions in both instances (Fig. 5).

DISCUSSION

To determine whether the Na^+ and P^- of the Na^+P^- ion pair formed by an ion-exchange reaction [2] are eluted together or separately, we prepared a sample solution containing $^{22}NaCl$ and $H_3{}^{32}PO_4$ in 0.025 *M* sodium (or potassium) phosphate buffer. We assumed that because of the much lower concentrations of $^{22}Na^+$ and $^{32}P^-$ than those of Na^+ (or K^+) and P^- of sodium (or potassium) phosphate in the sample, the $^{22}Na^+$ and $^{32}P^-$ would promptly associate with the P^- and Na^+ (or K^+), respectively, to form $^{22}Na^+P^-$ and $Na^+{}^{32}P^-$ (or $K^+{}^{32}P^-$) ion pairs. Saunders and Pecsok [5] also observed similar ion exchange. The $^{22}Na^+Cl^-$ ion pair in the sample, if it existed, would also be subjected to the ion-exchange reaction during elution with 0.025 *M* sodium (or potassium) phosphate buffer, the eluent, to form a $^{22}Na^+P^-$ ion pair. As $^{22}Na^+$ and $^{32}P^-$ are eluted at the same velocity as Na^+ and P^-, respectively, the elution behaviours of $^{22}Na^+$ and $^{32}P^-$ should indicate whether the $^{22}Na^+$ and P^- of the $^{22}Na^+P^-$ ion pair formed are eluted together or not.

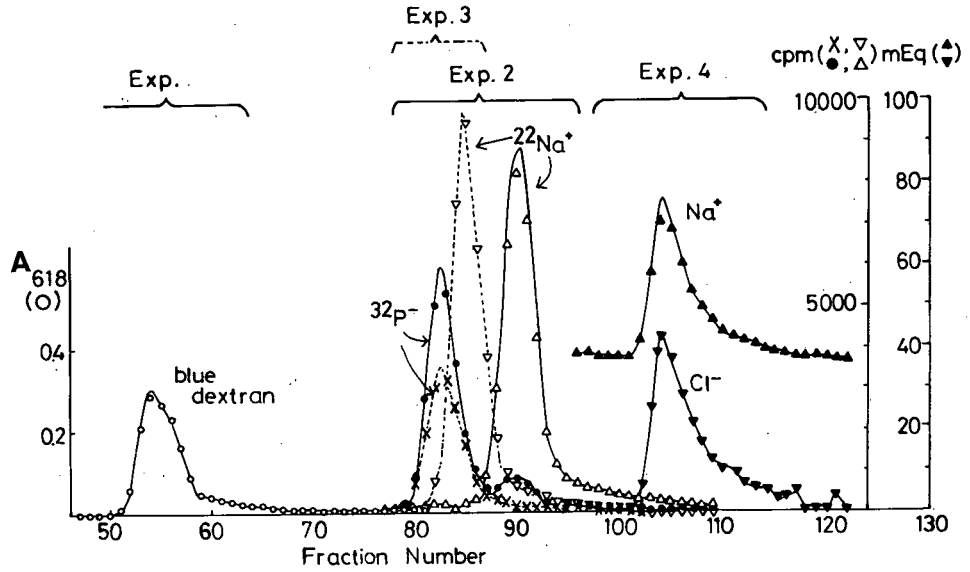

Fig. 6. Elution profiles of blue dextran and ions in four independent experiments. Experiment 1, blue dextran 2000 (10 mg/ml) eluted with sodium phosphate buffer (data not shown); experiment 2, $^{22}Na^+$ and $^{32}P^-$ in the $^{22}NaCl \cdot H_3{}^{32}PO_4$–sodium phosphate buffer system (solid line, from Fig. 1); experiment 3, $^{22}Na^+$ and $^{32}P^-$ in the $^{22}NaCl \cdot H_3{}^{32}PO_4$–potassium phosphate buffer system (dotted line, from Fig. 3); experiment 4, Na^+ and Cl^- of the Na^+Cl^- ion pair formed by the ion-exchange reaction in the NaCl–sodium phosphate buffer system (from ref. 2).

The results obtained showed that $^{22}Na^+$ was eluted more slowly than $^{32}P^-$ (Figs. 1–4), but more rapidly than the Na^+Cl^- ion pair which was formed by the ion-exchange reaction (Fig. 6). A possible explanation of this phenomenon is that the Sephadex which had previously adsorbed P^- behaved as a cation exchanger and the $^{32}P^-$ in the sample is excluded from the gel beads (ion exclusion), whereas the $^{22}Na^+$ was adsorbed (adsorption) and retarded. However, this possibility was unlikely because the amount of P^- adsorbed on the gel was $6.3 \cdot 10^{-12}$ mmol per gram of gel [3] and 2.5 μM phosphate buffer could completely prevent the adsorption of P^- on the gel under the present conditions [3]. Therefore, the amount of adsorbed P^- may be too small to affect the elution behaviour of P^- from 0.025 M phosphate buffer. With Na^+, $3.2 \cdot 10^{-3}$ mmol of Na^+ was adsorbed on 1.0 g of gel [3]. This amount is much more than that of P^- adsorbed on the gel, but is negligible compared with the high concentration of Na^+ in the buffer. Therefore, the retardation of $^{22}Na^+$ may not be due to its adsorption on the gel.

We performed additional experiments in which 1 M monosodium phosphate was eluted with distilled water from fresh and phosphate-treated gel to ascertain whether the Na^+ and P^- from the monosodium phosphate in the sample are eluted together or separately. If P^- is excluded from the gel and Na^+ is adsorbed, P^- and Na^+ should be eluted separately. However, the results showed that they were eluted together in approximately the same fractions from both fresh and phosphate-treated columns (Fig. 5). Therefore, ion exclusion and adsorption, if they occurred, did not affect the elution behaviour of the bulk of the Na^+ and P^- in the sample.

From these observations, we conclude that the differential elutions of $^{22}Na^+$ and $^{32}P^-$ in the sample were not due to ion exclusion of the P^- from and adsorption of Na^+ on the gel, but to exchange of Na^+ with the partner P^- in the eluent. In other words, acceptor P^- in the eluent is essential for exchange of the partner of Na^+, and Na^+ is pulled down by the P^-, released gradually from the P^- and bound to other P^- flowing through later (Fig. 7). This change of partners occurs repeatedly during the passage through the column. Na^+ or K^+ is separated from P^- in the column owing to their differences in penetrability into the gel particles, resulting in weakening of the cation–anion bond. Hence not only the different elution velocities of the different ions in the column, but also the separation of the different ions by the Sephadex network may be involved in changing partners. The phenomenon of ion exchange also supports the changing-partner hypothesis, because if the binding of Na^+ to P^- in the Na^+P^- ion pair is tight, there will be no exchange of ions between the sample and the eluent.

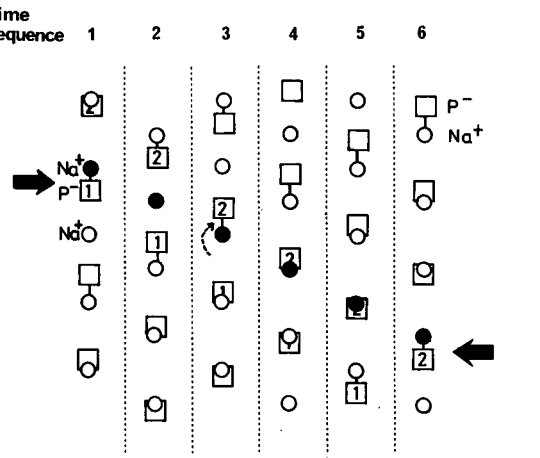

Fig. 7. Hypothetical scheme of the mechanism of changing partners. The sample was a solution containing sodium chloride labelled with ^{22}Na ($^{22}NaCl$) and phosphoric acid labelled with ^{32}P ($H_3{}^{32}PO_4$) in 0.025 M sodium phosphate buffer (the eluent). The $^{22}Na^+$ and $^{32}P^-$ promptly associated with P^- and Na^+ from the buffer to form $^{22}Na^+P^-$ and $Na^+{}^{32}P^-$ ion pairs, respectively, because the concentrations of $^{22}Na^+$ and $^{32}P^-$ were much lower than those of Na^+ and P^- in the buffer. When the sample was eluted with sodium phosphate buffer ($^{22}NaCl \cdot H_3{}^{32}PO_4$–sodium phosphate buffer system), $^{22}Na^+$ was eluted more slowly than $^{32}P^-$ but more rapidly than Na^+ of the Na^+Cl^- ion pair, which was formed by the ion-exchange reaction. As $^{22}Na^+$ and $^{32}P^-$ are eluted at the same velocity as Na^+ and P^-, respectively, the result indicates that Na^+ from the sample is gradually released from the partner P^- and binds to other P^- in later eluent. The figure shows one cycle of changing partners. The time sequence of elution is from left to right (1–6). Na^+ of the Na^+(●) P^-(1) ion pair is gradually released from P^-(1) and associates with P^-(2) which comes later to form the Na^+(●)P^-(2) ion pair. The Na^+ in the eluent (○) also changes partners by the same mechanism.

Our results also showed that $^{22}Na^+$ was less separated from $^{32}P^-$ when eluted with potassium phosphate buffer (Fig. 3) than when eluted with sodium phosphate buffer (Fig. 1). As potassium phosphates are more soluble than Na_2HPO_4 in distilled water, the phenomenon is independent of the solu-

bility of the phosphates in the eluent, but might be due to the higher electronegativity of K^+ than Na^+, resulting in stronger binding of K^+ than of Na^+, and a lower efficiency of changing partners of $^{22}Na^+$ in the potassium phosphate buffer than in sodium phosphate buffer.

ACKNOWLEDGEMENTS

The authors are indebted to Professor Tsutomu Ohashi of Kanazawa Medical University for valuable discussions. They thank Miss Naoko Kawara for her help in preparing the manuscript.

REFERENCES

1 N. Yoza, *J. Chromatogr.*, 86 (1973) 325.
2 T. Okada, Y. Nakabayashi, K. Teraoka, M. Miyakoshi and M. Inoue, *J. Chromatogr.*, 481 (1989) 299.
3 T. Okada, M. Miyakoshi and M. Inoue, *J. Chromatogr.*, 475 (1989) 412.
4 C. H. Fiske and Y. Subbarow, *J. Biol. Chem.*, 66 (1925) 375.
5 D. Saunders and R. L. Pecsok, *Anal. Chem.*, 40 (1968) 44.

Journal of Chromatography, 604 (1992) 225–232
Elsevier Science Publishers B.V., Amsterdam

CHROM. 24 182

Mixed retention mechanism in gas–liquid chromatography of hydrocarbon and dialkyl ether solutes on squalane-coated silica gel

Kunishige Naito, Yuuki Watanabe and Shinsuke Takei

Department of Materials Science, Faculty of Engineering, Ibaraki University, Hitachi, Ibaraki 316 (Japan)

(First received October 30th, 1991; revised manuscript received March 18th, 1992)

ABSTRACT

A mixed retention mechanism in gas–liquid chromatography was studied in order to elucidate the dependence of the retention volume of some hydrocarbons and dialkyl ethers on squalane-coated silica gel on the liquid phase loading. Two adsorption equilibria on the solid surface of silica gel and the surface of a monolayer of squalane dominantly contribute to solute retention until the monolayer of squalane is formed on the silica gel surface. Subsequently, excess of squalane formed a double layer on the deactivated surface of the silica gel, so bulk solution partition concurrently contributes to solute retention together with adsorption equilibria on the monolayer and/or the double layer of squalane. The distribution constants of bulk solution partition and adsorption equilibria on the solid surface of silica gel and the surface of the monolayer of squalane were calculated as reasonable values for any solute.

INTRODUCTION

It is well known that interfacial adsorption equilibria, together with bulk solution partition, contribute to solute retention in gas–liquid chromatography at different rates depending on the nature of the solute, the type of solid support and the polarity of and the loaded amount of liquid stationary phase. In such cases, the retention volume of a given solute, V_R, can be written as a linear combination of contributions of bulk solution partition and interfacial adsorption equilibria taking part in solute retention [1–8]:

$$V_R = K_L V_L + K_A A_L + K_S A_S$$

where K_L, K_A and K_S are distribution constants of solution partition into a bulk liquid layer (volume V_L) and adsorption equilibria on the liquid layer (surface area A_L) and on the solid surface (surface area A_S), respectively. V_R and V_L can be experimentally determined but A_L and A_S cannot be directly measured when the solid support surface is partly covered with the liquid layer. For practical use of the above equation it is therefore necessary to establish a reasonable relationship relating A_L and A_S to the liquid phase loading.

In a previous study using silica gel as a solid support [9], we found that the experimental plot of the reduced retention volume of a given solute, V_{NR}, against the liquid phase loading, X_L, could be divided into two or three parts. The respective parts were fitted with straight lines of different slopes and intercepts. From this result, we proposed a model in which the silica gel surface essentially consisted of two subsurfaces with high and low adsorption capacities and was gradually covered first with a monolayer of the liquid phase and then with a double layer with increasing liquid phase loading. On the basis of this model, the specific surface area of liquid-coated silica gel and the reduced retention volume of a given solute could be written as a linear function of the liquid phase loading in each part. By

Correspondence to: Dr. K. Naito, Department of Materials Science, Faculty of Engineering, Ibaraki University, Hitachi, Ibaraki 316, Japan.

0021-9673/92/$05.00

fitting these relationships to the experimental data, distribution constants could be calculated for adsorption equilibria on the solid surface and the monolayer of the liquid stationary phase, but the distribution constant of bulk solution partition could not be calculated. Because of the large specific surface area of silica gel and the strong polarity of the liquid stationary phase, the effects of interfacial adsorption equilibria dominated over the contribution of bulk solution partition to solute retention.

In this study, silica gel with a smaller specific surface area than that studied previously was used as a solid support for avoiding the dominant effects of interfacial adsorption equilibria on the retention volume of any solute. A non-polar liquid stationary phase, squalane, was used to observe the contribution of bulk solution partition to solute retention. The retention volume of a given solute and the specific surface area of liquid-coated silica gel were determined as a function of the liquid phase loading. The experimental data were analysed and are discussed on the basis of the previous model of the solid support surface and the distribution of the liquid phase on the solid support.

EXPERIMENTAL

Fujigel KC-5, silica gel for preparative column chromatography, was used as a solid support after sizing into a 60–80 mesh fraction. Chromosorb P NAW (60–80 mesh) was used as a reference solid support without further purification. Ten grams of Chromosorb P and silica gel were dried at 120°C for 3 and 12 h, respectively, and weighed accurately. They were suspended in dichloromethane containing the desired amount of squalane. Squalane was deposited on the solid support as evenly as possible by evaporating the solvent with occasional stirring. After drying under vacuum at 50°C for 3 h for removal of any volatile component, the material was packed into a stainless-steel tube (100 × 0.3 cm I.D.) with tapping. The newly packed column was conditioned at 120°C for 15 h in a stream of nitrogen (flow-rate 40 cm^3 min^{-1}) and then for 3 h in a stream of helium (flow-rate 40 cm^3 min^{-1}) before use.

A Hitachi Model 263-30 gas chromatograph equipped with a thermal conductivity detector was used in conjunction with a Hitachi Model 561 recorder. Chromatographic measurements were made at a column temperature of 120°C using helium as the carrier gas at a flow-rate of 40 cm^3 min^{-1}. The retention volume of a given solute was measured from the air peak to the particular peak maximum and corrected for the vapour pressure of water in a flow meter and the pressure drop in the column. The specific surface area of the column packings was determined by the BET nitrogen adsorption method at liquid nitrogen temperature. To account for any variations of the retention data with different amounts of the column packings used, the reduced retention volume, V_{NR}, was calculated by dividing the net retention volume by the weight of liquid-free solid support packed into the column. The liquid phase loading, X_L, was taken as the

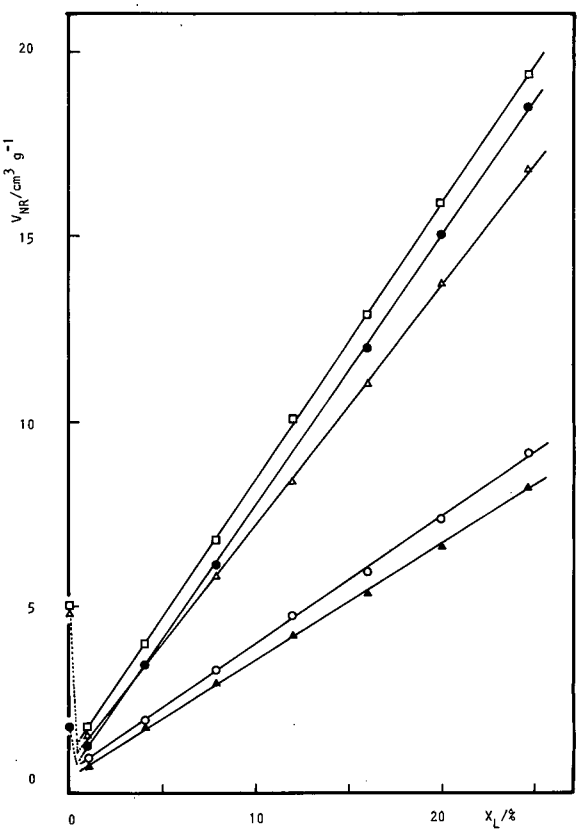

Fig. 1. Dependence of reduced retention volume on liquid phase loading on squalane-coated Chromosorb P. Solutes: ▲ = 1-hexene; ○ = *n*-hexane; △ = 1-heptene; ● = *n*-heptane; □ = 2-heptene.

weight ratio of the liquid stationary phase to the solid support.

RESULTS AND DISCUSSION

When Chromosorb P was coated with different amounts of squalane, the reduced retention volume of any solute increased linearly with increasing liquid phase loading. Fig. 1 shows such linear plots of V_{NR} *vs.* X_L for some hydrocarbon solutes. The small, positive intercepts of these graphs on the ordinate suggest less importance of concurrent contributions of interfacial adsorption equilibria to solute retention in this instance. Thus, the slope of the V_{NR} *vs.* X_L graph is regarded as the distribution constant of the bulk solution partition, K'_L, for each solute.

Table I summarizes the K'_L values calculated from the experimental data. The K'_L values show that all the solutes except *tert.*-butyl methyl ether are readily soluble in the bulk liquid layer of squalane under the present conditions. The K'_L values of alkenes are very close to those of alkanes with the same carbon number and similar molecular shape, suggesting very similar solubilities of these compounds in squalane. The V_{NR} *vs.* X_L graphs of dialkyl ethers and aromatic hydrocarbons gave larger intercepts on the ordinate than those of aliphatic hydrocarbons. Taking their large K'_L values into account, possible interfacial adsorption in this instance is considered to occur at the liquid–solid interface but not at the gas–liquid interface. Only one straight line was fitted to the experimental data except for a zero liquid phase loading for each solute. This indicates that a bulk liquid layer of squalane is formed on the surface of the Chromosorb P support even at low liquid phase loadings.

When silica gel was coated with squalane, the reduced retention volume of alkanes and cyclohexene increased monotonically. V_{NR} of aromatic hydrocarbons and alkenes except cyclohexene first decreased and then increased with increasing liquid phase loading. The profiles of these curves are different from those of the corresponding graphs ob-

TABLE I

DISTRIBUTION CONSTANTS OF BULK SOLUTION PARTITION, K'_L, and K'_{exp}

Solute	K'_L ($cm^3\ g^{-1}$)	K'_{exp} ($cm^3\ g^{-1}$)
2-Methylpentane	28	31
n-Hexane	36	37
Cyclohexane	62	66
1-Hexene	31	28
2-Hexene	35	29
Cyclohexene	66	76
2-Methylhexane	73	74
n-Heptane	73	81
1-Heptene	65	65
2-Heptene	74	68
Benzene	51	56
Toluene	108	106
Ethylbenzene	205	205
Diethyl ether	34	−169
tert.-Butyl methyl ether	8.3	−460
Di-*n*-propyl ether	183	−873
Diisopropyl ether	51	−492
Methyl *n*-propyl ether	48	−174
Ethyl *n*-propyl ether	75	−508

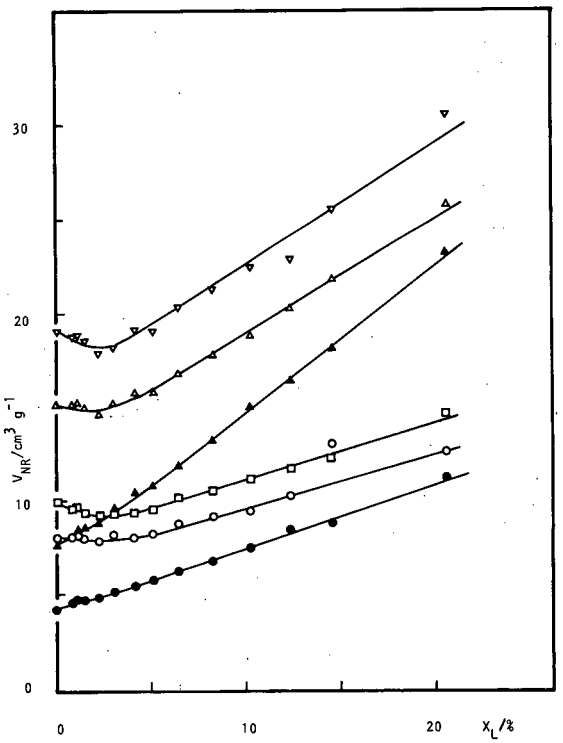

Fig. 2. Dependence of reduced retention volume on liquid phase loading on squalane-coated silica gel. Solutes: ● = *n*-hexane; ○ = 1-hexene; □ = 2-hexene; ▲ = *n*-heptane; △ = 1-heptene; ▽ = 2-heptene.

tained previously using modified alumina as a solid support [10]. In Fig. 2, the V_{NR} *vs.* X_L curve for any hydrocarbon solute shows no sudden decrease at low liquid phase loadings. It appears that the silica gel surface is less adsorptive than the modified alumina surface towards hydrocarbon solute molecules. An increase in V_{NR} with increasing X_L indicates that the non-polar surface of the thin film of squalane can interact more strongly than the polar surface of silica gel with hydrocarbon solute molecules. The reduced retention volumes of alkenes are always larger than those of the corresponding alkanes, although their K'_L values are very similar. The difference in the V_{NR} values of these compounds gradually decreases with increasing X_L. This result indicates that, with increasing X_L, interfacial adsorption equilibria become less significant and bulk solution partition becomes more important with respect to solute retention. Even at high liquid phase loadings, the apparent effects of interfacial adsorption equilibria remain in V_{NR} because of the considerable difference in the V_{NR} values of the solutes.

Fig. 3 shows plots of V_{NR} *vs.* X_L for some dialkyl ethers. Their reduced retention volumes decrease with increasing X_L. The profiles of these graphs are similar to those for the experimental data measured on the modified alumina coated with polar stationary liquid phases [11,12]. This suggests that dialkyl ether molecules may interact more strongly with the polar surface of silica gel than with the non-polar surface of the thin layer of squalane. The decrease in V_{NR} of each dialkyl ether with increasing X_L is probably due to deactivation of the silica gel surface

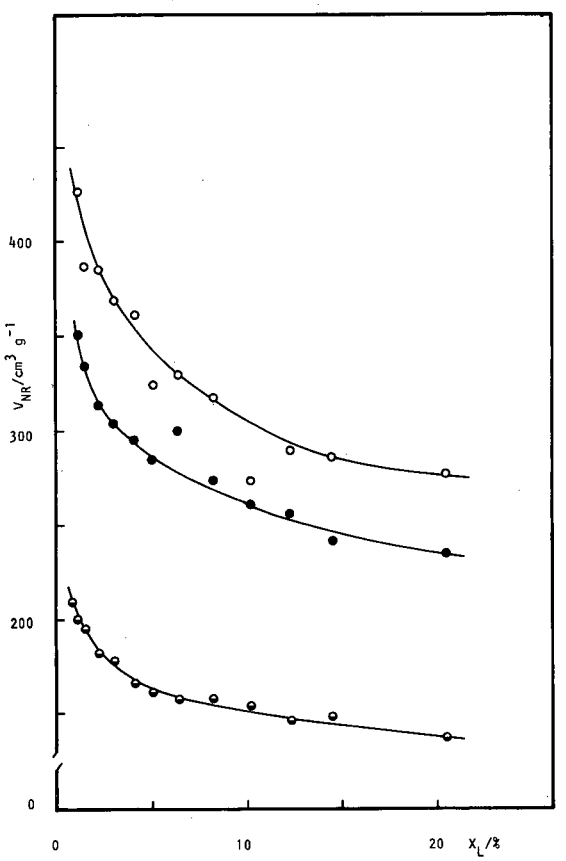

Fig. 3. Dependence of reduced retention volume on liquid phase loading on squalane-coated silica gel. Solutes: ◒ = diethyl ether; ● = ethyl *n*-propyl ether; ○ = diisopropyl ether.

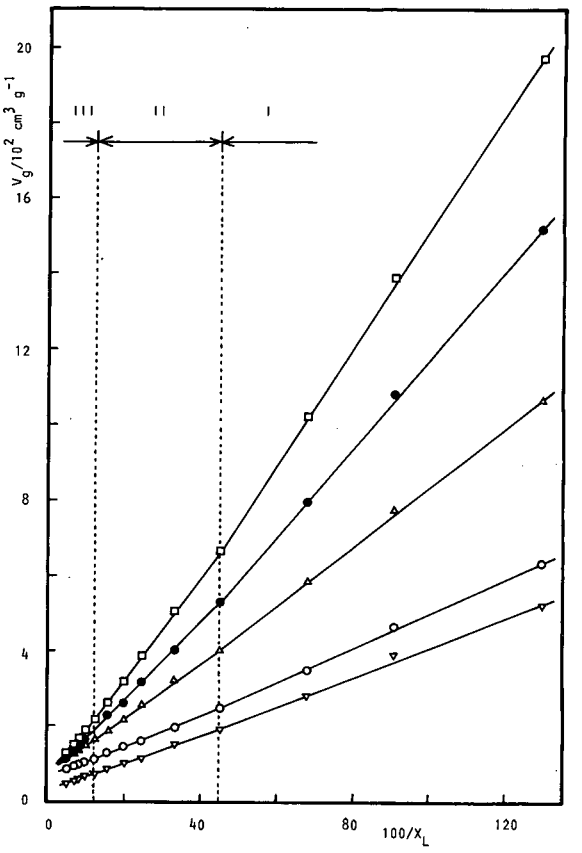

Fig. 4. V_g *vs.* $1/X_L$ plot. Solutes: ▽ = 2-methylpentane; ○ = cyclohexane; △ = *n*-heptane; ● = cyclohexene; □ = 1-heptene. I = region 1; II = region 2; III = region 3.

caused by gradual coverage with some types of liquid layers of squalane. In this instance interfacial adsorption equilibria may play an important role in solute retention.

As shown in Fig. 4, the V_g *vs.* $1/X_L$ curves are divided into three linear parts. Two liquid phase loadings, X_{L1} and X_{L0}, were calculated as 2.23 and 8.27%, respectively, at the intersection of two adjacent straight lines regardless of the nature of the solutes. The occupied area of a squalane molecule (0.99 nm^2), calculated from the X_{L0} value and the specific surface area of liquid-free silica gel, is consistent with the cross-sectional area of the same molecule (0.99 nm^2), calculated from density and molecular weight of squalane according to Emmett and Brunauer's equation [13]. Thus, we regarded X_{L0} as the liquid phase loading at which the silica gel surface was completely covered with a monolayer of squalane. This supports the idea that the silica gel surface is first covered with a monolayer of squalane when the squalane is loaded on silica gel.

The specific surface area of the liquid-coated silica gel, S_P, decreased linearly, at first rapidly with increasing X_L up to about 8% and then slowly with further increase in X_L. The S_P *vs.* X_L curve can be approximated by two straight lines which intersect near X_{L0}. This result shows that the decrease in S_P is proportional to X_L or $X_L - X_{L0}$. The V_{NR} *vs.* X_L curve for hydrocarbons hardly reflected this change in S_P with X_L. Althought the V_{NR} *vs.* X_L curve for ethers showed a decreasing trend similar to that of the S_P *vs.* X_L curve, V_{NR} of ethers was not always proportional to S_P. These results indicate that the surface of the liquid-coated silica gel involves some types of subsurfaces at different ratios depending on X_L. We then examined the quantitative interpretation of the experimental X_L dependence of V_{NR} and S_P by considering a model for the solid surface of silica gel and the distribution of the liquid stationary phase on the solid surface.

At liquid phase loadings below X_{L0}, the V_g *vs.* $1/X_L$ curve can be approximated by two straight lines. This means that the original surface of the silica gel shows essentially heterogeneous characteristics on adsorption of solute molecules. We simply considered that the original surface of the silica gel consisted of two subsurfaces with high and low adsorption capacities, as assumed previously [9–12]. As previously, we regarded the subsurface with a high adsorption capacity (subsurface 1) as being occupied first with squalane molecules and then the subsurface with a low adsorption capacity (subsurface 2) was covered. Hence X_{L1} (2.23%) should correspond to the liquid phase loading at which subsurface 1 was completely covered with the monolayer of squalane.

At liquid phase loadings above X_{L0}, one straight line of V_g *vs.* $1/X_L$ was drawn for each solute. For hydrocarbon solutes, the intercepts of these linear graphs are in good agreement with the K'_L values for the corresponding solutes listed in Table I. However, for dialkyl ethers, this linear graph gave a negative intercept on the ordinate, indicating that interfacial adsorption equilibria still contribute significantly to solute retention. According to previous considerations [9,10], a double layer of squalane should be formed on the silica gel surface in this region. We expect that, on the deactivated surface of silica gel, shielded with a monolayer of squalane, a double layer of squalane may possess a loose structure like a bulk liquid, because non-polar molecules of squalane cannot orient to the silica gel surface as strongly as polar molecules. It is likely that such a loose structure will lead to the same sorption properties as those of a bulk liquid layer. Hence we considered that, in this region, the silica gel surface is also covered with the same type of bulk liquid layer of squalane as is formed on a Chromosorb P support.

At liquid phase loadings below X_{L1} (region 1), the monolayer of squalane gradually expands on subsurface 1 of the silica gel surface with increasing X_L. The surface of the liquid-coated silica gel involves an uncoated part of subsurface 1, bare subsurface 2 and the surface of the monolayer of squalane with which subsurface 1 was partly covered. Then, the specific surface area of the liquid-coated silica gel, S_P, can be written as the sum of the surface areas of the above three surfaces:

$$S_P = S_1 - a X_L + S_2 + b X_L$$
$$= S_S^0 - (a - b) X_L$$

where $S_S^0 = S_1 + S_2$, S_S^0, S_1 and S_2 are the specific surface area of the liquid-free silica gel, subsurface 1 and subsurface 2, respectively, and a and b are proportionality constants that relate X_L to the covered area and surface area of the monolayer of squalane. We considered that the monolayer of squalane has

such a rigid structure that solute molecules cannot penetrate or dissolve in the monolayer. In this instance, interfacial adsorption equilibria on these three surfaces take part in solute retention. Hence the reduced retention volume of a given solute can be written as a linear combination of the contributions of these adsorption equilibria:

$$V_{NR} = K_1 (S_1 - a X_L) + K_2 S_2 + K_A b X_L \quad (1)$$

where K_1, K_2 and K_A are distribution constants of adsorption equilibria on subsurface 1, subsurface 2 and the surface of the monolayer of squalane, respectively. Dividing both sides of eqn. 1 by X_L and using the relationship $K_{ad} S_S^0 = K_1 S_1 + K_2 S_2$, the specific retention volume, V_g, can be expressed as

$$V_g = b K_A - a K_1 + K_{ad} S_S^0/X_L \quad (2)$$

where $K_{ad} S_S^0$ is equal to V_{NR} at $X_L = 0$. Eqn. 2 should give a straight line with a positive intercept on the ordinate of the V_g *vs.* $1/X_L$ plot if $b K_A > a K_1$ and with a negative intercept if $b K_A < a K_1$.

In the range of liquid phase loadings between X_{L1} and X_{L0} (region 2), the monolayer of squalane completely covered subsurface 1 and gradually expanded on subsurface 2 with increasing X_L. The specific surface area of the liquid-coated silica gel in this region is the sum of the surface areas of an uncoated part of subsurface 2 and the surface of the monolayer of squalane. S_P can be written as the same linear function of X_L using the same a and b as defined in region 1:

$$S_P = S_S^0 - (a - b) X_L$$

This equation can be fitted to the experimental plot of S_P *vs.* X_L if $a > b$. In this instance, adsorption equilibria on these surfaces take part in solute retention. We considered that the distribution constant of adsorption was the same on the monolayer of squalane formed on subsurface 1 and on subsurface 2. The following equation can be written:

$$V_{NR} = K_2 (S_S^0 - a X_L) + K_A b X_L \quad (3)$$

Dividing both sides of eqn. 3 by X_L, V_g can be expressed as follows:

$$V_g = b K_A - a K_2 + K_2 S_S^0/X_L \quad (4)$$

This equation should plot as a straight line of V_g *vs.* $1/X_L$ with a positive slope. The intercept of this linear graph on the ordinate is positive if $b K_A > a K_2$ and negative if $b K_A < a K_2$. We assumed that $K_1 > K_2$, so it is valid that $b K_A > a K_2$ if $b K_A > a K_1$, but it is not always true that $b K_A < a K_2$ when $b K_A < a K_1$.

At liquid phase loadings above X_{L0} (region 3), the silica gel surface was completely covered with a monolayer of squalane and further partly covered with a double layer of squalane. The surface of the liquid-coated silica gel involves the surface of an uncoated part of the monolayer and the double layer. Hence the specific surface area of the liquid-coated silica gel can be written as

$$\begin{aligned} S_P &= S_{LM} - a' (X_L - X_{L0}) + b' (X_L - X_{L0}) \\ &= S_{LM} + (a' - b') X_{L0} - (a' - b') X_L \end{aligned}$$

where a' and b' are proportionality constants that relate the excess liquid loading to the covered area and the surface area of the double layer of squalane. We simply assumed that the covered area and the surface area of the double layer of squalane were proportional to the excess liquid loading, $X_L - X_{L0}$. Assuming that the double layer of squalane shows the same sorption properties as a bulk liquid layer of squalane, solute molecules can dissolve in the double layer. In this instance, bulk solution partition, together with interfacial adsorption equilibria on the surface of the monolayer and/or the double layer, takes part in solute retention. V_{NR} can be written as

$$\begin{aligned} V_{NR} = {} & K_A [S_L^0 - a' (X_L - X_{L0})] + \\ & + K_S a' (X_L - X_{L0}) + K'_A b' (X_L - X_{L0}) + \\ & + K'_L (X_L - X_{L0}) \end{aligned} \quad (5)$$

where K_S and K'_A are distribution constants of adsorption equilibria on the monolayer through the double layer (at the liquid–solid interface) and the surface of the double layer of squalane (at the gas–liquid interface). Using the relationship $K'_{exp} = K'_L - (a' K_A - b' K'_A) + a' K_S$ and dividing both sides of eqn. 5 by X_L, the following equation can be written:

$$V_g = K'_{exp} + (K_A S_L^0 - K'_{exp} X_{L0})/X_L \quad (6)$$

If $K'_L < a'K_A - b'K'_A - a'K_S$, K'_{exp} will be negative, indicating that adsorption equilibrium on the monolayer surface is important in solute retention. If $K'_L >> a'K_A - b'K'_A - a'K_S$, K'_{exp} will be equal to K'_L, that is, bulk solution partition contributes dominantly to solute retention.

TABLE II

DISTRIBUTION CONSTANTS OF ADSORPTION, K_1, K_2 AND K_A

Solute	K_1 (10^{-5} cm)	K_2 (10^{-5} cm)	K_A (10^{-5} cm)		
			Region 1	Region 2	Region 3
2-Methylpentane	0.39	0.31	0.73	0.72	0.73
n-Hexane	0.45	0.36	0.87	0.86	0.86
Cyclohexane	0.51	0.35	1.15	1.15	1.14
1-Hexene	0.89	0.64	1.16	1.17	1.16
2-Hexene	1.07	0.75	1.33	1.33	1.33
Cyclohexene	1.27	0.91	1.86	1.86	1.92
2-Methylhexane	0.76	0.56	1.46	1.46	1.46
n-Heptane	0.77	0.64	1.60	1.70	1.67
1-Heptene	1.77	1.17	2.23	2.25	2.24
2-Heptene	2.24	1.44	2.70	2.70	2.68
Benzene	2.60	1.65	2.87	2.92	2.92
Toluene	5.88	3.87	6.61	6.61	6.60
Ethylbenzene	9.21	7.18	12.2	12.2	12.2
Diethyl ether	26.4	16.4	19.8	19.9	19.9
tert.-Butyl methyl ether	55.4	37.9	43.0	43.2	43.3
Di-*n*-propyl ether	79.2	46.7	54.3	56.3	56.4
Diisopropyl ether	53.7	35.2	40.1	39.9	40.0
Methyl *n*-propyl ether	25.7	15.1	19.5	18.7	19.1
Ethyl *n*-propyl ether	47.4	28.2	34.4	34.5	34.6

For each solute, the equations derived could be well fitted to the corresponding linear parts of the experimental plot of V_g *vs.* $1/X_L$. Distribution constants as unknown constants in these equations could be calculated from the intercepts and slopes of the respective straight lines. For hydrocarbons, K'_{exp} is in good agreement with K'_L, indicating the dominant contribution of bulk solution partition to solute retention in region 3. However, negative values of K'_{exp} for dialkyl ethers indicate dominant effects of adsorption equilibria on V_{NR} even at high liquid phase loadings. Unfortunately, distribution constants of bulk solution partition for dialkyl ethers could not be calculated from K'_{exp} because a' and b' were not determined from experimental data.

Almost the same value could be calculated as K_A for each solute separately in three regions of the liquid phase loading (Table II). This indicates that heterogeneous characteristics of the solid surface of silica gel on adsorption of solute molecules could be converted into homogeneous surface properties. As K_A of an unsaturated hydrocarbon is still larger than that of the corresponding saturated compound, the original surface properties of silica gel were not completely shielded with a monolayer of squalane. Table II shows that the previous assumption that $K_1 > K_2$ is satisfied for any solute. It appears that hydrocarbon molecules can interact more strongly with the non-polar surface of silica gel, as $K_A > K_1$ and $K_A > K_2$. It is strange that $K_A > K_2$ for dialkyl ethers, although V_{NR} decreases monotonously with increasing X_L. It is probable that non-polar alkyl groups of ether molecules can interact through non-specific interaction with the squalane monolayer although specific interactions through ether-type oxygen are weakened significantly by shielding with the monolayer of squalane.

From the above results and discussion, we concluded that adsorption equilibria on the bare surface of the silica gel and the surface of the monolayer of squalane contributed dominantly to solute retention until the silica gel surface was completely covered with a monolayer of squalane. Subsequently, bulk solution partition and adsorption equilibria on the monolayer and/or the double layer of squalane concurrently contributed to solute retention

when an excess amount of squalane was loaded on silica gel. It was found that a considerable amount of squalane was necessary for deactivation of the surface of a solid support such as silica gel with a large surface area. A mixed retention mechanism was successfully applied for understanding the dependence of the retention volume of a solute on the liquid phase loading, taking into account a model of the solid surface and the distribution of the liquid phase molecules on the solid support.

REFERENCES

1 J. R. Conder, D. C. Locke and J. H. Purnell, *J. Phys. Chem.*, 73 (1972) 700.
2 V. G. Berezkin, *J. Chromatogr.*, 159 (1978) 358.
3 A. Waksmundzki, W. Rudzinski and Z. Suprynowicz, *J. Chromatogr.*, 74 (1972) 3.
4 Z. Suprynowicz, A. Waksmundzki and W. Rudzinski, *J. Chromatogr.*, 67 (1972) 21.
5 J. Å. Jönsson and L. Mathiasson, *J. Chromatogr.*, 179 (1979) 1.
6 D. F. Fritz, A. Sahil and E. Sz. Kováts, *J. Chromatogr.*, 186 (1978) 63.
7 J. Å. Jönsson and L. Mathiasson, in J. Å. Jönsson (Editor), *Chromatographic Theory and Basic Principles (Chromatographic Science Series*, Vol. 38), Marcel Dekker, New York, Basle, 1982, p. 189.
8 R. N. Nikolov, *J. Chromatogr.*, 241 (1982) 237.
9 K. Naito, T. Sagara and S. Takei, *J. Chromatogr.*, 503 (1990) 25.
10 K. Naito, H. Ogawa, S. Igarashi and S. Takei, *Anal.Sci.*, 4 (1988) 185.
11 K. Naito, S. Wada and S. Takei, *Anal. Sci.*, 4 (1988) 105.
12 K. Naito, H. Ogawa, S. Moriguchi and S. Takei, *J. Chromatogr.*, 299 (1984) 73.
13 S. J. Gregg and K. S. W. Sing, *Adsorption, Surface Area and Porosity*, Academic Press, London, 1967, p. 67.

Journal of Chromatography, 604 (1992) 233–241
Elsevier Science Publishers B.V., Amsterdam

CHROM. 24 187

Response characteristics and operating limits of thermal conductivity detectors at reduced pressure in capillary gas chromatography

Yafeng Guan, Liangmo Zhou, Daoqian Zhu and Wenqiang Jiang

Laboratory of Analytical Chemistry, Dalian Institute of Chemical Physics, Chinese Academy of Sciences, P.O. Box 100, Dalian 116012 (China)

(First received December 13th, 1991; revised manuscript received March 10th, 1992)

ABSTRACT

The response characteristics of thermal conductivity detectors (TCDs) at reduced pressure, especially in the pressure range 0.2–25 Torr, was studied systematically. It was found that there existed an operational pressure limit (P_{min}) below which the gas flow in the detector cell was no longer laminar and the detector response became pressure dependent. In addition, the noise level increased exponentially as the pressure decreased below P_{min}. When the detector was operated at pressures above P_{min}, both the responses and relative responses of the TCD were constant for a given concentration of a sample. P_{min} as a function of temperature, cell structure and carrier gas properties was interpreted theoretically and verified experimentally. Using this technique, coupling of capillary columns directly with a conventional TCD without make-up gas was realized while maintaining the efficiency of the capillary columns and the concentration sensitivity of the detector.

INTRODUCTION

The thermal conductivity detector (TCD) has enjoyed great popularity in packed column gas chromatography since the 1950s. Apart from its simple construction, sturdiness, lack of destruction of samples and ease of operation, this detector has a universal nature and the same relative response towards different classes of components of similar molecular size, regardless the differences in their chemical properties. This is different from ionization detectors. Another important feature of the TCD is that it is concentration sensitive, which implies that the minimum detectable concentration with the TCD is independent of the column diameter when the detector cell volume is small enough to be neglected. As capillary columns have replaced conventional packed columns in almost all gas chromatographic analyses, the combination of the advantages of the TCD with those of capillary columns has significant practical importance.

The main obstacle that prevents the coupling of capillary columns with TCDs has been the stringent requirements on the detector cell volume in capillary gas chromatography. The maximum permissible detector cell volume ($V_{d,max}$) for a 530 μm I.D. wide-bore capillary column is less than 10 μl, which is far below the cell volume of a conventional TCD. For use with smaller diameter columns, the required condition is even more severe, as $V_{d,max}$ is proportional to of the column inner diameter to the power 2–3. One solution to this problem is to add make-up gas to the TCD in order to increase the total gas flow through the cell, but this has the drawbacks of dilution of the column eluent, resulting in a decrease in sensitivity and a reduction in the working range of the column–detector system [1].

Reduction of the cell volume is another solution

Correspondence to: Dr. Y. Guan, Laboratory of Analytical Chemistry, Dalian Institute of Chemical Physics, Chinese Academy of Sciences, P.O. Box 100, Dalian 116012, China.

0021-9673/92/$05.00

adopted by several groups [2–4]. The 3.5-μl micro-TCD from Hewlett-Packard (Avondale, PA, USA) meets the requirement of capillary columns with I.D. $\geqslant$ 390 μm. Make-up gas has to be added when using smaller diameter columns. A TCD fabricated on a silica wafer [2] offers a 1.5-nl cell volume, and can match $\geqslant$ 50 μm I.D. capillary columns theoretically. The coupling of a micro-detector with capillary columns of various diameters is difficult as the dead volume of the connection is much larger than the cell volume itself, unless the capillary column and the TCD are fabricated on one silicon wafer. Adding make-up gas in the connecting part can eliminate the effect of the dead volume, but at the same time dilutes the eluent. The dilution becomes more severe when a narrow-bore capillary column is used because the flow ratio of the make-up gas to the eluent is rather high.

A third solution is to reduce the cell pressure. The effective cell volume is reduced by a factor P_o/P, where P_o and P are the atmospheric pressure and cell pressure, respectively. Actually, the use of a TCD at reduced pressure was first reported in 1963 [5] for other purposes. The first successful work on the vacuum operation of a TCD to couple with a capillary column was reported by Shirrmeister [6], and there have been further publications on this subject since then [7–10]. However, there are misunderstandings about the influence of the cell pressure on the detector responses in the low-pressure range, and there is no report of studies of the effect of cell pressure on the detector relative response, noise level and stability of operation and, in particular, the operating limits of the cell pressure. There is also a lack of study of the response characteristics as the pressure under intermediate flow conditions.

In this work, the relationships between cell pressure and the above-mentioned factors were studied systematically. The limit of the operating pressure of a TCD as a function of carrier gas properties and cell structure was determined and interpreted theoretically, and was verified experimentally. The influence of cell pressure on the relative response for molecules with different molecular weights and diameters was also studied.

THEORY

The ideal flow conditions inside the TCD cell are laminar, the thermal conductivity of a gas then being independent of pressure [11]. The noise level of a TCD is low and insensitive to pressure changes. As the pressure decreases, the flow pattern changes from laminar to intermediate and then to molecular. The boundaries between these different flows is defined by the value of the Knudsen number, *i.e.*,

$D/\lambda > 110$	laminar flow	(1)
$1 < D/\lambda < 110$	intermediate flow	(2)
$D/\lambda < 1$	molecular flow	(3)

where λ is the mean free path of the gas molecules and D is the diameter of the tube with sufficient length. In the TCD, the filament is placed in the centre axis of the cylindrical cell and the D term in above equations is replaced by the radius (R) of the cell. As the cell length is short, the above definition is only an approximation.

In the range of intermediate flow, an irregular flow pattern occurs and the degree of irregularity depends on the ratio D/λ. The thermal conductivity of the gas becomes poorer and pressure dependent under these conditions, resulting in higher noise levels and a higher filament temperature when the TCD is operated in the constant-current or constant-voltage mode. The main source of the detector noise comes from the irregular flow when other conditions are fixed, and the noise level is proportional to the degree of irregularity of the flow pattern. In the range of molecular flow, the flow pattern becomes random and the noise level reaches a maximum.

Because the TCD is designed to operate under laminar flow conditions, the lowest cell pressure that can be used in TCD operation is limited by inequality 1. Substituting $\lambda = 2.33 \cdot 10^{-20} T/(P\phi^2)$ (cm) into inequality 1, we obtain the desired equation,

$$P_{min} = 2.56 \cdot 10^{-18} T/(R\phi^2) \text{ (Torr)} \quad (4)$$

where ϕ is the molecular diameter of the carrier gas R is the radius of the TCD cell, and T is the wall temperature of the cell (K). For a TCD of fixed cell volume, the lower is P_{min} the smaller is V_e, which is what we require.

From eqn. 4, we know that there are three ways to reduce P_{min}: (i) using a low operating temperature T, which is limited by the volatility of the sam-

ple and the column temperature; (ii) increasing the cell radius R, which also increases the cell physical volume (V_o), and the decrease in P_{min} cannot compensate for the increase in V_e; in fact, V_e can be reduced efficiently by using a smaller cell radius; and (iii) using a carrier gas of larger molecule size; unfortunately, the optimum carrier gas velocity is also reduced when a large-molecule carrier gas is used, and columns under these conditions require a smaller $V_{d,max}$.

When hydrogen is used as the carrier gas, $\phi = 2.75 \cdot 10^{-8}$ cm, we have

$$P_{min} = 3.39 \cdot 10^{-3} T/R \text{ (Torr)} \quad (5)$$

The effective cell volume (V_e) therefore cannot be reduced arbitrarily because P_{min} sets the lowest limit. As a result, the minimum effective volume $V_{e,min}$ is

$$V_{e,min} = V_o P_{min}/P_o \quad (6)$$

Only columns for which the maximum permissible detector volume $V_{d,max}$ meets the condition $V_{d,max} \geqslant V_{e,min}$ are suitable for coupling with a TCD without make-up gas. The peak shape will be distorted when using columns with $V_{d,max} < V_{e,min}$.

EXPERIMENTAL

A Type 102G gas chromatograph from Shanghai Analytical Instruments (Shanghai, China) was fitted with a common capillary inlet system and a six-port gas sampling valve, which was connected between the carrier gas line and the injection port. Two types of TCD were used. Type I was a four-element flow-through TCD with two cells of total volume 600 μl and $S = 6000$ from Sichuan Analytical Instruments (Sichuan, China), and type II was a laboratory-made two-element flow-through TCD with a cell volume of 300 μl and $S = 1500$ [S is the response of a TCD for a given substance at a given concentration, *i.e.*, S = mV/(mg/ml), at a noise level $\leqslant$ 20 μV]. The diameters of both types of cells were 3.60 mm. The outlet of the TCD cells was enlarged to 2.0 mm I.D. and was connected via 2.0 mm I.D. copper tubes to a vacuum line through a needle valve, which was used to adjust the cell pressure. A U-tube manometer, connected with the TCD outlet, was used to measure the operating pressure. The cell pressure was then calculated by using eqns. 3.26 and 3.52 in ref. 11. The accuracy of temperature control of the TCD body was kept at $\pm$ 0.01°C.

Cross-linked fused-silica capillary columns were used: (a) 30 m × 0.25 mm I.D. SE-30, film thickness 0.2 μm; and (b) 14 m × 0.53 mm I.D. SE-30, film thickness 1.0 μm. A 15 cm × 50 μm I.D. fused-silica tube was used as a restrictor between the analytical column and the TCD to eliminate the effect of low pressure on the column performance and to maintain the mass flow-rate of the carrier gas constant. An empty silica tube with an inside diameter and length identical with those of the analytical column was used on the reference side. Other columns were also used in the examples of applications, and are described in the figure legends.

The carrier gas was high-purity hydrogen (minimum concentration 99.995%). Standard samples were all of analytical-reagent grade. Chromatograms were recorded on a CDMC-2A integrator (Shanghai Research Institute of Computer Technology, Shanghai, China).

RESULTS AND DISCUSSION

The concept of P_{min} is very important for both the design and operation of TCDs. Theoretically, we expected that the detector performance would change drastically when P varied from $P > P_{min}$ to $P \leqslant P_{min}$. This assumption was examined experimentally in the following way.

Noise level V_n

The influence of the cell pressure (P) on the V_n value of the TCD was studied in the constant-voltage and constant-current modes. For better comparison, the filament bridge current (I) was adjusted to about 100 mA at 30 Torr for both operational modes. As the λ value, and hence P_{min}, is temperature dependent, the measurement was carried out at two given TCD body temperatures, 60 and 170°C. The resulting of V_n *versus* P plot in the constant-voltage mode is shown in Fig. 1. The noise remained at a very low level when P was higher than 15 Torr. V_n began to increase slowly as P decreased, and then there was a sharp increase in V_n at $P < P_{min}$, which was the turning point of the curve. Fig. 2 shows the V_n–P relationship in the constant-current mode. The turning point of the curve, for

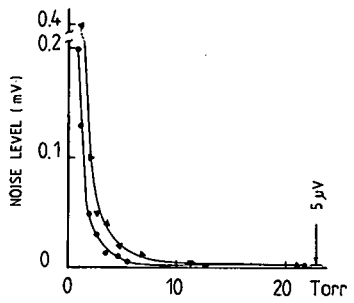

Fig. 1. Plots of detector noise level *vs.* detector cell pressure for TCD Type I in the constant-voltage mode. TCD body temperature: ● = 60°C; ▲ = 170°C.

the same TCD body temperature, is the same as in Fig. 1, but the change in V_n was more abrupt. Measurement of the filament resistance indicated that the filament temperature increased near and below P_{min} for both operational modes, but was higher for the constant-current mode. The filament temperature in the constant-current mode is shown in Fig. 3A and B for reference. In the theoretical discussion, we expected that V_n would change drastically near the region of intermediate flow, *i.e.*, $R/\lambda \leqslant 110$ or $P \leqslant P_{min}$. Substituting the experimental conditions of $R = 0.18$ cm and $MW(H_2) = 2$ into inequality 5, we found that $P_{min}(60°C)$ was 6.3 Torr and $P_{min}(170°C)$ was 8.3 Torr. The values agreed well with the experimental results.

Substituting the above P_{min} values into eqn. 6, we obtained the values of $V_{e,min}$ for the type II TCD, *i.e.*, $V_{e,min}(60°C) \approx 2.5$ μl and $V_{e,min}(170°C) \approx 3.3$ μl. The corresponding $V_{e,min}$ values were double these for the type I TCD.

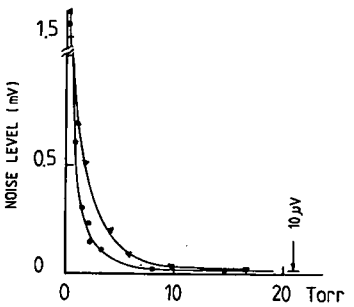

Fig. 2. Plots of the noise level *vs.* detector cell pressure for TCD type II in the constant-current mode. Body temperature: ● = 60°C; ▲ = 170°C.

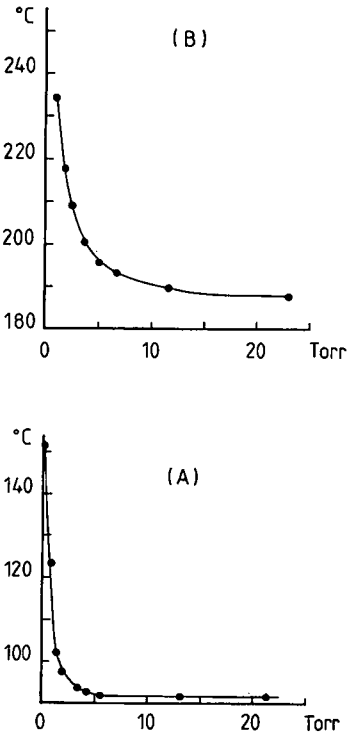

Fig. 3. Relationship between filament temperature and cell pressure in the constant-current mode. TCD type II; body temperature, (A) 60°C and (B) 170°C.

Responses

The detector response for nitrogen was investigated over a wide pressure range from 550 down to 0.5 Torr. A fixed-volume valve sampling was used in conjunction with fixed split injection after the valve. A constant flow of make-up gas was added to the detector in the pressure range 550–30 Torr, in order to reduce the peak distortion and to keep the mass flow through the detector cell constant. This measure ensured the integration of the concentration profile unchanged for a given amount of sample. A stable detector response for nitrogen was observed in this pressure range, as shown in Fig. 4A. This was in good agreement with theory.

At pressures around and below 30 Torr, no make-up gas was used. The change in column outlet pressure is negligible compared with the column inlet pressure (above 1100 Torr). Further, as the main pressure drop is on the restrictor, the mass flow-rate of carrier gas through the column, and then through the detector cell, was constant at a given

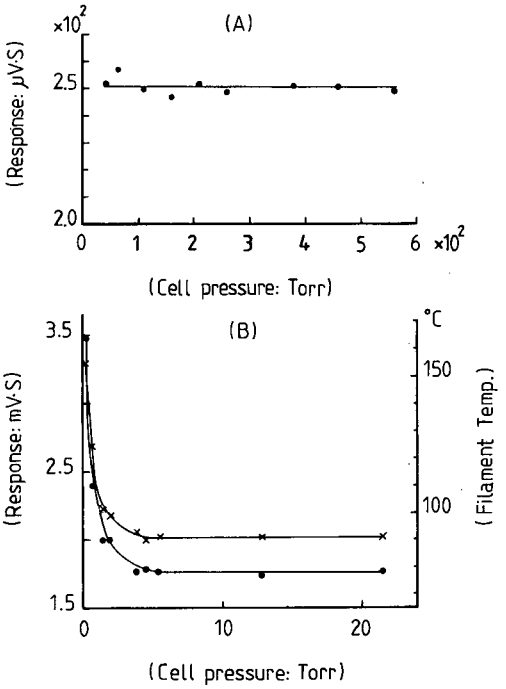

Fig. 4. (A) Detector response to nitrogen. TCD type I, 25°C. Bridge current, 50 mA. Column A, make-up gas flow-rate 25 ml/min. Sample size, 50 μl of pure nitrogen; splitting ratio, 1:100. (B) (●) Plot of the detector response to nitrogen *vs.* cell pressure and (x) plot of filament temperature at different cell pressures. TCD type I, 60°C, constant-voltage mode. Column B. Sample size, 20 μl; splitting ratio 1:40.

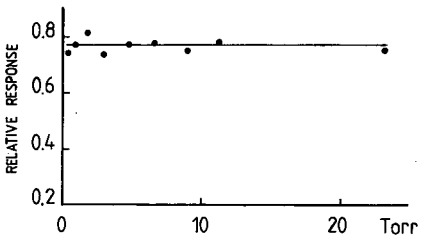

Fig. 6. Plot of detector relative response to CCl_4 *vs.* cell pressure. The response is relative to that of nitrogen. TCD, type II, 170°C. Column B. Headspace sampling.

column temperature. Subsequent measurements were all carried out under these conditions.

The response for nitrogen from 22 to 0.5 Torr is demonstrated in Fig. 4B. The response was constant at cell pressures $P > P_{min}$, and increased at $P \leqslant P_{min}$. The increase in detector response was caused mainly by the increase in filament temperature. Because the noise level increased faster than the response (see Fig. 1), the signal-to-noise ratio was poorer at $P \leqslant P_{min}$.

The detector responses, relative to nitrogen, for propane and isobutane are shown in Fig. 5. The responses of the sample were pressure dependent until the cell pressure was higher than 7 Torr, which is slightly above P_{min}. Another interesting compound was tetrachloromethane (CCl_4). The response of CCl_4 relative to nitrogen is illustrated in Fig. 6. Because of its fairly constant relative response, CCl_4 was chosen as the reference com-

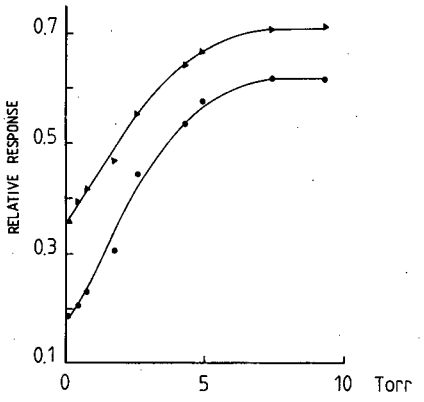

Fig. 5. Plot of detector relative response *vs.* cell pressure. ▲ = Propane; ● = isobutane. TCD type II, 30°C. Sample, mixture of nitrogen, propane and isobutane. Other conditions as in Fig. 4B.

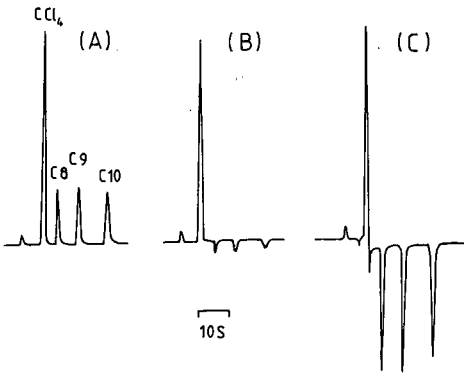

Fig. 7. Detector response to CCl_4, n-C_8H_{18}, n-C_9H_{20} and n-$C_{10}H_{22}$ at three cell pressures: (A) 3.8, (B) 1.8 and (C) 0.5 Torr. TCD, type II, 170°C. Column B. Sample size, 0.2 μl; splitting ratio, 1:40.

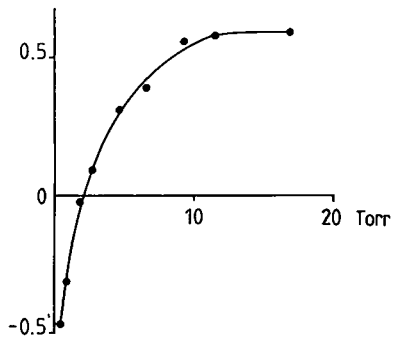

Fig. 8. Plot of detector relative response to n-C_9H_{20} *vs.* cell pressure. The response is relative to that of CCl_4. Other conditions as in Fig. 7.

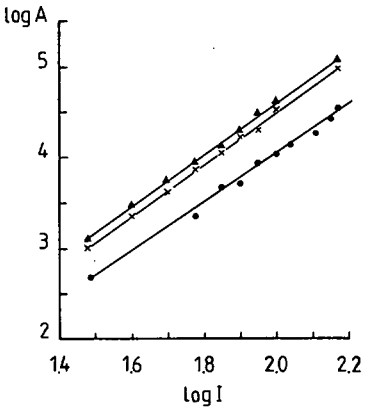

Fig. 9. Detector response (A) *vs.* filament current (I). TCD, type II, 25°C, constant-current mode. Sample, nitrogen. ● = Atmospheric pressure, column 2 m × 2 mm I.D., 60–80 mesh Carbosieve B; × = 8 Torr, column A; ▲ = 2 Torr, column A.

pound for liquid samples. The high molecular weight (MW = 152) and smaller molecular diameter of CCl_4 compared with propane and isobutane, suggested that the cross-sectional area of the molecule is the dominant factor in thermal conductance under intermediate flow conditions.

The situation became more complex with samples of larger molecular size. The chromatograms of a four-compound mixture, obtained at three different P values, are depicted in Fig. 7. The negative peak phenomenon led us study the responses of the compounds more carefully. The example given in Fig. 8 shows the change in the response toward n-nonane around the intermediate flow region. Note that the response of n-nonane became zero at 2.0 Torr, then negative at lower pressures. The response became constant at pressures higher than 9.0 Torr. This result demonstrated again that the detector response was normal and stable only at cell pressures higher than P_{min}. For convenience, we chose $1.2P_{min}$ as the practical pressure limit.

A comparison of the detector relative responses for various compounds at normal pressure (760 Torr) and at 15 Torr is shown in Table I. Peak area (A) was used in the measurement. The values were correlated with benzene for easy comparison with other published data. The relative responses of the TCD at normal pressure can be used directly in situations with reduced pressure, as long as $P \geqslant 1.2P_{min}$.

The response (peak area, A)–filament current (I) relationship was also studied using nitrogen as the sample. The lines in Fig. 9, obtained at three different pressures, were parallel to each other. This shows that the relationship $A = kI^y$ applies and the pressure has no influence on y. The value of y is determined by the slope of the log A *vs.* log I plot, which was 3.14 in the example.

Detection limit

Two detection limits can be given for a detector, the minimum detectable concentration (Q_c) and the minimum detectable amount (Q_m). At cell pressures higher than $1.2P_{min}$, Q_c was constant because the response and the noise level were unchanged in this

TABLE I

RELATIVE RESPONSES OF SELECTED COMPOUNDS AT DIFFERENT PRESSURES

Pressure	CO_2	CH_4	C_2H_6	C_2H_4	C_3H_8	C_3H_6	i-C_4H_{10}	n-C_4H_{10}	n-C_8H_{18}	n-C_9H_{20}	n-$C_{10}H_{22}$
15 Torr	1.52	2.01	1.43	1.56	1.24	1.23	1.01	0.97	0.70	0.72	0.71
Normal	1.62	2.04	1.43	1.54	1.23	1.23	1.03	1.00	0.71	0.72	0.71

TABLE II

THE DETECTOR RESPONSE TO ISOBUTANE AT DIFFERENT CONCENTRATIONS

Measurements were carried out on column B, carrier gas velocity 30 cm/s, column temperature 25°C, sample size 1 ml, splitting ratio 1:150, detector temperature 68°C, detector cell pressure 7.6 Torr, filament bridge current 150 mA, constant-voltage mode. The baseline noise was 0.005 mV.

Concentration (%)	60	6	0.6	0.06	0.006
Response (mV)	540	51	4.4	0.44	0.032

pressure range. Factors affecting Q_c at reduced pressure are the same as at normal pressure, as discussed thoroughly in 1960s [12]. However, the influence of cell pressure on Q_m was substantial. Q_m, the amount of sample of concentration Q_c entering the TCD cell in unit time, is given by

$$Q_m = Q_c F_d \quad (7)$$

where F_d was the gas flow-rate through the detector cell.

When the column is coupled directly to the detector without make-up gas, $F_d = \pi r^2 u P$, where u is the linear velocity of the carrier gas at the column outlet and r is the radius of the column. Substituting F_d in eqn. 6, we have $Q_m = \pi Q_c u r^2 P$. When u and P are constant, then

$$Q_m \propto r^2 \quad (8)$$

This means that the smaller the detector cell volume, the lower is Q_m.

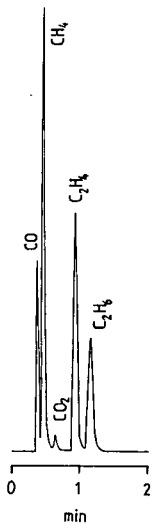

Fig. 10. Chromatogram of the residual gases from an oil refinery plant. TCD, type I, 15 Torr, 120°C. Column, 2 m × 0.46 mm I.D., 60–80 mesh Porapak QS, 50°C. Sample size, 50 μl; splitting ratio, 1:100.

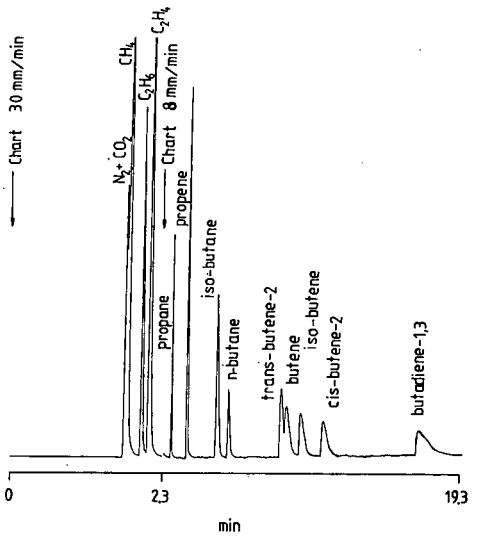

Fig. 11. Analysis of the gas mixture produced in the cracking process in a crude oil refinery. Column, 44 m × 0.46 mm I.D. coated with γ-alumina, 50°C. Others conditions as in Fig. 10.

Fig. 12. Chromatogram of a gasoline. TCD, type II, 68°C, 15 Torr. Column B, 68°C. Sample size, 0.1 μl; splitting ratio, 1:50.

The constant Q_c characteristic of the TCD opened the way to use smaller diameter columns while maintaining the practical sensitivity for a given sample concentration, as long as $V_{d,max} \leqslant V_{e,min}$.

The above discussion was concentrated on the detector itself. The detection limit of column–detector systems has been treated extensively by Noij and co-workers [1,8].

The dynamic range of the TCD at reduced pressure was determined experimentally. Isobutane mixed with hydrogen was used as the sample. Different concentrations of isobutane were prepared by step dilution. Two gas-tight glass syringes of volume 100 ml and 10 ml, were used for the sample mixing and dilution. The syringe was flushed with hydrogen three times before preparing a given concentration of sample. The experimental result, shown in Table II, indicated that the linear range of the response was about four orders of magnitude, and the minimum detectable concentration Q_c was around 0.01%, at reduced pressure. Both of these characteristics were the same as at normal pressure. The deviation of the data in Table II was caused mainly by the error in the sample concentration.

Examples of application

A gas mixture, which had been analysed on a conventional packed column with a TCD of 600-μl cell volume, was analysed on a micro-packed capillary column with the same detector operated at 15 Torr. The chromatogram is illustrated in Fig. 10; the analysis time was halved and the sample volume injected on to the column was 0.5 μl. The effective volume V_e of the detector at 15 Torr was 11.8 μl, much smaller than 600 μl but still too large even for the 0.48 mm I.D. column used. As a result, the peaks in Fig. 10 show some extra tailing.

The analysis of the gas mixture released from the cranking process in a oil refinery plant was performed on a PLOT column coated with alumina; the chromatogram is shown in Fig. 11. The TCD cannot be replaced with a flame ionization detector (FID) because the samples contained both hydrocarbons and permanent gases such as nitrogen and carbon dioxide.

The following two samples were analysed using a TCD with a cell volume of 300 μl operated at 15 Torr. V_e of the detector was about 6 μl, which is smaller than $V_{d,max}$ (*ca.* 6.6 μl) of the 0.53 mm I.D. capillary column. The chromatogram of the first fraction of gasoline was shown in Fig. 12, in which the peak shape is satisfactory. The analysis of a higher boiling sample, the raw material for making

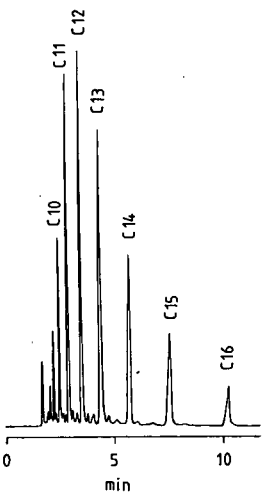

Fig. 13. Analysis of an alcohol mixture. TCD, type II, 15 Torr, 160°C. Column B, 160°C. Other conditions as in Fig. 12.

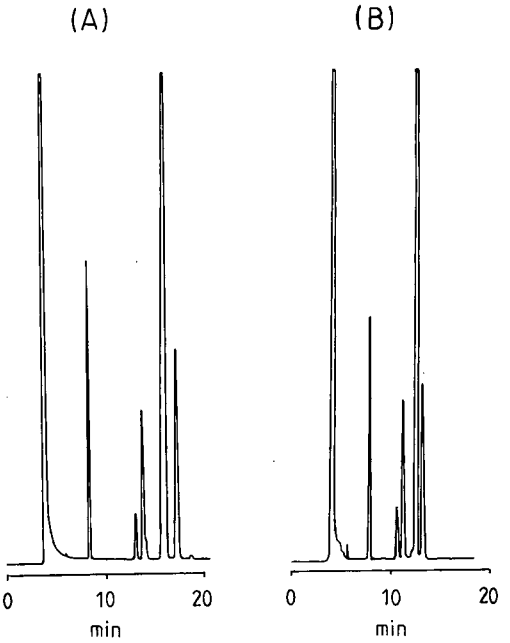

Fig. 14. Comparison of FID and TCD. Sample, esterified evening primrose oil. (A) FID: column, 20 m × 0.25 mm I.D., PEG-20M, 190°C. (B) TCD: column, 26 m × 0.46 mm I.D., PEG-20M, 226°C. TCD, type II, 18 Torr, 226°C.

an anti-freeze agent, is illustrated in Fig. 13. The main components of the sample were C_{10}–C_{16} alcohols.

A comparison of the TCD and FID for the analysis of esterified evening primrose oil is demonstrated in Fig. 14A and B, respectively. The chromatograms were almost identical. As the $V_{d,max}$ of a 20 m × 0.25 mm I.D. column is about 1.5 μl, we had to use a larger diameter column to couple with the TCD ($V_e \approx 6$ μl).

The wide range of operating temperature of the TCD and the variety of columns used in the five examples demonstrated that capillary columns coupled with TCDs can be used to analyse a broad range of samples. Because the TCD is operated at reduced pressure, the detector can be operated at the same temperature as the column without the problem of sample deposition. In addition, the optimum linear velocity of the carrier gas was much faster at a reduced outlet pressure [13], which will benefit faster analyses.

REFERENCES

1 Th. Noij, J. Curvers and C. Cramers, *J. High Resolut. Chromatogr. Chromatogr. Commun.*, 9 (1986) 752.
2 S. C. Terry, J. H. Jerman and J. B. Angell, *IEEE Trans. Electron Devices*, ED-26(12) (1979) 1880.
3 H. Wohltjen, *Anal. Chem.*, 56 (1984) 87A.
4 B. J. Lambert, R. J. Laub, W. L. Roberts and C. A. Smith, in S. Ahuja (Editor), *Ultrahigh Resolution Chromatography (ACS Symposium Series*, No. 250), American Chemical Society, Washington, DC, 1984, p. 59.
5 D. C. Locke and W. W. Brandt, in L. Fowler (Editor), *Gas Chromatography 1963*, Academic Press, New York, 1963, pp. 55–76.
6 H. Shirrmeister, *J. Chromatogr.*, 137 (1977) 13.
7 M. G. Proske and M. Bencler, *Chromatographia*, 715 (1978) 11.
8 Th. Noij and C. Cramers, *J. High Resolut. Chromatogr. Chromatogr. Commun.*, 11 (1988) 264.
9 A. van Es, C. Cramers and J. Rijks, *J. High Resolut. Chromatogr.*, 12 (1989) 303.
10 A. van Es, C. Cramers and J. Rijks, in P. Sandra (Editor), *10th International Symposium on Capillary Chromatography, Riva del Garda, May 22–25, 1989*, Huethig, Heidelberg, 1989, Vol. 1, p. 109.
11 A. Roth, *Vacuum Technology*, Elsevier North-Holland, Amsterdam, 1982.
12 A. E. Lawson, Jr. and J. M. Miller, *J. Gas Chromatogr.*, 8 (1966) 273.
13 C. A. Cramers, G. J. Scherpenzeel and P. A. Leclercq, *J. Chromatogr.*, 203 (1981) 207.

Journal of Chromatography, 604 (1992) 243–246
Elsevier Science Publishers B.V., Amsterdam

CHROM. 24 173

Determination of maleic hydrazide residues in cured tobacco by gas chromatography☆

J. M. Renaud, I. Keller and G. Vuillaume

Research & Development, Philip Morris Europe SA, P.O. Box 11, CH-2003 Neuchâtel (Switzerland)

(First received November 29th, 1991; revised manuscript received March 12th, 1992)

ABSTRACT

A rapid and sensitive method for measuring maleic hydrazide (6-hydroxy-2*H*-pyridazin-3-one) residues in cured tobacco is described. A mixture of free and bound maleic hydrazide is extracted with hydrochloric acid in which maleic hydrazide glycoside is simultaneously hydrolysed. The free maleic hydrazide obtained is methylated using dimethyl sulphate and the derivative is partitioned into chloroform and determined by capillary gas chromatography using a nitrogen–phosphorus detector. The limit of detection of maleic hydrazide is 5 ppm.

INTRODUCTION

Maleic hydrazide (6-hydroxy-2*H*-pyridazin-3-one) (MH) is a systemic plant growth regulator, widely used for tobacco-sucker control. After application to the upper part of the tobacco plant, MH is transcolated within the plant where it inhibits cell division, but not cell extension. Maleic hydrazide can exist in three tautomeric forms [1] (**I–III**) and shows phenolic properties under physiological conditions.

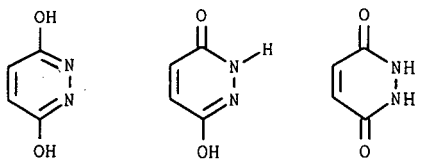

I II III

Towers *et al.* [2] showed that about 15% of the maleic hydrazide in young wheat leaf segments was present as a glycoside. In tobacco, MH is gradually converted into the bound form, mainly during curing but also during storage; conversion rates of up to 50% were observed during curing [3].

Because of growing restriction concerning agricultural chemical residues on tobacco, interest in the determination of MH has arisen. Methods for the determination of total MH on tobacco involve reduction with zinc and hydrolysis with hot alkali to hydrazine [4–9]. The hydrazine is isolated by distillation and determined spectrophotometrically as an azine by addition of *p*-dimethylaminobenzaldehyde. The spectrophotometric procedure was adopted by the International Organization for Standardization (ISO) as a standard method [9]. In addition to the low sample capacity of this method, its major drawback is a lack of specificity and possible interferences [10]. More specific methods utilizing GC have been proposed, but they are restricted to free MH [10,11] and also involve tedious sample preparation steps.

A method is presented here for the routine determination of total, *i.e.*, free and glycosidically bound MH on tobacco. MH glycoside is hydrolysed by

Correspondence to: Dr. J. M. Renaud, Research & Development, Philip Morris SA, P.O. Box 11, CH-26043 Neuchâtel, Switzerland.

Presented in part at the *CORESTA Symposium, Kallithea, Greece, October 7–11, 1990.*

0021-9673/92/$05.00

hydrochloric acid, methylated in aqueous medium with dimethyl sulphate, transferred into an organic solvent and determined by gas chromatography (GC) with nitrogen–phosphorus detection (NPD).

EXPERIMENTAL

Reagents

All solvents were of analytical-reagent grade (Fluka, Buchs, Switzerland). Maleic hydrazide (Riedel-de Haën, Seelze, Germany) and 6-methyluracil (Aldrich, Steinheim, Germany) were of Pestanal grade and 97% purity, respectively. Concentrated hydrochloric acid (32%, $d = 1.16$) and dimethyl sulphate of analytical-reagent grade were obtained from Fluka. An internal standard stock solution was prepared by dissolving 30 mg of 6-methyluracil in 100 ml of water. In order to obtain the extraction solution, 400 ml of concentrated hydrochloric acid and 20 ml of internal standard stock solution were made up to a total volume of 2 l with water. A standard stock solution of MH was prepared by dissolving 40 mg of MH in 100 ml of water. The calibration solution was obtained by dissolving 10 ml of standard MH stock solution and 200 ml of concentrated hydrochloric acid in 1 l of water.

Analytical procedure

Extraction and hydrolysis. A 5-g amount of cut filler or ground tobacco was introduced into a 250-ml flask and extracted with 100 ml of extraction solution for 2 h under reflux. After cooling and filtration, a 1-ml aliquot was transferred into a 5-ml reaction vessel for derivatization.

Derivatization. The 1.0-ml aliquot was made alkaline by addition of exactly 0.4 ml of 10 *M* NaOH; an exact amount of dimethyl sulphate (200 μl) was then added using a disposable syringe and the flask was tightly closed and kept at 75°C for 1 h in a heating module (Pierce, Rockford, IL, USA). At the beginning of the reaction, the flask was shaken regularly until the dimethyl sulphate layer disappeared (usually 7–10 min). After cooling, the dimethyl derivative obtained was extracted with 500 μl of chloroform. Optimum extraction yields were obtained by shaking in a vortex mixer for 3 min and the final phase separation was achieved by centrifugation. An aliquot (200 μl) of the lower organic layer was transferred into a GC vial and analysed by GC–NPD.

Calibration. A 1-ml volume of calibration solution was introduced into a 5-ml reaction vessel and derivatized in parallel with the tobacco extract. Three replicates were required.

Instrumentation. A Carlo Erba Model 5160 gas chromatograph with split injector and a nitrogen–phosphorus detector was used, equipped with a 30 m × 0.25 mm I.D. fused-silica column coated with a 0.25-μm layer of DB-17 (J&W, Rancho Cordova, CA, USA). A Spectra-Physics DP-700 integrator was used for data processing. The injector and detector temperatures were set at 250 and 270°C, respectively. The column temperature was initially 140°C for 3 min, then programmed from 140 to 200°C at 5°C/min and from 200 to 250°C at 20°C/min; the final temperature was held for 15 min. The column head pressure was set at 120 kPa of 99.999% helium. A 30 ml/min flow of 99.99% nitrogen was used as make-up gas. A 1-μl volume of sample was injected with a splitting ratio of 1:30. Quantification was performed by the internal standard technique using 6-methyluracil as internal standard.

GC–MS apparatus and conditions. A Hewlett-Packard Model 5988 GC–MS system was used. The chromatographic conditions were identical with those mentioned above. The spectra were recorded in the electron impact mode with the following conditions: interface temperature, 250°C; source temperature, 190°C; and ionization energy, 70 eV. Ions were detected at *m/z* 140 (92%, $M^{+\cdot}$), 112 (36%), 82 (29%), 80 (47%) and 69 (100%).

Nuclear magnetic resonance. ^{1}H NMR spectra were recorded in deuterated chloroform at 200 MHz on a Bruker WP 200 spectrometer. Tetramethylsilane was taken as the reference for the calculation of chemical shifts. The ^{1}H NMR chemical shifts were 3.6 (s, 3H), 3.8 (s, 3H) and 6.9 ppm (s, 2H).

RESULTS

The chromatogram of an extract of flue-cured tobacco is shown in Fig. 1. The retention times of methylated MH and 6-methyluracil are 5.32 and 14.29 min, respectively. A recovery of 95% was determined on tobacco samples fortified with 80 ppm of MH. The precision of the method was determined at two concentration levels by analysing two

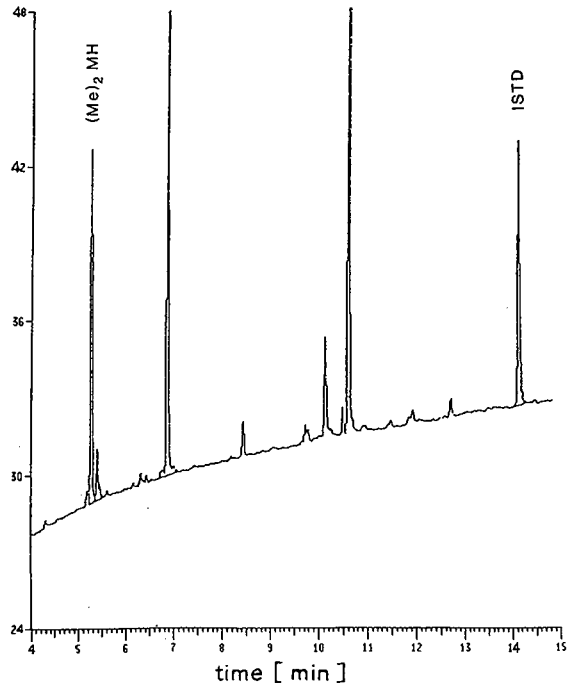

Fig. 1. Gas chromatogram of a Virginia tobacco extract containing 209 ppm of MH.

different tobacco samples containing 70 and 150 ppm of MH. At both levels the relative standard deviation based on eleven replicates was 3%. The detection limit, corresponding to a signal-to-noise ratio of 3, was 5 ppm.

The linearity of MH detection was examined for standard solutions and for fortified tobacco extracts between 10 and 550 ppm (Figs. 2 and 3). The amounts detected by the GC method increased linearly in the range considered for both the standard solutions and the tobacco extracts with a good correlation (r^2 = 0.999 and 0.997, respectively).

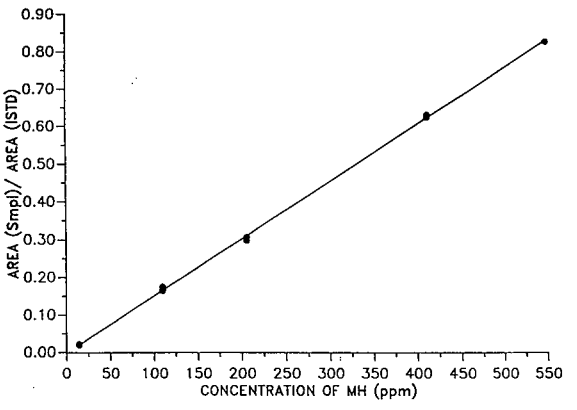

Fig. 2. Linearity of MH detection in standard solutions.

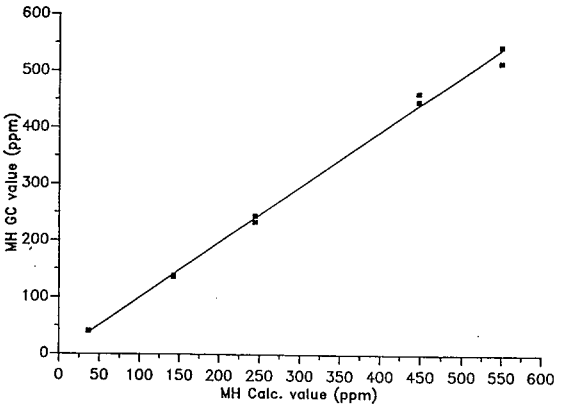

Fig. 3. Linearity of MH detection in fortified tobacco extracts.

The method was further validated by comparing the amounts of MH detected by the GC procedure with the amounts detected by the ISO reference method [9]. Thirty tobaccos with MH contents ranging from 0 to 300 ppm were analysed and, as shown in Fig. 4, an excellent correlation was obtained (r^2 = 0.9775).

DISCUSSION

The very low solubility of MH in non-polar organic solvents and the necessity to hydrolyse the

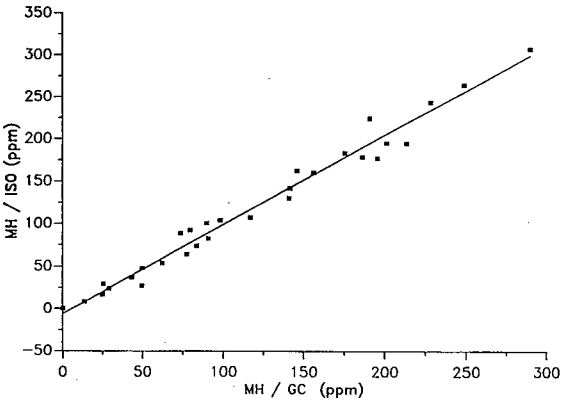

Fig. 4. Correlation between MH residues determined by GC and by spectrophotometry by the ISO 4876 method [9].

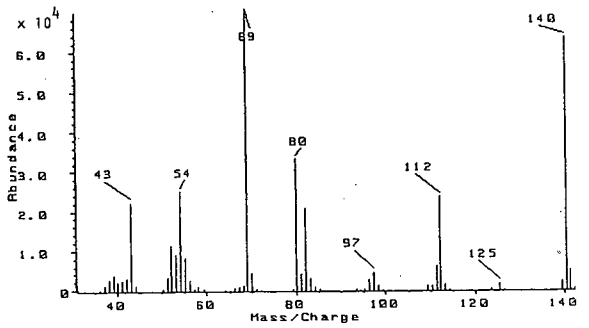

Fig. 5. Electron impact mass spectrum of the methylated derivative of MH.

MH glycoside require and aqueous medium for the initial step. Under such conditions, the tobacco material gives a very complex mixture that is not compatible with any direct chromatographic analysis. Therefore, the "*in situ*" methylation with dimethyl sulphate presented several advantages: free MH is converted into its dimethyl derivative, which can be quantitatively extracted from the aqueous phase with chloroform; the partitioning into the organic phase, associated with specific GC detection, was sufficient to ensure an interference-free analysis. On decreasing its polarity by methylation, MH was also made more suitable for GC analysis.

Although MH can exist in three tautomeric forms (**I–III**) [1], methylation with dimethyl sulphate produces only the derivative of one isomer (**II**, 6-methoxy-2-methylpyridazin-3-one). Positive proof of the identity of the derivative was obtained by GC–MS and ^{1}H NMR.

In the ^{1}H NMR spectrum, the two signals (singlets) at 3.6 and 3.8 ppm correspond to methyl groups in different environments, *i.e.*, CH_3–N (3.6 ppm) and CH_3–O (3.8 ppm). In addition, the measured chemical shifts are in accordance with values reported by Katritzky and Waring [1], *i.e.*, 3.53 and 3.78 ppm for CH_3–N and CH_3–O, respectively, in 6-methoxy-2-methylpyridazin-3-one.

The mass spectral data (Fig. 5) are in agreement with the fragmentation of pyridazine reported by Porter [12]: The molecular ion at *m/z* 140 loses a molecule of CO, producing the signal at *m/z* 112, and this ion loses CH_3N_2, resulting in the base peak at *m/z* 69 and the signal at *m/z* 43. Fragments at *m/z* 80 and 82 orginate from the ion at *m/z* 112 by loss of methanol and formaldehyde, respectively.

CONCLUSIONS

A GC method for the routine determination of MH residues in tobacco has been presented and validated. The method is specific, rapid and requires little manual labour. Including the hydrolysis step, which is the most time-consuming step in the method, 20 samples can be processed daily. The use of an internal standard added to the hydrolysis solution at the beginning of the procedure guarantees a high precision, as it allows corrections for occasional losses during sample preparation, variations in injection volume and changes in detector sensitivity. However, owing to the efficiency of the extraction procedure (>95% recovery) and the stability of the NP detector, these corrections were minor.

ACKNOWLEDGEMENTS

The authors express their thanks to Dr. S. Claude, University of Neuchâtel, for measuring the NMR spectra.

REFERENCES

1 A. R. Katritzky and A. J. Waring, *J. Chem. Soc.*, (1964) 1523.
2 G. U. N. Towers, A. Hutchinson and W. A. Andreae, *Nature (London)*, 181 (1958) 1535–1536.
3 A. F. Haeberer and O. T. Chortyk, *J. Assoc. Off. Anal. Chem.*, 62 (1979) 171–175.
4 P. R. Wood, *Anal. Chem.* 25 (1957) 1879–1883.
5 C. Anglin and J. H. Mahon, *J. Assoc. Off. Agric. Chem.*, 41 (1958) 177–182.
6 J. R. Lane, D. K. Gullstrom and J. E. Newell, *J. Agric. Food Chem.*, 6 (1958) 671–674.
7 I. Hofmann, *J. Assoc. Off. Agric. Chem.*, 44 (1961) 723–725.
8 M. Ihnat, J. Robert and I. Hoffman, *J. Assoc. Off. Anal. Chem.*, 56 (1973) 1164–1172.
9 *International Standard, ISO 4876*, International Standards Organization, Geneva, 1980.
10 A. F. Haeberer, W. S. Schlotzhauer and O. T. Chortyk, *J. Agric. Food Chem.*, 22 (1974) 328–330.
11 Y. Y. Liu and D. Hofman, *Anal. Chem.*, 45 (1973) 2270–2273.
12 A. N. Porter, *Mass Spectrometry of Heterocyclic Compounds*, Wiley, New York, 1985, p. 715.

Journal of Chromatography, 604 (1992) 247–253
Elsevier Science Publishers B.V., Amsterdam

CHROM. 24 225

New analytical methods for quantitation of four fungicides by gas and high-performance liquid chromatography

Joseph A. Akkara, Marvin Greenberger and David L. Kaplan

US Army Natick Research, Development & Engineering Center, Natick, MA 01760-5020 (USA)

(First received September 6th, 1990; revised manuscript received March 21st, 1992)

ABSTRACT

New analytical methods were developed for the quantitation of para-nitrophenol, 2,2'-methylenebis(4-chlorophenol), salicylanilide and copper 8-quinolinolate, by high-performance liquid and gas chromatography. The first three were extracted for 4–8 h from leather, cotton and felt samples, respectively, by acetonitrile in a Soxhlet, and then quantitated by high-performance liquid chromatography using a C_{18} reversed-phase column and a UV detector. Copper 8-quinolinolate was extracted by dilute sulfuric acid and the acid extract was treated with a chelating agent to release 8-hydroxyquinoline. 8-Hydroxyquinoline was in turn extracted and quantitated by gas chromatography with a flame ionization detector.

INTRODUCTION

Treatments with fungicides are usually part of a functional finish for materials, which may include treatments for water repellency, coloring, and flame retardation. Present specifications for the quantitation of the fungicides *p*-nitrophenol (pNP), 2,2'-methylenebis(4-chlorophenol) (dichlorophene, G-4), salicylanilide and copper 8-quinolinolate (Cu-8) are based on colorimetric techniques, which are not precise, specific, sensitive or reproducible [1–5]. Therefore new analytical methods, high-performance liquid chromatography (HPLC) with UV detection, and gas chromatography (GC) with flame ionization detection (FID), were evaluated for the precise and sensitive quantitation of these fungicides in the presence of other functional finishes. Fig. 1 gives the chemical structures of the four fungicides studied.

Earlier studies for the determination of Cu-8 have shown that the yellow color extracted from the

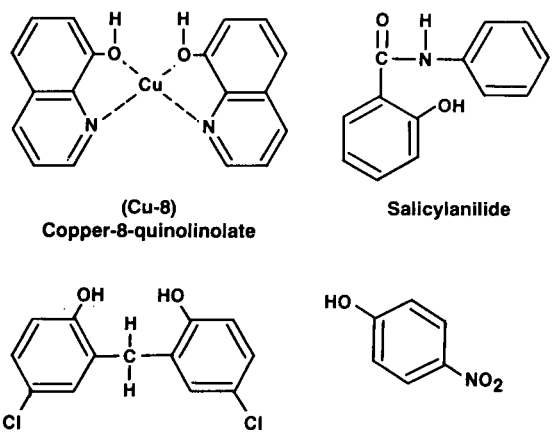

Fig. 1. Chemical structures of fungicides.

Correspondence to: Joseph A. Akkara, Biotechnology Division, Box 20, US Army Natick Research, Development & Engineering Center, Natick, MA 01760-5020, USA.

test material interfered with the analytical method. To prevent interference in the quantitation of Cu-8, column chromatographic removal of the dye was recommended [6,7]. There was significant interference with a number of phenolic compounds including *o*-phenylphenol, salicylanilide, 4,4′-isopropylidenebis(2-chlorophenol), and 2,4-dichlorophenol by the present colorimetric method used for quantitation of G-4 [8]. Some of these interferences with the colorimetric procedures used in the quantitation could result in incorrect values, which would result in incorrect recommendations for the optimum treatment of material with these fungicides. The new analytical methods developed and reported here are reliable, accurate, sensitive and free from interferences from other substances generally present in the material being evaluated.

EXPERIMENTAL

Materials

Materials tested

Leather treated with *p*-nitrophenol; wool felt treated with salicylanilide; and cotton duck and tent lining with flame retardant [tetrakis(hydroxymethyl)phosphonium hydroxide–ammonia (THPOH–NH_3)] and treated with G-4 or Cu-8 were used for the fungicide quantitation.

Fungicides

The following fungicides were purchased from commercial sources: Cu-8 (Monsanto, St Louis, MO, USA); *p*-nitrophenol (J. T. Baker, Phillipsburg, NJ, USA); G-4 (Givaudan, Clifton, NJ, USA); and salicylanilide (Aldrich, Milwaukee, WI, USA).

Other chemicals

The following chemicals were purchased from sources indicated: 2-hydroxyquinoline, 5-hydroxyquinoline, 8-hydroxyquinoline, 2,4-quinolinediol, isoquinoline, 5,7-dibromo-8-hydroxyquinoline, 2-hydroxypyridine, 8-hydroxyquinaldine, 8-hydroxyquinoline N-oxide, salicylaldehyde, salicylic acid, salicylamide, phenylsalicylate, phenol, nitrobenzene, *m*-nitrotoluene, *o*-nitrotoluene and *p*-nitrotoluene (Aldrich); 2,2′-methylenebis(3,4,6-trichlorophenol) (Givaudan) and *p*-nitrophenol (J. T. Baker). These chemicals were selected based on the functional groups, precursors, and breakdown products of the fungicides for which new analytical methods were to be developed, and to determine the potential interference of these compounds.

Solvents

Acetonitrile and methyl alcohol (HPLC grade, with UV cut-off at 190 nm and 205 nm, respectively, Caledon, Ontario, Canada) were used for extractions, preparation of standard solutions, and HPLC analysis. Cu-8 was solubilized in pyridine (Aldrich) and used in recovery studies. Methylene chloride (HPLC grade, 233 nm cut-off, Burdick & Jackson, Baxter Travenol, Muskegon, MI, USA) was used for the extraction and the preparation of standard solution of 8-hydroxyquinoline.

High-performance liquid chromatography

An HPLC System (Waters Div., Millipore, Bedford, MA, USA) with Model 721 system controller, Model 730 data module, Model 6000A solvent pump, Model 710B WISP and Model 441 UV detector was used for the quantitation of G-4, pNP and salicylanilide.

Gas chromatography

Hewlett-Packard gas chromatography (Model 5880A; Hewlett-Packard, Avondale, PA, USA) with flame ionization detector and a glass column (305 cm × 4 mm I.D.) with packing of 1.5% OV-17 with 1.95% QF-1 on Gas-Chrom Q, 100–120 mesh (lot SP 981; Applied Science Laboratories, State College, PA, USA) was used to quantitate Cu-8.

Methods

Treatment of material

Ca. 0.1–0.5 g of material (leather, felt, cotton duck and tent lining) containing fungicide was cut up and weighed. Control samples [leather, felt, cotton duck, tent lining, etc., without any fungicide, but with other functional finishes (flame retardant, water repellent, etc., present in the test materials)] were also extracted to determine the potential interference of these functional finishes in the analytical methods being developed. These control samples were spiked with a known amount of fungicide, and used for recovery studies. The treatment level in re-

covery samples represents the actual spiking concentrations. These samples were extracted and fungicides quantitated as described below.

Preparation of fungicide solutions

p-Nitrophenol, G-4 and salicylanilide were solubilized in methanol and used to spike control samples for recovery studies. These fungicides, dissolved in 86.7% (v/v) acetonitrile (ACN) in Milli-Q water, were used as the HPLC standards. A solution of Cu-8 in pyridine was used in the recovery studies because of the solubility of the fungicide in this solvent of the many solvents tested.

Method of extraction

Two procedures were developed for the extraction of fungicides from the test materials. The first procedure was for the extraction of pNP, G-4, and salicylanilide by acetonitrile solution and the second one was for the extraction of Cu-8 by H_2SO_4 solution.

Extraction of pNP, G-4 and salicylanilide. Soxhlet extraction was used for the extraction of *p*-nitrophenol, G-4 and salicylanilide. This extraction setup consisted of a heating mantle with a rheostat, 250 ml flat bottom flask for the solvent, 100 ml Soxhlet extractor to hold the sample in a thimble and a water-cooled condenser. Fungicides were extracted with 86.7% (v/v) ACN in Milli-Q water. The boiling point of this azeotrophic mixture is 76.5°C. Time required for the complete extraction of the above fungicides from test samples was from 4–8 h. Afterwards the extract was concentrated to less than 25 ml volume using the same solvent. An aliquot of the extract was quantitated using HPLC as described below.

Extraction of copper 8-quinolinolate. Cu-8 is a chelated compound of 8-hydroxyquinoline with copper and the analytical method developed and reported is for the quantitation of 8-hydroxyquinoline. The extraction procedure used involved extraction of Cu-8 from the test material, treatment of extracted Cu-8 with a strong chelating agent to remove copper from Cu-8 and the extraction of 8-hydroxyquinoline released. Cu-8 treated fabric was extracted three times with hot, 0.5 *M* H_2SO_4 solution (8.0 ml each time) and the extracts were pooled and brought up to 25 ml with 0.5 *M* H_2SO_4. A 1-ml volume of this acid extract was treated with 1.0 ml of tetrasodium ethylenediaminetetraacetate (Na_4-EDTA, 1.0 *M*) and mixed on a Vortex mixer for 1 min. This treatment of Cu-8 solution with EDTA was to remove copper present in Cu-8 and release 8-hydroxyquinoline. 8-Hydroxyquinoline that was released (from Cu-8) was extracted with 0.2 ml methylene chloride by vortexing the mixture for 1 min. The supernatant containing copper salt was aspirated off and 8-hydroxyquinoline present in methylene chloride was quantitated by GC as described below.

Recovery studies

Recovery studies were carried out by spiking control samples [0.2–1.0 g cut piece of the test material (leather, felt, or cotton duck with no prior fungicide treatment, but with other functional finishes)] with a known amount of the fungicide solution. The amount of fungicide used to spike the control samples varied from fungicide to fungicide and depended upon the amount of the commercial fungicide treatment normally required for protection. These spiked samples were extracted and the amount of the fungicide in the extract was quantitated by the methods developed. The fungicides (except Cu-8) dissolved in methyl alcohol were applied onto the test materials and the solvent was removed by air drying. Cu-8 dissolved in pyridine was applied to test materials as above, and pyridine was removed by air drying. Since not enough cotton duck without G-4 pretreatment was available, the cotton duck commercially treated with this fungicide plus other functional finishes was also used for the G-4 recovery studies.

HPLC operating conditions

Reversed-phase column (C_{18}, 10 μm, Waters, Millipore) with either acetonitrile or methanol solution and a UV detector were used for the HPLC analysis. The wavelength selected for the HPLC detector was based on the absorption maximum determined by UV–VIS scanning in a spectrophotometer (Model Lambda 3; Perkin-Elmer, Oak Brook, IL, USA).

GC operating conditions

Nitrogen, with a flow-rate of 30 ml/min, was the carrier gas for GC. The flow-rates of air and hydrogen to the flame ionization detector were 400 and 40

ml/min, respectively. The injector temperature was 170°C, and the column temperature was programmed from 170–250°C at a rate of 10°C per min for 8 min. A 10-μl volume of the sample was injected into the column and the data were collected for 4 min.

Standard curves

The standard curves of the four fungicides were prepared from standard solutions by HPLC and GC methods described above. The range, linearity and correlation coefficient of the standard curves of fungicides were determined by 2–4 independent analyses.

RESULTS AND DISCUSSION

p-Nitrophenol

Leather samples commercially treated with pNP were extracted by Soxhlet for 4–8 h with 86.7% (v/v) ACN in water as described earlier. The retention time of the fungicide eluted from the C_{18} (10 μm) column was 10.7 min, using 25% (v/v) ACN in Milli-Q water as the eluent. Other details of the extraction procedure and the HPLC method used for the analysis of pNP are given in Table I. The following compounds were evaluated for potential interference in the quantification of pNP: phenol, nitrobenzene, *o*-nitrotoluene, *m*-nitrotoluene and *p*-nitrotoluene. These compounds eluted at times different from the retention time of pNP. There was also no interference from other substances extracted from untreated leather by the acetonitrile solution. The standard curve for pNP was linear from 2–12 mg/l (correlation coefficient = 0.9982, intercept = $-0.0278 \cdot 10^6$ and slope = $0.0792 \cdot 10^6$). Fig. 2A gives the chromatogram obtained with a typical HPLC run. The average amount of moisture in the leather samples tested was 9.3%. Mean value for the *p*-nitrophenol (after the moisture correction) in the leather samples tested varied from 0.26–0.27% (g/100 g) and standard deviation varied from 0.002–0.007. With extraction times from 4–8 h, there was no significant difference in the levels of pNP quantitated by HPLC.

p-Nitrophenol recovery studies were carried out with 0.5 g control leather samples (without any fungicide treatment) after spiking with 1.5 mg of the fungicide. These recovery samples were extracted for 4, 6, and 8 h and the fungicide in the extract was quantitated as described above. Recovery studies indicate that the amount of pNP recovered was from 102–111% (mean value 106 ± 3.9% S.D.) and the extraction of pNP was complete from the fungicide-spiked leather samples after 4 h of the Soxhlet extraction.

2,2'-Methylenebis(4-chlorophenol)

Cotton fabrics commercially treated with G-4 and flame retardant (THPOH–NH_3) treatment were used for the HPLC analysis. The Soxhlet extraction with acetonitrile was carried out for 4, 6 and 8 h, to determine the extraction efficiency. G-4 extracted was quantitated by HPLC using a C_{18} (10

TABLE I

SUMMARY OF ANALYTICAL METHODS FOR FUNGICIDES

Reference details in Experimental.

	pNP	G-4	Salicylanilide	Cu-8
Extraction solvent	86.7% ACN	86.7% ACN	86.7% ACN	0.5% *M* H_2SO_4
Extraction time (h)	4–8	4–8	4–8	1.5
Chromatography	HPLC	HPLC	HPLC	GC
Column packing	C_{18}, 10 μm	C_{18}, 10 μm	C_{18}, 10 μm	1.7% OV-17 with 1.95% QF-1
Eluent/carrier gas	25% ACN	50% ACN	75% Methanol	Nitrogen
Flow-rate (ml/min)	1.0	1.0	1.0	30
Retention time (min)	10.7	9.0	3.25	2.8
Detector	UV	UV	UV	FID
Wavelength (nm)	340	214	229	–

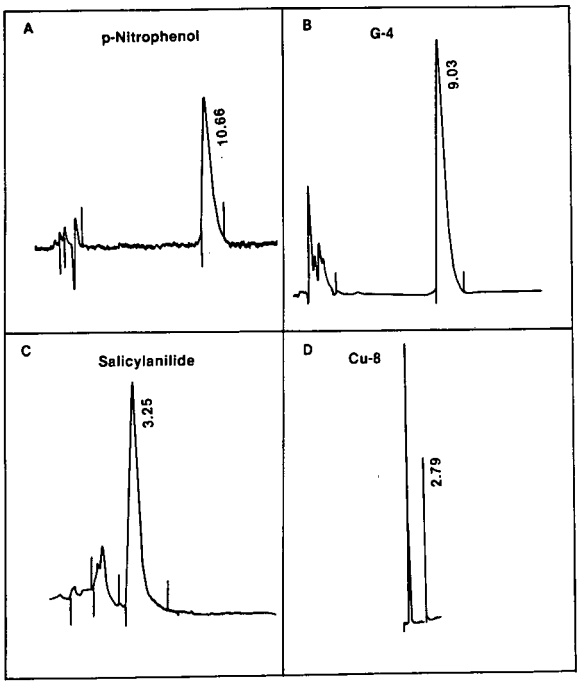

Fig. 2. Chromatograms of fungicides with retention times in min.

μm) column and eluted with 50% (v/v) ACN in Milli-Q water. Other details of the HPLC method are given in Table I. The amount of G-4 in fabric samples (extracted for 4–8 h) varied from 0.98–1.2% with a mean value of 1.08 ± 0.11% S.D. The results indicate that there was no significant difference between 4 and 8 h of extraction. 4-Chloro-3-methylphenol and 2,2′-methylenebis(3,4,6-trichlorophenol) did not interfere with the HPLC analysis of G-4. Fig. 2B shows a representative chromatogram with a G-4 by the HPLC method. The standard curve indicates that the response of the LC detector was linear up to 100 mg/l of G-4 (correlation coefficient 0.9998, intercept $-0.017 \cdot 10^6$ and slope $0.093 \cdot 10^6$).

The G-4 recovery studies were carried out with 627–773 mg control samples (commercially treated with THPOH–NH_3 but without G-4 pretreatment), spiked with 3.0 mg of the fungicide in methanol, and extracted for 6 h. The G-4 (commercially) treated fabric (141–213 mg) was additionally spiked with 0.5 mg of G-4 per sample and Soxhlet extracted for 4–8 h as described above. The amount of G-4 present in the sample (unspiked) was subtracted from the spiked sample to determine the percentage of recovery from the spiked sample. The data indicate that the G-4 extraction was complete in 6 h and the mean value of the recovery was 101 ± 15.2% S.D.

Salicylanilide

Felt samples were Soxhlet extracted for 6 and 8 h, and the extract was analyzed by HPLC using a C_{18} (10 μm) column with 75% (v/v) methanol in Milli-Q water as the eluent. Other details of the extraction and HPLC parameters are given in Table I. Fig. 2C is a typical HPLC chromatogram with salicylanilide with a retention time of 3.25 min. The standard curve was linear from 10–500 mg/l of salicylanilide (correlation coefficient 0.9685, intercept $0.702 \cdot 10^6$ and slope $0.064 \cdot 10^6$). The HPLC data indicate that there was no difference in the amount of salicylanilide quantitated in felt samples extracted for 6 or 8 h, and salicylanilide in felt samples varied from 1.01–1.05% (w/w), with a mean value of 1.03 ± 0.014% S.D. Salicylaldehyde, salicylic acid, salicylamide and phenylsalicylate did not interfere with the quantitation of G-4 by this HPLC method. The amount of salicylanilide-like substances was 0.03% or less in those felt samples untreated by salicylanilide but treated with other functional finishes.

Recovery studies were carried out with salicylanilide-spiked felt samples. Untreated felt samples (*ca.* 200 mg in weight each) were spiked with 4 mg of salicylanilide and extracted for 6 and 8 h with 86.7% (v/v) ACN in Milli-Q water as described above. The salicylanilide extracted was quantitated by HPLC method described earlier. This study indicates that 94% (w/w) of the salicylanilide was recovered from felt samples after 6 h of extraction, and the percentage of recovery ranged from 90–95% (mean value 92 ± 2.0% S.D.).

Copper 8-quinolinolate

Since Cu-8 is a chelated compound of 8-hydroxyquinoline with copper, repeated attempts to quantitate this chelated compound by HPLC and GC were not successful. HPLC methods using normal- and reversed-phase column packing, with a number of eluents from polar to non-polar solvents were tried for the separation of Cu-8. The column packings evaluated included Bondapak, Phenyl, CN,

and NH_2 (Waters, Millipore) and ion-exchange columns. In many instances, the Cu-8 broke down slowly and irreversibly bound with the column packing, and thus changed the retention time and shape of the fungicide peak from run to run. Separation of this fungicide by GC was equally unsuccessful with and without derivatization of Cu-8 (including in-column derivatization) using a number of GC column packings. Since 8-hydroxyquinoline is the major (82%) and expensive ingredient of Cu-8, it was decided to quantitate 8-hydroxyquinoline, to measure the amount of Cu-8 present in samples.

Cu-8 was extracted three times from cotton fabrics (*ca.* 1 g) with hot 0.5 *M* H_2SO_4 solution. The total treatment time was 1.5 h. The three extracts were pooled and diluted to 25 ml volume. An aliquot of the extract was treated with an equal volume of 1.0 *M* Na_4EDTA solution and shaken vigorously for 1.0 min to release copper-bound 8-hydroxyquinoline from Cu-8. 8-Hydroxyquinoline that was released was extracted with methylene chloride by vigorous shaking again for 1.0 min. Other details of the extraction procedure are given in Fig. 3. The supernatant was aspirated off, and an aliquot of the methylene chloride containing 8-hydroxyquinoline was injected directly into the GC column. The GC parameters used for the quantitation of 8-hydroxyquinoline are given above and in Table I.

Two standard curves were prepared for the quantitation of Cu-8 in cotton fabrics; the first standard curve was prepared using 8-hydroxyquinoline solution in methylene chloride; and the second one was prepared using 8-hydroxyquinoline in methylene chloride prepared from Cu-8 as described above (dissolving Cu-8 in 0.5 *M* H_2SO_4, followed by Na_4EDTA treatment, and extraction of 8-hydroxyquinoline by methylene chloride as illlustrated in Fig. 3). The values obtained with the 8-hydroxyquinoline standard curve were converted to Cu-8 by multiplying the 8-hydroxyquinoline values by 1.2195. This conversion factor was calculated from the theoretical amount of 8-hydroxyquinoline (82%) in Cu-8. The standard curve was linear from 50–500 mg/l for both 8-hydroxyquinoline and Cu-8 (correlation coefficient 0.9978, intercept $-1.107 \cdot 10^3$ and slope $0.107 \cdot 10^3$). Fig. 2D shows the chromatogram obtained with 8-hydroxyquinoline by

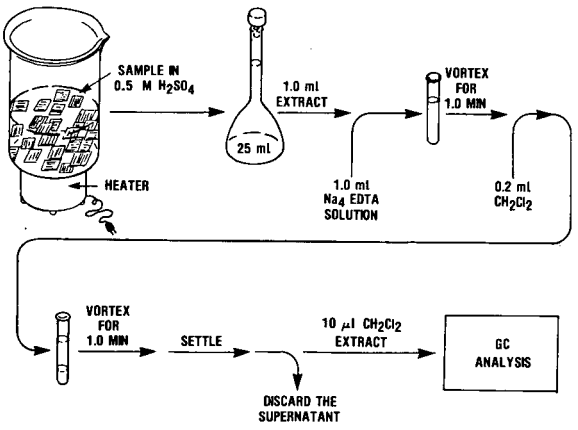

Fig. 3. Procedure for the extraction of copper 8-quinolinolate for the GC analysis.

GC, with a retention time of 2.79 min. Cu-8 values obtained with GC indicate that the amount of Cu-8 present in cotton fabric samples as calculated from 8-hydroxyquinoline and Cu-8 standard curves was comparable (0.64 ± 0.079 and 0.69 ± 0.079% S.D., respectively). GC studies with 2-hydroxyquinoline, 5-hydroxyquinoline, 2,4-quinolinediol, isoquinoline, 5,7-dibromo-8-hydroxyquinoline, 2-hydroxypyridine, 8-hydroxyquinaldine, and 8-hydroxyquinoline-N-oxide indicated that there was no interference from these compounds in the quantitation of 8-hydroxyquinoline (by GC).

Cu-8 recovery studies were carried out with cotton fabric samples (*ca.* 1.0 g each) spiked with 8.0 mg of the fungicide in pyridine and the solvent removed by air drying. Cu-8 was extracted and quantitated as described previously. The Cu-8 standard curve was used for the quantitation of 8-hydroxyquinoline in the Cu-8 spiked cotton fabric samples. The amount of Cu-8 extracted and quantitated by the GC method varied from 91–114% (with mean value of 101 ± 7.8% S.D.) of the spiked amount. The results indicate that the method will be able to quantitate accurately the amount of Cu-8 present in the test material [2,5,7].

The Cu-8 GC method developed and described here is reproducible, sensitive and could be automated. Cu-8 values calculated from 8-hydroxyquinoline data were consistent with those reported from copper determination (by atomic absorption) and colorimetric methods.

REFERENCES

1 *Federal Standard for Textile Test Methods, Federal Test Method Standard No. 191 A: Dihydroxydichlorodiphenylmethane, Colorimetric Method, Method 2011,* US Government Printing Office, Washington, DC, July 1978.
2 *Federal Standard for Textile Test Methods, Federal Test Method Standard No. 191 A: Copper 8-Quinolinolate Content of Textiles, Spectrophotometric Method, Method 2060,* US Government Printing Office, Washington, DC, July 1978.
3 *Federal Standard for Leather, Methods of Sampling and Testing No. 311: Para-nitropenol, Colorimetric Method, Method 6711,* US Government Printing Office, Washington, DC, January 1969.
4 *Military Specification, MIL-F-2312E, Felt, Hair or Wool: Mildew Resistant and Moisture Resistant Treatment,* US Government Printing Office, Washington, DC, 1984.
5 A. D. Baskin and A. M. Kaplan, *Analysis of Copper 8-Quinolinate and Copper Naphthenate Applied to Cotton Duck as an FWWMR Formulation,* in *Microbiological Deterioration Series No. 3,* Headquarters, Quartermaster Research & Engineering Command, US Army Quartermaster Research & Engineering Center, Natick, MA, September 1957.
6 S. Gottlieb and P. B. Marsh, *Ind. Eng. Chem.,* 18 (1946) 16–19.
7 A. G. Kempton, M. Greenberger and A. M. Kaplan, *Discrepancies between the Spectrophotometric and Total Copper Methods of Analysis of Copper 8-Quinolinate in Webbing,* in *Microbiological Deterioration Series No. 4,* Headquarters, Quartermaster Research & Engineering Command, Quartermaster Research and Engineering Center, Natick, MA, July 1961.
8 L. B. Hilliard and H. Freiser, *Anal. Chem.,* 24 (1952) 752–754.

Journal of Chromatography, 604 (1992) 255–260
Elsevier Science Publishers B.V., Amsterdam

CHROM. 24 216

Separation of non-steroidal anti-inflammatory agents using supercritical fluid chromatography

Nirdosh K. Jagota and James T. Stewart

Department of Medicinal Chemistry, College of Pharmacy, University of Georgia, Athens, GA 30602 (USA)

(First received November 5th, 1991; revised manuscript received February 18th, 1992)

ABSTRACT

Supercritical fluid chromatography (SFC) was investigated for the separation of non-steroidal anti-inflammatory agents (NSAIs). Three different stationary phases (SB-methyl-100, SB-biphenyl-30, and SB-cyanopropyl-50) were compared for the separation of the compounds. Baseline separation of a flufenamic acid, mefenamic acid, fenbufen and indomethacin mixture was achieved on the SB-biphenyl-30 column using a pressure gradient. A mixture containing flufenamic acid, mefenamic acid, acetylsalicylic acid, ketoprofen and fenbufen and another mixture containing ibuoprofen, fenoprofen, naproxen, ketoprofen and tolmetin were well separated on the SB-cyanopropyl-50 column using pressure gradients. Typical analysis time for a mixture of NSAIs on the biphenyl or cyanopropyl column was approximately 20–25 min. Application of the method using the biphenyl column to the determination of NSAIs present in selected commercial dosage forms was demonstrated.

INTRODUCTION

Supercritical fluid chromatography (SFC) is a complementary technique to high-performance liquid chromatography (HPLC) and gas chromatography (GC). The advantages of SFC include the possibility of analysis of thermally labile compounds and the use of both HPLC and GC type detectors including the UV–Vis and flame ionization detectors. Other advantages of SFC are that a supercritical fluid possesses solvating properties similar to those of a liquid, and the solute diffusion coefficients are more than two orders of magnitude greater than those found in liquids [1]. Commercial SFC instruments are available that can utilize both open-tubular capillary and packed columns. Capillary SFC offers the advantage of GC-type efficiency yielding a high number of theoretical plates.

There have been reports of the use of SFC in pharmaceuticals [2–6]. Wong and Dellafera [2] demonstrated the use of capillary SFC in therapeutic drug monitoring of phenobarbital in serum using a polymethylsiloxane stationary phase and a carbon dioxide mobile phase. Later *et al.* [3] have reported the analysis of steroids, antibiotics and cannabinoids on polymethylsiloxane capillary columns using carbon dioxide mobile phase. Crowther and Henion [4] demonstrated the SFC–mass spectrometric analysis of codeine, caffeine, cocaine, phenylbutazone and methocarbamol by using packed amino and silica columns and a modified direct liquid-introduction interface. The mobile phase was carbon dioxide modified with methanol. Smith and Sangi [5] have reported the SFC analysis of barbiturates using polystyrene–divinylbenzene or octadecylsilane stationary phases with methanol-modified carbon dioxide as mobile phase. Perkins *et al.* [6] have reported the analysis of veterinary antibiotics (levamisol, furazolidone, chloramphenicol and lincomycin) on an amino-bonded stationary phase also utilizing carbon dioxide with methanol modifier.

In this paper, the separation of non-steroidal anti-inflammatory agents (NSAIs) using capillary SFC was explored. NSAI analgesics were chosen as

Correspondence to: Dr. J. T. Stewart, Department of Medicinal Chemistry, College of Pharmacy, University of Georgia, Athens, GA 30602, USA.

model compounds due to their wide use and applicability. These studies were concerned with separation of NSAI mixtures using three different stationary phases (SB-methyl-100, SB-biphenyl-30 and SB-cyanopropyl-50) with carbon dioxide as mobile phase. The SFC method using the biphenyl column was then applied to the determination of NSAIs in selected dosage forms.

EXPERIMENTAL

Reagents and chemicals

HPLC-grade absolute methanol was purchased from J. T. Baker (Phillipsburg, NJ, USA). Puradisc 25TF, 0.45-μm filters were obtained from Whatman (Maidstone, UK). Supercritical fluid chromatography grade carbon dioxide was obtained from Scott Specialty Gases (Plumsteadville, PA, USA).

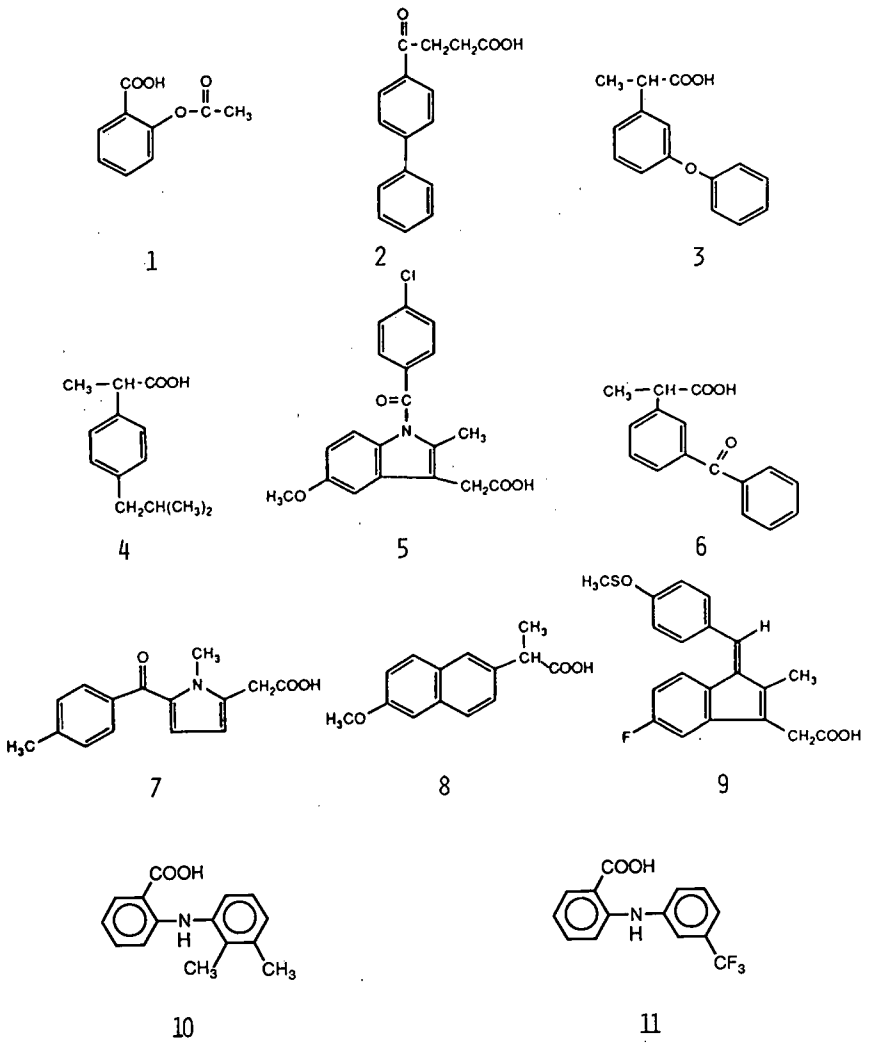

Fig. 1. Structural formulae of NSAI compounds studied. 1 = Acetylsalicylic acid; 2 = fenbufen; 3 = fenoprofen; 4 = ibuprofen; 5 = indomethacin; 6 = ketoprofen; 7 = tolmetin; 8 = naproxen; 9 = sulindac; 10 = mefenamic acid; 11 = flufenamic acid.

The structural formulae of the compounds studied are shown in Fig. 1. Fenoprofen calcium and naproxen sodium were purchased from the United States Pharmacopeial Convention (Rockville, MD, USA). Acetylsalicylic acid was obtained from Aldrich (Milwaukee, WI, USA). Fenbufen, ibuprofen, indomethacin, ketoprofen, sulindac, flufenamic acid and mefenamic acid were purchased from Sigma (St. Louis, MO, USA). Commercial tablet and capsule dosage forms of the various NSAI analgesics were obtained from a local pharmacy.

Instrumentation

Chromatography was performed on a Lee Scientific Model 600D supercritical fluid chromatograph (Salt Lake City, UT, USA) equipped with a pump, oven and flame-ionization detector and controlled by a Dell computer (ACI 600D, software version 2.2). SFC was performed on three different stationary phases: a 5 m × 100 μm I.D. SB-methyl-100 (200 μm O.D. and 0.25 μm film thickness), 10 m x 50 μm I.D. SB-biphenyl-30 and a SB-cyanopropyl-50 (both 195 μm O.D. and 0.25 μm film thickness). All three columns were purchased from Lee Scientific.

Preparation of drug solutions

Solutions of each NSAI drug were prepared by accurately weighing 5 mg of each drug and dissolving in 5 ml of absolute methanol to give a final concentration of approximately 1 mg/ml.

Chromatographic parameters

Pump program. Multilinear pressure program: 7 min hold at an initial pressure of 100 atm, then 25 atm/min ramp to 250 atm, followed by a 4.0 atm/min ramp to 290 atm.

Oven program. Isothermal at 130°C.

Columns. 5 m × 100 μm SB-methyl-100, 10 m × 50 μm SB-biphenyl-30 and 10 × 50 μm SB-cyanopropyl-50.

Injection type. Time split set at 200 ms. Injection ratio approximately 20:1, giving an injection volume of approximately 25 nl.

Detector. Flame ionization at 375°C.

Mobile phase. Supercritical fluid chromatography grade carbon dioxide. Analysis time: 20–25 min.

RESULTS AND DISCUSSION

The goal of this study was to investigate the separation of NSAIs using capillary SFC. These widely used drugs exhibit variation in structure and functional group chemistry to provide a representative sample of acidic compounds of pharmaceutical interest. There have been no reports in the scientific literature describing the use of SFC in the analysis of these compounds.

Three different capillary columns, SB-methyl-100, SB-biphenyl-30 and SB-cyanopropyl-50, were compared for the separation of these drugs. The SB-methyl-100 column is coated with 100% methylpolysiloxane and is cross-linked for SFC use. Several different temperature and pressure gradients were investigated. The NSAIs could not be chromatographed on this column due to poor peak shape and overlapping of peaks.

The SB-biphenyl-30 column is coated with 30% biphenyl and 70% methylpolysiloxane and is also cross-linked for SFC use. After investigating several pressure gradients (25 atm/min to 3 atm/min), the gradient described above in the Experimental section was found to give the best separation of NSAIs. The SFC oven temperature was investigated in the range 80–140°C in the isothermal mode.

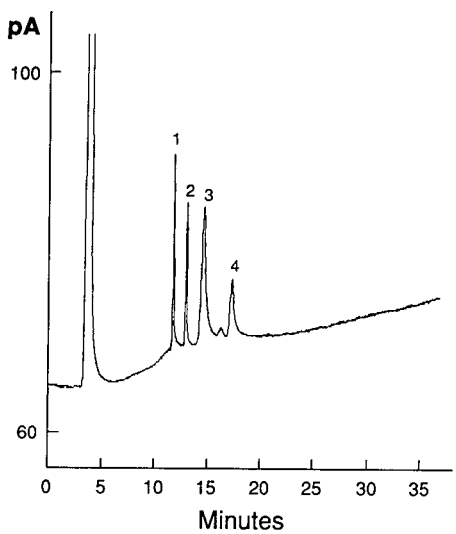

Fig. 2. Typical SFC separation of flufenamic acid (1), mefenamic acid (2), fenbufen (3) and indomethacin (4) on a SB-biphenyl-30 column.

TABLE I

ANALYTICAL FIGURES OF MERIT WITH SB-BIPHENYL-30 COLUMN

Compound	Retention time (min)	Tailing factor[a]	LOD (μg/ml)[b]	Amount injected on column (ng)
Ibuprofen	11.8	1.05	100	2.5
Flufenamic acid	11.9	1.00	75	1.8
Fenoprofen	12.4	1.25	100	2.5
Mefenamic acid	13.1	1.06	75	1.8
Naproxen	13.5	1.43	100	2.5
Tolmetin	14.6	1.40	150	3.8
Fenbufen	14.7	1.50	100	2.5
Ketoprofen	15.0	1.13	100	2.5
Indomethacin	17.5	1.50	100	2.5
Sulindac	21.5	0.63	250	6.3

[a] Calculated according to the USP XXII method (ref. 7).
[b] Signal-to-noise ratio 3.

The separation of the compounds on the biphenyl column was adequate, but the compounds were not all separated in a single injection. However, certain groups of NSAIs can be efficiently separated. Fig. 2 shows the SFC separation of a flufenamic acid, mefenamic acid, fenbufen and indomethacin mixture on the biphenyl column. The analytical figures of merit for each drug on the biphenyl column are shown in Table I. Tailing factors were generally in the 1.0–1.5 range except for sulindac, which exhibited some frontal tailing. The limits of detection (LOD) based on a signal-to-noise ratio of 3 were in the range of 75–250 μg/ml corresponding to approximately 1.8–6.3 ng of analyte injected on col-

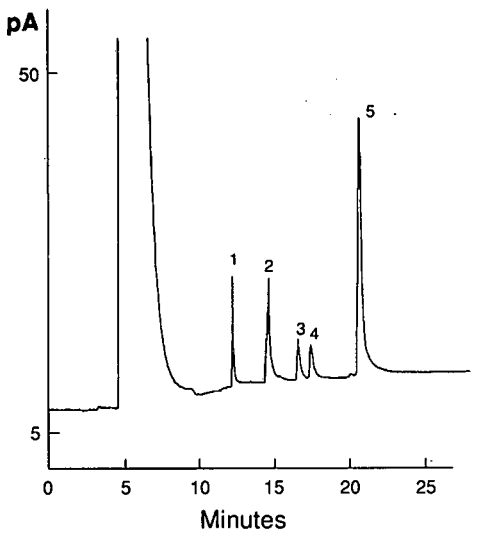

Fig. 3. Typical SFC separation of ibuprofen (1), fenoprofen (2), naproxen (3), ketoprofen (4) and tolmetin (5) on a SB-cyanopropyl-50 column.

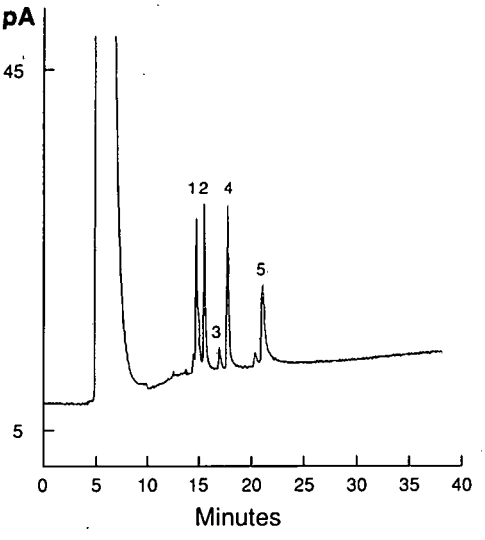

Fig. 4. Typical SFC separation of flufenamic acid (1), mefenamic acid (2), acetylsalicylic acid (3), ketoprofen (4) and fenbufen (5) on a SB-cyanopropyl-50 column.

TABLE II

ANALYTICAL FIGURES OF MERIT WITH SB-CYANOPROPYL-50 COLUMN

Compound	Retention time (min)	Tailing factor[a]	LOD (μm/ml)[b]	Amount injected on column (ng)
Ibuprofen	12.3	1.25	100	2.5
Sulindac	13.9	1.50	250	6.3
Flufenamic acid	14.5	1.00	80	2.0
Fenoprofen	14.7	1.38	100	2.5
Mefenamic acid	15.2	1.05	80	2.0
Naproxen	16.7	1.31	200	5.0
Acetylsalicylic acid	16.7	1.13	400	10.0
Ketoprofen	17.5	1.33	80	2.0
Fenbufen	20.8	1.50	150	3.8
Tolmetin	20.8	1.76	150	3.8

[a] Calculated according to the USP XXII method (ref. 7).
[b] Signal-to-noise ratio 3.

umn. One of the disadvantages of SFC instrumentation at the present time is its inability to allow for larger sample volumes to be injected on column and hence, improve the sensitivity of the method.

The SB-cyanopropyl-50 column is coated with 50% cyanopropyl and 50% methylpolysiloxane. It is considered the most polar column among the commercially available SFC columns. The same chromatographic parameters that were applied to the SB-biphenyl-30 column above were also used for comparison purposes. Retention increased for all of the analytes compared to that obtained on the

TABLE III

COMPARISON OF RELATIVE RETENTION BEHAVIOR OF SELECTED NSAIs ON OCTADECYLSILANE AND UNDERIVATIZED SILICA HPLC COLUMNS *VERSUS* SB-BIPHENYL AND SB-CYANOPROPYL SFC COLUMNS

HPLC Columns				SFC Columns			
Octadecylsilane[a]		Underivatized Silica[b]		SB-biphenyl[c]		SB-cyanopropyl[c]	
Compound	k'	Compound	k'	Compound	k'	Compound	k'
Tolmetin	3.77	Sulindac	0.7	Ibuprofen	1.4	Ibuprofen	0.8
Sulindac	5.02	Fenoprofen	1.1	Fenoprofen	1.5	Sulindac	1.0
Ketoprofen	5.98	Ibuprofen	1.1	Naproxen	1.7	Fenoprofen	1.1
Naproxen	6.59	Naproxen	1.3	Tolmetin	1.9	Naproxen	1.4
Fenbufen	7.46	Tolmetin	1.4	Fenbufen	2.0	Aspirin	1.4
Fenoprofen	8.54	Ketoprofen	1.5	Ketoprofen	2.0	Ketoprofen	1.5
Indomethacin	8.86	Fenbufen	2.6	Indomethacin	2.6	Fenbufen	2.0
Ibuprofen	10.01	Indomethacin	3.6	Sulindac	3.3	Tolmetin	2.0

[a] Solvent programming using acetonitrile–0.05 *M* acetate buffer, pH 4.5; column temperature 35°C; flow-rate 0.8 ml/min; detector set at 254 nm (ref. 8).
[b] 5 m*M* Sodium phosphate buffer, pH 2.6–acetonitrile (95.5, v/v); 1 ml/min; and detector set at 254 nm (ref. 9).
[c] See chromatographic parameters, Experimental section.

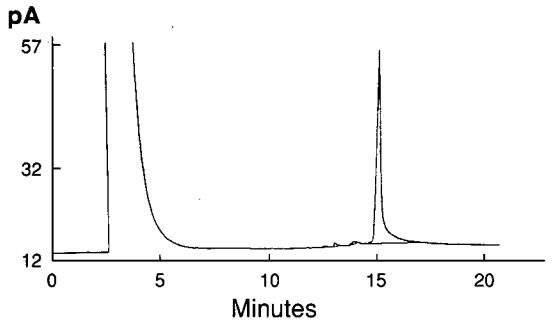

Fig. 5. Typical SFC chromatogram of ketoprofen in a dosage form on a SB-biphenyl-30 column.

SB-biphenyl-30 column. Figs. 3 and 4 show a comparison of chromatographic separations of two groups of NSAIs on the SB-cyanopropyl-50 column. The analytical figures of merit for each drug on the cyanopropyl column are shown in Table II. Tailing factors were generally in the 1.0–1.76 range. Limits of detection based on signal-to-noise ratio of 3 were in the range of 80–400 μg/ml corresponding to 2.0–10.0 ng of analyte injected on column.

A comparison of the relative retention behavior of selected NSAIs using two HPLC stationary phases *versus* our SFC stationary phases is shown in Table III. Capacity factors (k') are being used here only for comparison purposes since the SFC separations all involved pressure gradients and one of the HPLC separations was obtained under solvent programming conditions. However, the SFC capacity factors can be utilized as system suitability parameters for day-to-day SFC operations.

Since our studies indicated that both the biphenyl and cyanopropyl columns were suitable for the separation of NSAIs, the biphenyl column was arbitrarily chosen to demonstrate the applicability of the SFC method to selected pharmaceutical dosage forms. Linear calibration curves in the range 0.5–4 mg/ml were obtained for each of the three NSAIs chosen for study. The correlation coefficients calculated were better than 0.99 ($n=4$). A typical chromatogram obtained for a ketoprofen dosage form is shown in Fig. 5. The results obtained in Table IV suggest that the proposed SFC method can be a useful procedure for the routine determination of

TABLE IV

AMOUNTS OF NSAIs IN PHARMACEUTICALS

The contents of a NSAI tablet or capsule were dissolved in absolute methanol with the aid of sonication, filtered if necessary, and injected into the SFC chromatograph. R.S.D. = Relative standard deviation.

Compound	Labeled strength (mg)	Amount found ± S.D. (mg) ($n=3$)
Ibuprofen[a]	800	760.5 ± 38.70 (R.S.D. 5.1%)
Ketoprofen[b]	75	77.1 ± 3.45 (R.S.D. 4.5%)
Mefenamic acid[c]	250	252.4 ± 8.37 (R.S.D. 3.3%)

[a] IBU, Boots, Lot No. B6132.
[b] Orudis, Wyeth Lab., Lot No. 9880476.
[c] Ponstel, Parke-Davis, Lot No. 06449FA.

NSAIs in pharmaceuticals. No claim is made that the assay is stability-indicating since the separation of by- and degradation products of each drug was not investigated.

ACKNOWLEDGEMENT

This work was supported by a grant from Hoffmann–La Roche, Inc., Nutley, NJ, USA.

REFERENCES

1 I. K. Barker, J. P. Kithji, K. D. Bartle, A. A. Clifford, G. F. Shilstone, P. A. Halford-Malu and M. W. Raynor, *Analyst (London)*, 114 (1989) 41.
2 S. H. Y. Wong and S. S. Dellafera, *J. Liq. Chromatogr.*, 13 (1990) 1105.
3 D. W. Later, B. E. Richter and M. R. Andersen, *LC · GC*, 4 (1988) 992.
4 J. B. Crowther and J. D. Henion, *Anal. Chem.*, 57 (1985) 2711.
5 R. M. Smith and M. M. Sangi, *J. Chromatogr.*, 481 (1989) 63.
6 J. R. Perkins, D. E. Games, J. R. Startin and J. Gilbert, *J. Chromatogr.*, 540 (1991) 257.
7 *United States Pharmacopeia, 22nd ed.–National Formulary*, 17th ed., The United States Pharmacopeial Convention, Rockville, MD, 1991, p. 1566.
8 H. J. Battista, G. Wehinger and R. Henn, *J. Chromatogr.*, 345 (1985) 77.
9 B. M. Lampert and J. T. Stewart, *J. Chromatogr.*, 504 (1990) 381.

Journal of Chromatography, 604 (1992) 261–265
Elsevier Science Publishers B.V., Amsterdam

CHROM. 24 129

Determination of the reactivity of uracil derivatives with respect to methyl iodide by high-performance thin-layer chromatographic densitometry

G. Vampa, S. Benvenuti and P. Pecorari

Dipartimento di Scienze Farmaceutiche, Università degli Studi di Modena, Via Campi 183, 41100 Modena (Italy)

(First received November 19th, 1991; revised manuscript received February 24th, 1992)

ABSTRACT

A high-performance thin-layer chromatographic method is described for the investigation of the methylation rates of uracil, 5-fluoro-, 5-chloro-, 5-bromo-, 5-methyl- and 5-nitrouracil and their N^1- and N^3-methyl derivatives. The method allowed the amounts of compounds obtained, the time required to complete the reaction and therefore the reactivity of the uracil derivatives to be determined. The N^1- and N^3-methyl and $N^{1,3}$-dimethyl derivatives were synthesized and separated by droplet countercurrent chromatography and/or medium-pressure liquid chromatography and their R_F values were determined in different solvent systems by thin-layer chromatography.

INTRODUCTION

A high-performance thin-layer chromatographic (HPTLC) investigation into the reactivity with respect to methyl iodide of uracil, 5-fluoro-, 5-chloro-, 5-bromo-, 5-methyl- and 5-nitrouracil and their N^1-methyl and N^3-methyl derivatives in anionic form and tautomeric equilibrium (Table I) was carried out. For this purpose, uracil derivatives (**II**, **VI–VIII**, **X–XII**, **XV**, **XVI**, **XVIII–XX**, **XXII–XXIV**) were synthesized and separated by droplet countercurrent chromatography (DCCC) and/or medium-pressure liquid chromatography (MPLC) and their R_F values were determined in suitable solvent systems by TLC. An HPTLC method was set up with the aim of following the course of the methylation reaction of uracil and its 5-substituted derivatives to give monomethyl and dimethyl derivatives and that of their N^1- and N^3-methyl derivatives to give $N^{1,3}$-dimethyl derivatives under different experimental conditions.

Correspondence to: Dr. G. Vampa, Dipartimento di Scienze Farmaceutiche, Università degli Studi di Modena, Via Campi 183, 41100 Modena, Italy.

EXPERIMENTAL

Materials

Compounds **I**, **III**, **IV**, **V**, **IX**, **XIII**, **XIV**, **XVII** and **XXI** were purchased from Sigma (St. Louis, MO, USA) and used after crystallization.

Silica gel 60 F_{254} TLC plates (20 × 20 cm, 0.25 mm) and silica gel 60 F_{254} HPTLC plates (10 × 20 cm, 0.20 mm) were supplied by Merck (Darmstadt, Germany).

All solvents were of analytical-reagent grade and were obtained from Merck.

Apparatus

Droplet countercurrent chromatography (DCCC). The separations were achieved on a Buchi (Flawil, Switzerland) DCCC 670 apparatus equipped with 200 columns (2.7 mm I.D.). The solvent system for all separations was chloroform–methanol–water (5:5:3, v/v/v) in the descending mode. A Buchi Model 683 UV detector with a 254-

0021-9673/92/$05.00

TABLE I

STRUCTURES OF URACIL COMPOUNDS

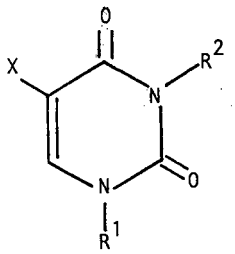

Compound	X	R^1	R^2	Compound	X	R^1	R^2
I	H	H	H	**XIII**	Br	H	H
II	H	CH_3	H	**XIV**	Br	CH_3	H
III	H	H	CH_3	**XV**	Br	H	CH_3
IV	H	CH_3	CH_3	**XVI**	Br	CH_3	CH_3
V	F	H	H	**XVII**	CH_3	H	H
VI	F	CH_3	H	**XVIII**	CH_3	CH_3	H
VII	F	H	CH_3	**XIX**	CH_3	H	CH_3
VIII	F	CH_3	CH_3	**XX**	CH_3	CH_3	CH_3
IX	Cl	H	H	**XXI**	NO_2	H	H
X	Cl	CH_3	H	**XXII**	NO_2	CH_3	H
XI	Cl	H	CH_3	**XXIII**	NO_2	H	CH_3
XII	Cl	CH_3	CH_3	**XXIV**	NO_2	CH_3	CH_3

nm filter, coupled with an LKB (Bromma, Sweden) Model 2210 recorder and an LKB Multirac 2111 fraction collector, was connected to the DCCC apparatus.

Medium-pressure liquid chromatography (MPLC). A Buchi Model 685 MPLC glass column (460 × 36 mm I.D.) was dry-filled with silica gel 60 (particle size 0.015–0.040 mm) (Merck) and connected to an LKB Multirac 2111 fraction collector. The fractions were monitored using 5 × 10 cm TLC plates.

The mobile phases for preparative MPLC separation were toluene–acetone (1:1, v/v) (system 2, Table II) for the separation of methyl derivatives of **I**, **XVII** and **XXI** and dichloromethane–ethylacetate (1:1, v/v) (system 5, Table II) for methyl derivatives of **V**, **IX** and **XIII**.

High-performance thin-layer chromatography (HPTLC). Samples were applied by means of a Linomat IV spotter (Camag, Muttenz, Switzerland) on 10 × 20 cm HPTLC plates. The solvent systems were system 2 for methyl derivatives of **I** and **XVII**, system 5 for methyl derivatives of **V**, **IX** and **XIII** and benzene–acetone (1:1, v/v) (system 1, Table II) for methyl derivatives of **XXI**.

All the plates were developed at room temperature using the ascending mode in a chromatographic tank previously saturated with eluent mixture. The layers were analysed at 254 nm by the fluorescence quenching method using a Camag TLC Scanner II linked to an Olivetti M280 PC operating the "Cats 3.04" (Camag) scanning program. The scanner was set up as follows: band with, 10 nm; span, 25; slit, 5 × 0.2 mm; and scanning speed, 5 mm/s.

Melting points were determined on a Buchi Model 510 apparatus and are uncorrected.

The compounds were analysed for C, H, N; the values obtained were within ± 0.3% of the theoretical values.

UV spectra were obtained with a Lambda 5 spectrophotometer (Perkin-Elmer, Norwalk, CT, USA) in 10^{-5} *M* buffered solution at pH 4 for the neutral form and at pH 13 or 11 for the monodeprotonated form: compounds **I**, **V**, **IX** and **XIII** are completely monodissociated at pH 11, whereas **XVII** and the N^1-methyl- and N^3-methyluracil derivatives **II**, **III**, **VI**, **VII**, **X**, **XI**, **XIV**, **XV**, **XVIII**, **XIX**, **XXII** and **XXIII** are completely dissociated at pH 13 [1,2].

Synthesis

Methylation of **I**, **V**, **IX**, **XIII**, **XVII** and **XXI** was carried out by suspending the compounds in acetonitrile and then adding tetrabutylammonium hydroxide (TBAH) (25% in methanol) (1–1.5 mol) and methyl iodide (1–1.5 mol). The mixture was stirred for 1 h at 40°C, thermostated at 40°C for 2 h and dried under vacuum; the crude material was then extracted with chloroform. The chloroform extract, consisting of starting product and N^1-methyl, N^3-methyl and $N^{1,3}$-dimethyl derivatives, was separated by DCCC and/or MPLC.

The melting points of the separated compounds were identical to those reported in the literature {**II**, **III**, **XV**, **XXII**, **XXIII** and **XXIV** [3]; **VI** [4]; **VII** [5]; **VIII** [6]; **X** [7]; **XII** [8]; **XVI**, **XVIII**, **XIX** and **XX**, [1]; **XI**, m.p. 189–191°C [acetone–light petroleum (b.p. 60–80°C] [9]}.

The physico-chemical properties of **I**–**XXIV** correspond to those reported in the literature [1,2,8].

Study of methylation reaction of uracil and 5-substituted uracil

TBAH (25% in methanol) (1 equiv.) was added to 0.2–0.3 mmol of **I**, **V**, **IX**, **XIII**, **XVII** and **XXI** in a 10-ml volumetric flask which was then filled to the mark with acetonitrile. The stirred solution was heated at 40°C and methyl iodide (1 equiv.) was added. Suitable volumes of standard solutions of starting product and of the respective methyl derivatives in acetonitrile were spotted alternately on to HPTLC plates with 2 μl of reaction mixture taken after 0, 3, 6, 10, 15, 30, 60 and 90 min.

The identities of the compounds were determined by means of the R_F values and by a computerized identity check procedure of UV spectra, which confirmed the correlation of the sample spectra with the standard spectrum. Calibration graphs were plotted for each plate by using the linear regression equation obtained from the area values under the peaks for different amounts of standard solution. The linearity correlation coefficient was between 0.997 and 0.998 for all compounds. The reproducibility of method was assessed from repeated analyses of spots containing 50 ng of compounds per spot; the relative standard deviations were between 1.8% and 3.5%. The recoveries of the compounds from artificial reaction mixtures were between 90.8% and 102.5%.

The study of the methylation reaction of N^1-methyl (**II**, **VI**, **X**, **XIV**, **XVIII** and **XXII**) and N^3-methyl derivatives (**III**, **VII**, **XI**, **XV**, **XIX** and **XXIII**) to the corresponding $N^{1,3}$-dimethyl derivatives was carried out following the procedure described above. Reactivity to the methylation of **I** was also determined at 0 and 25°C.

RESULTS AND DISCUSSION

DCCC and MPLC proved to be suitable techniques for separating the following reaction mixtures: **I**–**IV**, **V**–**VIII**, **IX**–**XII**, **XIII**–**XVI**, **XVII**–**XX** and **XXI**–**XXIV**.

In the case of the mixtures **I**–**IV**, **V**–**VIII**, **IX**–**XII**, **XIII**–**XVI** and **XVII**–**XX**, TLC analysis (Table II) revealed decreasing R_F values in the order $N^{1,3}$-di-

TABLE II

R_F VALUES OF URACIL DERIVATIVES

Compound	Solvent system[a]					
	1	2	3	4	5	6
I	0.25	0.16	0.09	0.21	0.07	0.53
II	0.33	0.23	0.10	0.21	0.12	0.69
III	0.43	0.34	0.14	0.32	0.18	0.73
IV	0.52	0.43	0.20	0.32	0.25	0.85
V	0.41	0.31	0.11	0.40	0.18	0.51
VI	0.52	0.43	0.20	0.43	0.27	0.62
VII	0.59	0.48	0.27	0.56	0.36	0.70
VIII	0.69	0.59	0.41	0.57	0.50	0.85
IX	0.45	0.39	0.21	0.51	0.28	0.63
X	0.58	0.52	0.31	0.54	0.40	0.75
XI	0.63	0.56	0.37	0.65	0.49	0.77
XII	0.76	0.67	0.51	0.67	0.61	0.91
XIII	0.45	0.39	0.17	0.54	0.29	0.55
XIV	0.60	0.52	0.32	0.58	0.44	0.70
XV	0.65	0.59	0.39	0.67	0.55	0.73
XVI	0.75	0.69	0.53	0.69	0.69	0.83
XVII	0.26	0.23	0.06	0.12	0.06	0.44
XVIII	0.42	0.37	0.12	0.20	0.15	0.61
XIX	0.53	0.48	0.22	0.35	0.22	0.62
XX	0.66	0.59	0.32	0.38	0.35	0.82
XXI	0.31	0.20	0.08	0.13	0.08	0.12
XXII	0.62	0.52	0.25	0.52	0.38	0.45
XXIII	0.55	0.47	0.25	0.38	0.30	0.41
XXIV	0.77	0.65	0.46	0.62	0.57	0.74

[a] 1 = Benzene–acetone (1:1, v/v); 2 = toluene–acetone (1:1, v/v); 3 = chloroform–ethylacetate (1:1, v/v); 4 = chloroform–ethylacetate (1:9, v/v); 5 = dichloromethane–ethylacetate (1:1, v/v); 6 = chloroform–methanol–water (5:5:3, v/v/v).

TABLE III

UV λ_{max} VALUES

Compound	Conditions[a]		Compound	Conditions[a]	
	1	2		1	2
I	259	261/262	**XIII**	276	283
II	267	272/271	**XIV**	283	289
III	259	261	**XV**	275	282
IV	266	270	**XVI**	283	288
V	266	272	**XVII**	265	269
VI	273	279	**XVIII**	273	277
VII	266	272	**XIX**	265	269
VIII	273	279	**XX**	272	276
IX	274	281	**XXI**	300	339
X	279	288	**XXII**	309	310
XI	274	282	**XXIII**	299	339
XII	280	287	**XXIV**	309	308

[a] 1 = In buffered solution at pH 4; 2 = on HPTLC plate, scanning in the reflectance mode.

TABLE IV

AMOUNTS OF $N^{1,3}$-DIMETHYL DERIVATIVES OBTAINED FROM 1 mmol OF N^1-METHYL- OF N^3-METHYL-5-URACIL DERIVATIVES AT 40°C AFTER 15 min

Starting compound	$N^{1,3}$-Dimethyl-5-uracil derivative	Amount obtained (mmol)
II	**IV**	0.83
VI	**VIII**	0.90
X	**XII**	0.88
XIV	**XVI**	0.92
XVIII	**XX**	0.98
XXII	**XXIV**	0.88
III	**IV**	0.89
VII	**VIII**	0.99
XV	**XVI**	0.69
XIX	**XX**	0.95
XXIII	**XXIV**	0.30

methyl- > N^3-methyl- > N^1-methyl > uracil, which correlated with the pK_a values [1,2].

The UV adsorption band used to identify the compounds was the higher wavelength band corresponding to the π–π^* transition of the chromophore N_1–C_6=C_5–C_4=O.

The pattern of the UV spectra of each compound was the same, whether in solution [1,2] or on the plate; in the latter instance, and with the exception of the pair **XXII**–**XXIV**, the λ_{max} was slightly higher (Table III). This difference may be attributed to a greater interaction between the substance and the chromatographic support with a consequent reduction in the π–π^* electronic transition energies, due to a lowering of π^*.

The reactions showed that, after 15 min at 40°C, methylation of the N^1-methyl and N^3-methyl derivatives with exception of the N^3-methyl-5-nitrouracil (**XXIII**) (table IV) was virtually complete and was independent of the nature of the substituent at the 5-position, and methylation of **I**, **V**, **IX**, **XIII** and **XVII** was rapid whereas that of **XXI** was slower (Table V). In every instance, mixtures of N^1-methyl and $N^{1,3}$-dimethyl derivative were formed together with small amounts of the substituted N^3-isomer and starting product.

TABLE V

AMOUNTS OF N^1-METHYL, N^3-METHYL AND $N^{1,3}$-DIMETHYL DERIVATIVES OBTAINED FROM 1 mmol OF 5-URACIL DERIVATIVES AT 40°C AFTER 15 min

Starting compound	N^1-Methyl-	Amount obtained (mmol)	N^3-Methyl-	Amount obtained (mmol)	$N^{1,3}$-Dimethyl-	Amount obtained (mmol)
I	**II**	0.56	**III**	0.01	**IV**	0.30
V	**VI**	0.33	**VII**	0.06	**VIII**	0.31
IX	**X**	0.43	**XI**	0.04	**XII**	0.23
XIII	**XIV**	0.46	**XV**	0.05	**XVI**	0.26
XVII	**XVIII**	0.29	**XIX**	0.07	**XX**	0.36
XXI	**XXII**	0.28	**XXIII**	0.03	**XXIV**	0.06

TABLE VI

AMOUNTS OF N^1-METHYL (**II**), N^3-METHYL (**III**) and $N^{1,3}$-DIMETHYL (**IV**) DERIVATIVES OBTAINED FROM 1 mmol OF 5-URACIL (**I**) AT 0, 15 and 40°C AFTER 15 min

Temperature (°C)	Amount obtained (mmol)		
	II	**III**	**IV**
0	0.18	0.30	0.15
15	0.44	0.04	0.26
40	0.56	0.01	0.30

Tests conducted on **I** at 0 and 25°C (Table VI) showed that as the temperature increased so did the yield of N^1- and $N^{1,3}$-dimethyl derivatives, whereas the percentage of N^3-methyl derivative remained almost constant.

CONCLUSIONS

The HPTLC apparatus gave rapid and accurate information about the reactivity of the uracil derivatives, the amount of compounds obtained and the time required to complete the reactions. In particular, it emerged that, with the exception of 5-nitrouracil, methylation, which hitherto has been continued for longer periods [1], is complete within the first 15 min. The HPTLC method allowed the reactivity of various uracil derivatives to be followed and could therefore be a helpful technique in optimizing organic reactions.

ACKNOWLEDGEMENT

The authors thank Miss S. Selmi for the microanalyses, carried out in the Microanalyses Laboratory of the Dipartimento di Scienze Farmaceutiche (Università di Modena).

REFERENCES

1 P. Pecorari, G. Vampa, A. Albasini, M. Rinaldi, M. Melegari and M. P. Costi, *Farmaco, Ed. Sci.*, 43 (1988) 311.
2 P. Pecorari, A. Albasini, M. P. Costi, M. Rinaldi, I. Baraldi, *Int. J. Purine Pyridine Res.*, in press.
3 D. J. Brown, E. Horger and S. F. Mason, *J. Chem. Soc.*, (1955) 211.
4 G. J. Durr, *J. Med. Chem.*, 8 (1965) 253.
5 M. Gacek and K. Undheim, *Acta Chem. Scand.*, 33 (1979) 515.
6 N. G. Kundu and S. A. Schmitz, *J. Pharm. Sci.*, 71 (1982) 935.
7 C. Bimal and J. Pal, *J. Am. Chem. Soc.*, 100 (1978) 5170.
8 T. Harayama, K. Kotoji, R. Yanada, F. Yoneda, T. Taga, K. Osaki and T. Nagamatsu, *Chem. Pharm. Bull.*, 34 (1986) 2354.
9 M. P. Costi, Thesis, Dottorato di Ricerca, Department of Pharmaceutical Science, University of Modena, Modena, 1988.

Journal of Chromatography, 604 (1992) 267–281
Elsevier Science Publishers B.V., Amsterdam

CHROM. 24 190

Rugged method for the determination of deamidation products in insulin solutions by free zone capillary electrophoresis using an untreated fused-silica capillary

Gitte Mandrup

Chromatographic Laboratory, Novo Nordisk A/S, Hallas Allé, DK-4400 Kalundborg (Denmark)

(First received January 8th, 1992; revised manuscript received March 20th, 1992)

ABSTRACT

Addition of zwitterions and acetonitrile to the running buffer provided a successful separation of insulin and deamidation products in an untreated fused-silica capillary. A high efficiency and reproducible migration times were obtained without a base wash between each run and without thermostating of the capillary. A comparison was made of results achieved using capillary zone electrophoresis (CZE), ion-exchange chromatography (IEC) and reversed-phase high-performance liquid chromatography. A good correlation was observed between CZE and IEC.

INTRODUCTION

The aim of this study was to find a rugged and reproducible method for the determination of deamidation products in insulin solutions. The most common technique used for analysing the neutral and the acidic desamido compounds in insulin samples is disc electrophoresis [1]. Ion-exchange chromatography (IEC) is also a very useful method for the determination of desamido products in insulin, but a faster and less time-consuming, and also less expensive, method is desirable. As capillary zone electrophoresis (CZE) seemed to be a good alternative to the above two methods, experiments with CZE were started. Furthermore, CZE apparatus requires a minimum of maintenance and is easy to operate. A readily accessible and reproducible application of CZE was developed.

In this study human insulin (HI) was used as the main component. The molecular mass of HI is 5808 [2] and the isoelectric point is 5.5 [1–4]. The primary structure of HI was published by Nicol and Smith in 1960 [5], and the structure is shown in Fig. 1. HI consists of two peptide chains, A and B. The A-chain and B-chain contain 21 and 30 amino acids, respectively, connected through two interchain disulphide bridges. On standing, insulin in solution decomposes owing to deamidation at rates depending *inter alia* on the storage temperature. Desamido-insulin generated in acidic medium is hydrolysed in position A21 and monodesamido-A21-insulin is formed [1,7], which in the following is referred to as acidic desamido-insulin. The product formed at neutral pH is deamidated in the B-chain by hydrolysis of Asn-B3, and in the following is referred to as neutral desamido-insulin.

Several strategies have been developed to overcome the problems resulting from adsorption of proteins on the silanol surface of fused-silica capillaries. Of the numerous approaches to prevent the protein from sticking to the wall, this work was focused on changing the pH of the running buffer and using additives in the buffer. At near neutral pH,

Correspondence to: Dr. G. Mandrup, Chromatographic Laboratory, Novo Nordisk A/S, Hallas Allé, DK-4400 Kalundborg, Denmark.

0021-9673/92/$05.00

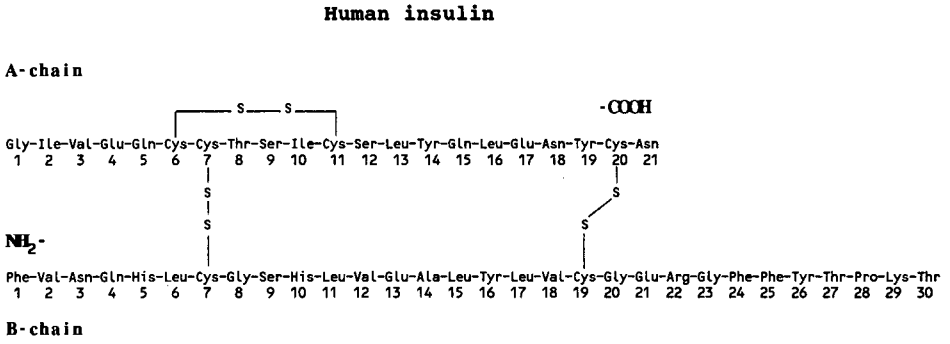

Fig. 1. Primary structure of human insulin [6].

the negatively charged exposed silanol groups in the bare silica capillary often cause protein samples to adsorb on the column walls. This silanol–protein attraction results in low-efficiency separations. At pH below 3, the silanols are fully protonated and the negative charge of the capillary surface is removed, so the problem of adsorption can be reduced. Buffers with a very low pH are generally unsuitable because of their high conductivity, which limits the use of high voltages. Working at high pH alters the charge of the protein, so that no significant regions of positive charge exist.

In addition to the problems caused by the high conductivity of the electrolytes, there will often be problems with the stability of the proteins under extreme pH conditions. To maintain optimum stability of the analyte, a buffer system with a pH in a suitable range for the protein is required.

Zwitterions consisting of sulphonic acid and quaternary amino groups have previously been investigated as buffer additives for use in CZE [8,9]. Zwitterions could be substitutes for the cation and its anion. Becuase a zwitterion contains no net charge, it has no net conductivity. Zwiterions will not contribute to the conductivity of the operating buffer, but are able to associate with the negatively charged surface of the capillary and with charged sites of the protein. Therefore, zwitterions are effective in reducing the interaction of proteins with the surface of a fused-silica capillary at neutral pH.

In 1989, CZE and reversed-phase high-performance liquid chromatographic (RP-HPLC) studies of biosynthetic human insulin (BHI) and its degradation were reported to give similar information [10]. Using a tricine buffer with morpholine and sodium chloride at pH 8, Nielsen *et al.* [10] separated BHI and acidic desamido-insulin. The buffer was replaced after every four to six runs. The smallest amount of acidic desamido-insulin determined by CZE was 9.7% of desamido compound as a percentage of total protein. This method was subjected to a critical examination in a parallel paper [11]. Later Lookabaugh *et al.* [12] described the determination of insulin using the same tricine buffer, with mixed results. The typical number of theoretical plates obtained with this application was 40 000.

The determination of insulin and related compounds has been accomplished with very reproducible results by RP-HPLC and IEC. The yield and purity were determined routinely at the different stages during the process of manufacturing insulin. In addition to large amounts of insulin-related substances, the separation of only the acidic desamido-insulin was obtained using RP-HPLC, whereas both acidic and neutral desamido-insulin of HI were separated by IEC. Addition of a different separation mechanism such as CZE gives valuable complementary information when validating the quality of a product. This paper presents a comparison of results obtained by the three different techniques.

EXPERIMENTAL

Materials

HI and acidic human desamido A-21 were obtained from Novo Nordisk (Bagsværd, Denmark). Sodium acetate, methanol, ethanol, triethylamine, ethanolamine, sodium hydroxide, sodium sulphate, phosphoric acid, acetic acid and hydrochloric acid

were purchased from, Merck (Darmstadt, Germany). CHES [2-(N-cyclohexylamino)ethanesulphonic acid], BES [N,N-bis(2-hydroxyethyl)-2-aminoethanesulphonic acid], AMPSO {3-[(1,1-dimethyl-2-hydroxyethyl)amino]-2-hydroxypropanesulphonic acid}, CAPSO [3-(cyclohexylamino]-2-hydroxy-1-propanesulphonic acid] and trizma base were obtained from Sigma (St. Louis, MO, USA). AccuPure Z1-Methyl (trimethylammonium propanesulphonate) was supplied by Waters (Waters Chromatography Division, Millipore, Milford, MA, USA). Acetonitrile was obtained from Rathburn (Walkerburn, UK).

Purified water obtained from a Milli-Q purification system (Millipore, Bedford, MA, USA) was used to prepare all solutions.

Equipment

Most of the experiments were performed on Quanta CZE apparatus from Waters. The Quanta CZE apparatus was equipped with untreated fused-silica capillaries of total length 60 cm (52.5 cm top detection) and three different inside diameters. Hydrostatic injection was performed by raising the injection end 10 cm relative to the detector end for various intervals measured in seconds. UV absorption was measured at 214 nm using a time constant of 0.1–1.0 s. Data were collected at a rate of 5 data points per second. The electrophoretic data system was a Waters 860 Data system operated on a Micro-Vax 3300 computer (Digital Equipment, Maynord, MA, USA).

To investigate the influence of controlling the outside temperature of the capillary, a P/ACE System 2050 CZE apparatus (Beckman, Palo Alto, CA, USA) was used. The samples were introduced on to this CZE unit by pressure (0.5 psi) for 3–5 s. Detection was effected at 214 nm. The temperatures was varied from 5°C below room temperature to 50°C.

Capillary zone electrophoresis

Prior to use, a fused-silica capillary was prepared by washing with 0.5 *M* sodium hydroxide solution for 30 min and running buffer for 15 min. Before each run the capillary was flushed with running buffer for 2 min. Between series of runs (typically 30–50 runs) and before new buffers were introduced, the capillary was treated with series of sodium hydroxide solutions and hydrochloric acid. The buffer in the electrode reservoirs was replaced after every 30–50 runs. When the capillary was stored for more than 24 h, it was flushed with 10% aqueous methanol.

The composition of the optimized running buffer was 50 m*M* sodium acetate and 0.85 *M* CHES in 10% aqueous acetonitrile adjusted to pH 7.8 with triethylamine.

The concentration of insulin in the introduced standards and samples was *ca.* 1 mg/ml.

Reversed-phase high-performance liquid chromatography

The RP-HPLC separation of HI and acidic desamido-insulin was performed on a C_{18} silica-based column packed with 5-μm, 120-Å particles. Eluent A consisted of 0.2 *M* sodium sulphate and 0.04 *M* phosphoric acid in 10% acetonitrile with the pH adjusted to 2.5 with ethanolamine. Eluent B was 50% acetonitrile. At approximately 28% acetonitrile the retention time of HI is 20 min. The temperature of the column was held at 50°C during the isocratic separation at a flow-rate of 1 ml/min. The components were detected at 214 nm. These conditions are used routinely in our in-process quality control of insulin.

Ion-exchange chromatography

HI and acidic and neutral desamido-insulin were separated using a Mono Q HR 5/5 anion-exchange column obtained from Pharmacia (Uppsala, Sweden). Eluent A was 18 m*M* Tris–4.5 m*M* acetic acid–53% ethanol (pH 8.4). Eluent B had the same composition as eluent A but with 0.33 *M* sodium acetate was added. The components were separated by gradient elution from 20 to 100% B in 30 min at a flow-rate of 1 ml/min with UV detection at 280 nm. The temperature of the column was ambient.

RESULTS AND DISCUSSION

Developing the running buffer

As mentioned previously, working with proteins using CZE in practice generally causes many problems. During the development phase of this application for insulin, several buffer systems such as phosphate, tricine and borate were tested. None of the buffers seemed to give the desired separation or reproducibility.

The effect of the cation and anion in the buffer on mobility in CZE was investigated by Atamna and co-workers [13,14]. When selecting a buffer for CZE studies, some of the issues to consider are the native pH of the solution and the conductivity. It has been reported that the migration time increases with increase in the atomic mass of the cation. The various anions turned out to give widely different currents at the same applied voltage. The observed current for sodium acetate was less than, *e.g.*, that for potassium acetate or sodium phosphate. It is important to know the values of the current in order to control the heat generated in the capillary [15]. The combination of sodium as the cation and acetate as the anion showed values interesting for this study of insulin. Therefore, sodium acetate (NaAc) was chosen as the running buffer.

Experimental runs showed that buffers without additives do not prevent the interaction between the capillary wall and the protein. For this reason, the addition of several zwitterions to the electrolyte was tested. Electropherograms obtained using selected zwitterions are shown in Fig. 2. The choice of zwitterions depends on the following practical points: (1) separation, (2) efficiency, (3) reproducible migration times, (4) solubility and (5) easy to reproduce with respect to pH and obtaining the same conductivity during the preparation of the running buffer. Observations regarding some of the zwitterions tested are listed in Table I. CHES was shown to fulfil the requirements mentioned, the other additives giving poor results with respect to at least one of the above points.

Adding organic solvents to the buffer improves the plate count considerably. The effect of adding methanol and acetonitrile to the buffer is shown in Table II, where the chromatographic data obtained are listed. Because of the improved efficiency (384 000 plates/m for HI) and resolution, acetonitrile was selected as the organic modifier. Adding acetonitrile to the buffer gave even better solubility of CHEs and also a more stable pH adjustment when preparing the electrolyte.

Optimization of the pH depends on the selectivity, resolution, efficiency and maximum acceptable current. Another important point to be aware of when optimizing pH is the sample matrix. First, the optimum pH for this buffer was determined to be

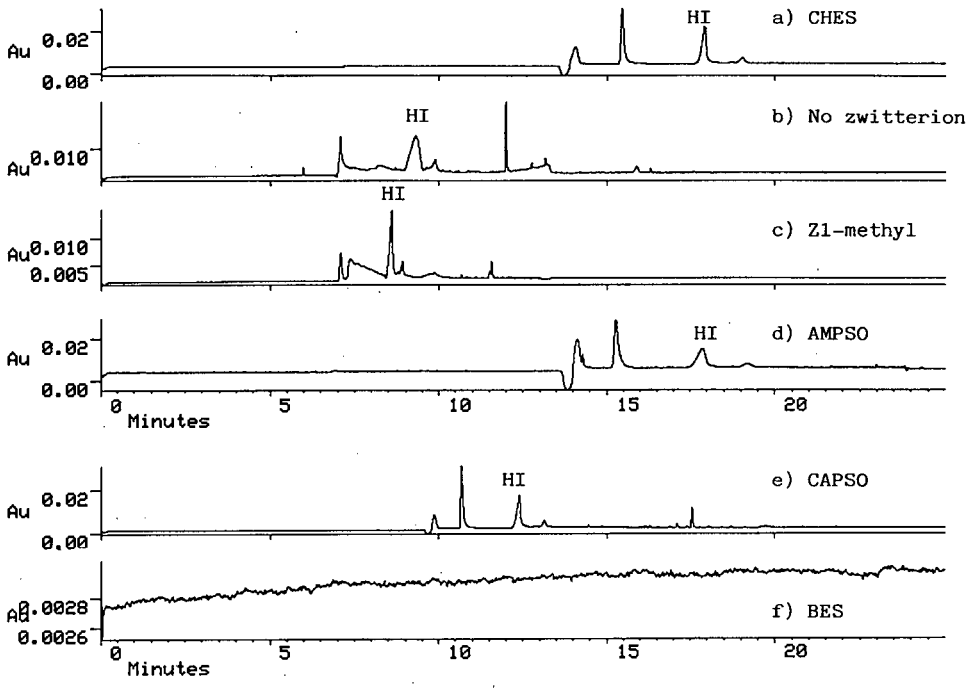

Fig. 2. Electropherograms of a formulation product of HI obtained using sodium acetate buffer with different additives. Detailed running conditions and information are given in Table II.

TABLE I

PRACTICAL POINTS OBSERVED WITH DIFFERENT ADDITIVES IN RUNNING BUFFER

Running buffer: 50 m*M* sodium acetate–10% acetonitrile.

Curve in Fig. 2	Additive	Parameter[a]						Comments
		I	II	III	IV	V	VI	
a	0.85 *M* CHES	6.53	2.42	7.76	3.01	15	48	Buffer easy to prepare Reproducible electropherograms
b	None	8.20	3.39	7.76	3.50	15	54	Irreproducible electropherograms
c	0.85 *M* Z1-methyl	7.96	2.92	7.78	3.21	15	45	Very sensitive to pH adjustment Irreproducible electropherograms
d	0.85 *M* AMPSO	5.65	2.28	7.76	3.38	15	53	Irreproducible electropherograms
e	0.50 *M* CAPSO	6.11	3.03	7.80	3.33	15	44	Low solubility Irreproducible electropherograms
f	0.85 *M* BES	5.67	3.01	7.79	14.51	5	66	No peaks

[a] I = pH in native solution; II = conductivity (mS) in native solution; III = pH after adjustment with triethylamine–acetic acid; IV = conductivity (mS) after pH adjustment; V = applied voltage (kV); VI = current (μA).

6.5. At this pH there is a good resolution between HI and desamido-insulin in a standard solution and the current is low. Also, very little pH adjustment in the buffer is necessary. When introducing a sample on to the capillary, additional peaks between the main peak of interest and the electroosmotic flow (EOF) front were discovered. To obtain a good separation of all the peaks, the pH was adjusted to pH 7.8. Fig. 3 shows the electropherograms of a formulation product obtained with buffers in the pH range 2–9.

Different concentrations of sodium acetate and CHES in the running buffer were examined. Electropherograms obtained under the various conditions are exhibited in Fig. 4. The content of the buffer ion is proportional to the resolution of the peaks. In addition, an increasing content of sodium acetate results in increased migration times. Concentrations of sodium acetate of 75 and 100 m*M* give very good separations of the components, but at the same time also more noise on the baseline, due to the high current (only obvious at an enlarged range). Increased amounts of CHES enhance the efficiency and give longer migration times. At 1 *M* concentration, CHES is difficult to dissolve in the electrolyte.

The buffer for the separation of HI and at least two forms of desamido-insulin was finally optimized to contain 50 m*M* sodium acetate, 0.85 *M* CHES and 10% acetonitrile (pH 7.8). A typical set of electropherograms for a formulation product of insulin and the corresponding reference standards of HI and acidic desamido-insulin is presented in Fig. 5. In the case of the sample solution the peak eluting near the EOF front is attributable to a preservative which was added to the the formulation.

Influence of base washing and replication of injections

It is often pointed out that base washing between runs is necessary to obtain reproducible migration times with untreated fused-silica capillaries [16]. The ruggedness of this method was investigated by several consecutive injections of a sample on to the capillary.

Using the P/ACE unit the temperature was set at 30°C. Several injections were made without base washing of the capillary, followed by nine injections made with base washing between each injection (2 min with 0.1 *M* sodium hydroxide solution). Results showing the reproducibility are presented for 36 successive runs of a formulation product using the optimized buffer. As shown in Table III, the method is highly reproducible with respect to the migration time, also without base washing. In spite of the large number of injections the relative standard deviation (R.S.D.) of the migration times is excellent (below 1%). Considering the number of injections, the decrease in efficiency of the HI peak is acceptable (from 503 000 to 265 000 plates/m).

TABLE II

EFFECT OF ADDING ORGANIC MODIFIER TO ELECTROLYTE

Electrolyte: 50 m*M* sodium acetate–0.85 *M* CHES (pH 7.8).

Organic modifier	Voltage (kV)	Current (μA)	HI migration time (min)	Plate count (10^3 N/m)[a]			Resolution[c]			Selectivity[d]		
				HI	Acidic des.[b]	Neutral des.	HI	Acidic des.	Neutral des.	HI	Acidic des.	Neutral des.
None	15	46	12.79	121	377	425	2.166	1.780		1.032	1.017	
None	25	103	5.88	78	43		–	–		–	–	
10% methanol	15	43	18.63	272	343	353	3.591	1.655		1.044	1.020	
10% methanol	25	97	8.03	189	109	192	2.971	1.258		1.049	1.020	
10% acetonitrile	15	46	15.26	384	576	553	4.846	2.187		1.047	1.018	
10% acetonitrile	25	102	6.67	169	–	146	–	–		1.051	1.016	

[a] Plate count per metre: $N = 5.54\,(t/w_{1/2})^2$. Dimensions of capillary: 60 cm × 75 μm I.D., 52.2 cm to detection.

[b] des. = desamido-insulin.

[c] Resolution: $R = 2(mt_2 - mt_1)/(w_2 - w_1)$, where mt = migration time, w = peak width at baseline using tangent lines drawn through 50th percentile points until they intercept the baseline.

[d] Selectivity: $a = (mt_2 - v)/(mt_1 - v)$, where v = void volume. Note: as the selectivity is compared relatively, v is taken as a constant.

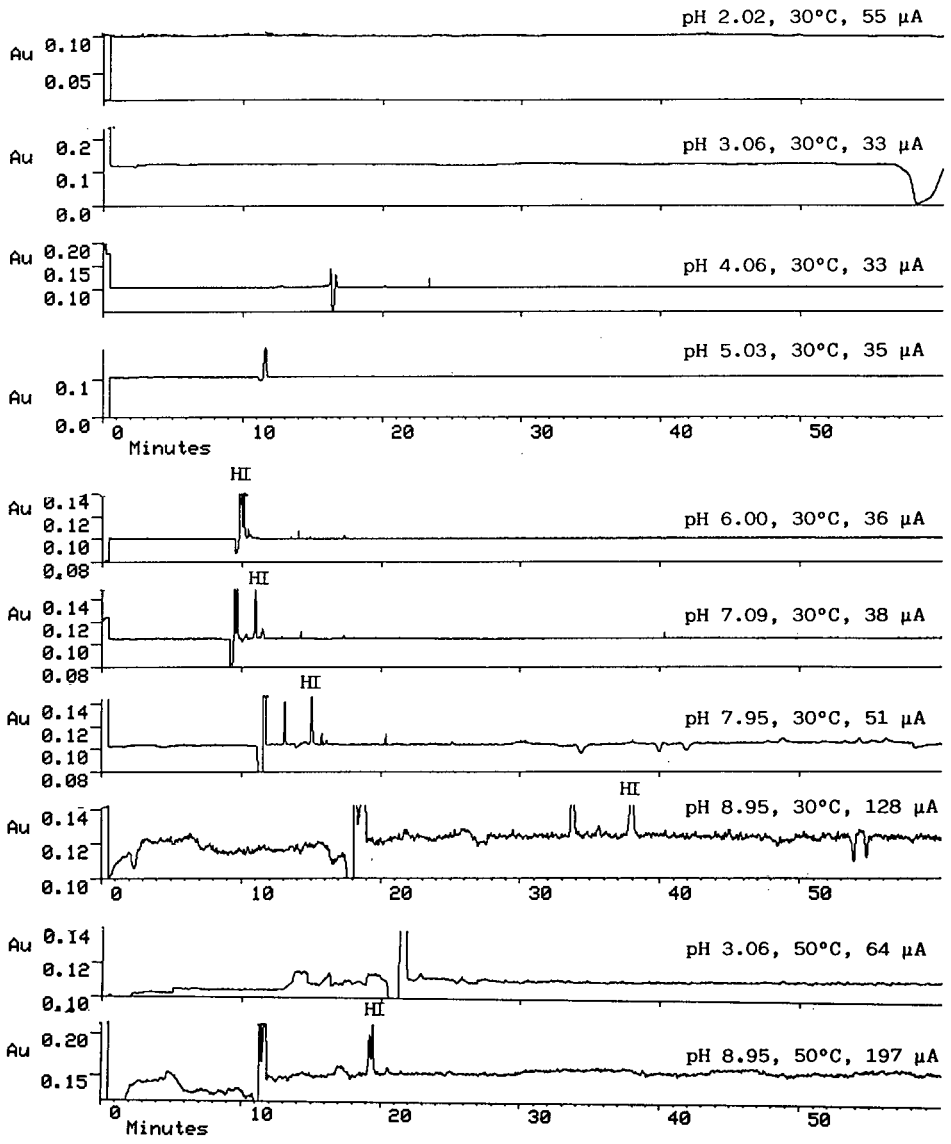

Fig. 3. Electropherograms showing the effect of pH in running buffer (50 m*M* NaAc–0.85 *M* CHES–10% CH_3CN). The applied voltage is 15 kV in all instances. The electropherograms were obtained with the P/ACE 2050 unit at 30 and 50°C.

With the Quanta CZE appratus eighteen continuous injections were made. This experiment was carried out without control of the external temperature of the capillary and without flushing with base between each run. The statistical data are given in Table IV. Also under these conditions the R.S.D. for the migration time is excellent (0.38%), especially in view of the number of injections executed.

The ruggedness of this method is underlined by these experiments on two different types of CZE apparatus. The migration times exhibited an R.S.D. in the order of 1% or less even without base washing and without thermostating the capillary.

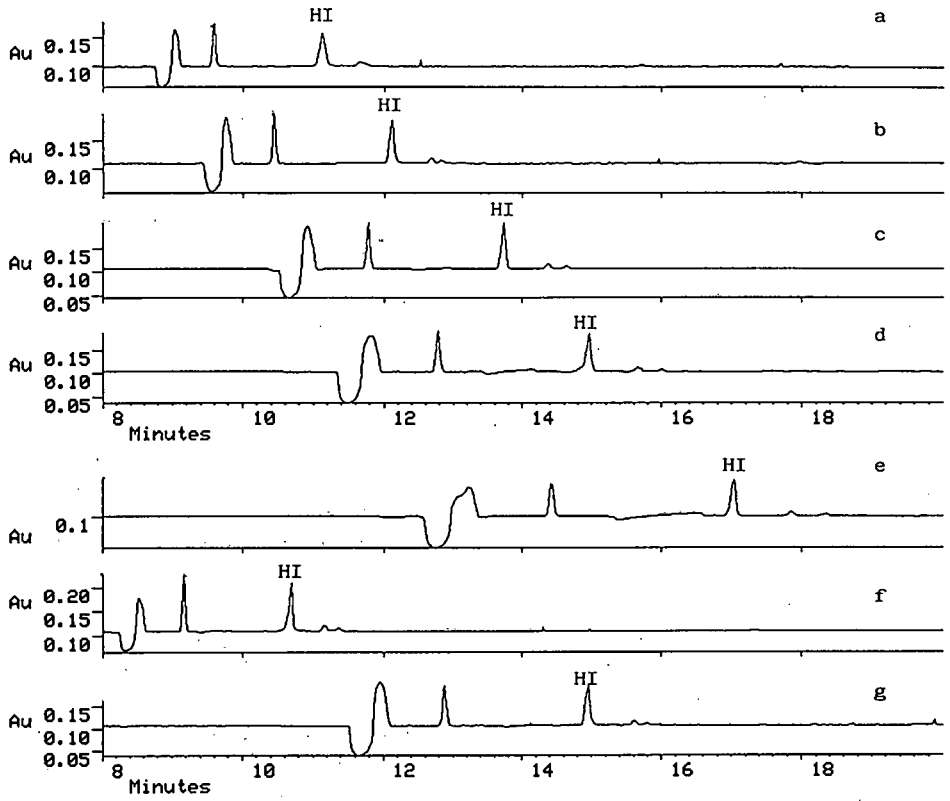

Fig. 4. Analysis of a formulation product of HI using various running buffers. Applied voltage, 15 kV; temperature, 30°C (P/ACE 2050). (a) 10 m*M* NaAc–0.85 *M* CHES–10% CH_3CN (pH 7.77) (17 μA); (b) 25 m*M* NaAc–0.85 *M* CHES–10% CH_3CN (pH 7.79) (27 μA); (c) 50 m*M* NaAc–0.85 *M* CHES–10% CH_3CN (pH 7.79) (45 μA); (d) 75 m*M* NaAc–0.85 *M* CHES–10% CH_3CN (pH 7.76) (60 μA); (e) 100 m*M* NaAc–0.85 *M* CHES–10% CH_3CN (pH 7.77) (81 μA); (f) 50 m*M* NaAc–0.5 *M* CHES–10% CH_3CN (pH 7.80) (48 μA); (g) 50 m*M* NaAc–1 *M* CHES–10% CH_3CN (pH 7.73) (43 μA).

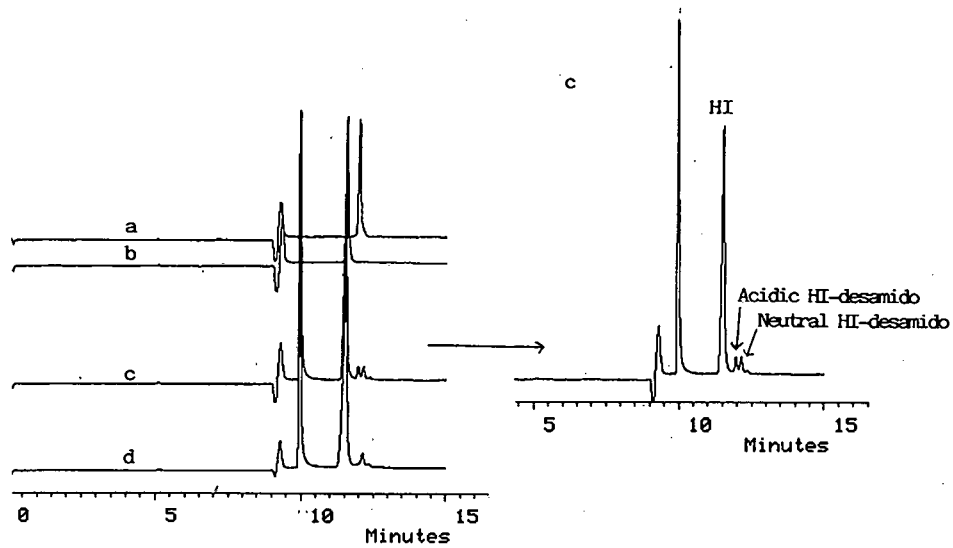

Fig. 5. Sample with corresponding reference standards. (a) Acidic desamido-insulin; (b) HI; (c) formulation product of HI (stored at 4°C for 15 months) containing standard of acidic desamido-insulin; (d) same sample as (c) but without acidic desamido-insulin added.

TABLE III

REPLICATION OF INJECTIONS AT 30°C (P/AGE 2050).

Statistical values for HI. Running buffer: 50 m*M* sodium acetate–0.85 *M* CHES–10% acetonitrile (pH 7.75) (15 kV, 45 μA).

Base wash between runs	Injection No.	Migration time (min)		Plate count ($10^3 \cdot N$/m)[a]		
		Mean	R.S.D. (%)	Mean	R.S.D. (%)	Range
No	1–27	12.413	0.61	382	14.69	503–322
No	1–9	12.452	0.17	466	7.62	503–399
No	10–18	12.410	0.98	363	2.90	376–349
No	19–27	12.377	0.20	351	5.77	385–322
Yes	28–36	12.457	0.51	288	6.65	317–265

[a] Plate count per metre: $N = 5.54(t/w_{1/2})^2$.

Additional optimization aspects

The influence of temperature control as a separation parameter was briefly studied. Fig. 6 shows electropherograms of a sample analysed at 30 and 50°C. Except for a shorter time of analysis at the higher temperature, no other advantages were obtained by raising the temperature. In this application no difference in selectivity was observed at the two temperatures. A higher current was observed with the higher temperature.

Capillaries with of I.D. 50, 75 and 100 μm were tested and the results obtained are shown in Table V. When deciding which inside diameter to use, the demands on sensitivity, need for resolution and efficiency, current, etc., should be considered.

As also observed in Table V, the amount of compound injected (which in this instances is directly proportional to the time of injection) is important when evaluating efficiency. A 1 mg/ml concentration of HI was introduced into the capillary (75 μm I.D.) for 1–20 s. The volume introduced into the capillary by hydrostatic injection was determined as *ca.* 1.4 nl/s (calculated using eqn. E3.7 in ref. 17). Depending on the injection volume, the range of the amount of HI injected was 1.4–28 ng. Fig. 7 shows the relationship between the time of injection and the plate count achieved. The efficiency decreases with increasing amount of sample applied to the capillary. The correlation between time of injection and efficiency of the HI peak shows linearity with $r^2 = 0.9510$, whereas $r^2 = 0.9985$ for the correlation between time of injection and peak area.

In order to achieve optimum utilization of the analysis time, four injections of a sample were made at 10-min intervals. The electropherogram is shown in Fig. 8. As shown, four samples are analysed in 50 min instead of four times 20 min.

Quantitative aspects

As described earlier, the precision of multiple injections was excellent for the reproducibility of migration times. Also, the R.S.D. of the peak area of

TABLE IV

REPLICATION OF EIGHTEEN INJECTIONS WITHOUT A BASE WASH BETWEEN RUNS AND WITHOUT TEMPERATURE CONTROL

Statistical values for HI. Running buffer: 50 m*M* sodium acetate–0.85 *M* CHES–10% acetonitrile (pH 7.76) (15 kV, 45 μA).

Migration time (min)		Plate count ($10^3 \cdot N$/m)[a]			R.S.D. (%)	
Mean	R.S.D. (%)	Mean	R.S.D. (%)	Range	Area	Height
13.177	0.38	333	2.39	346–325	1.75	1.79

[a] Plate count per metre: $N = 5.54(t/w_{1/2})^2$.

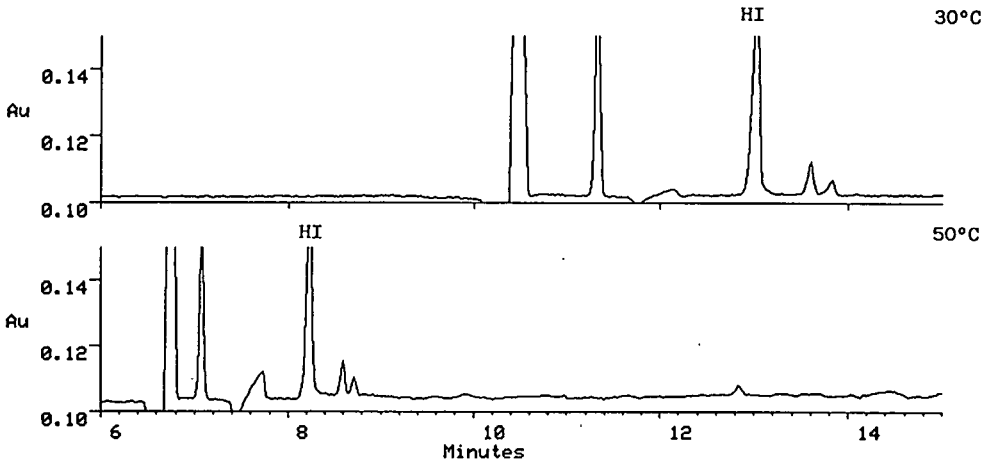

Fig. 6. Sample analysed at 30 and 50°C (P/ACE 2050). Running buffer: 50 m*M* NaAc–0.85 *M* CHES–10% CH_3CN (pH 7.75).

HI was satisfactory (Table IV). In addition to validation of precision, other important performance characteristics such as linearity and detection limit for the application were evaluated.

The linearity of response for HI was evaluated by varying the amount of material introduced into the capillary. First, the time of injection was held at 5 s while the concentration of the standard ranged from *ca.* 0.1 to 4 mg/ml, corresponding to an absolute amount from 0.7 to 28 ng. A plot of the peak area of HI *versus* amount of HI introduced gave good linearity (r^2 = 0.9998). The plate count ranged from 141 000 to 319 000 plates/m for 28 and 0.7 ng, respectively. In the second linearity experiment the injection time was 15 s, corresponding to 2.1–84 ng using the same concentrations of HI as in the previous test of linearity. This gave an excellent linearity (r^2 = 0.9999). With this test, the plate count ranged from 62 000 tot 294 000 plates/m for 84 and 2.1 ng, respectively. Data obtained from the two linearity experiments were combined into one calibration graph. As the experiments were carried out on two different days the normalized peak areas (area/migration time) were used. The linearity was acceptable (r^2 = 0.9986) for the range 0.7–84 ng of HI.

The detection limit was determined to be 80 pg of acidic desamido-insulin when introducing a standard 0.005 mg/ml for 30 s (signal-to-noise ratio = 8) or 0.0025 mg/ml for 60 s (signal-to-noise ratio = 3).

TABLE V

PERFORMANCE CHARACTERISTICS OBTAINED WITH CAPILLARIES WITH DIFFERENT INSIDE DIAMETERS

Electrolyte: 50 m*M* sodium acetate–0.85 *M* CHES–10% acetonitrile (pH 7.8).

I.D. (μm)	Injection time (s)	Voltage (kV)	Current (μA)	Migration time (min)	HI area ($\times 10^{-3}$)	Plate count (10^3 *N*/m)	Resolution	
							Acidic des.[a]	Neutral des.
75	5	15	45	13.150	103	344	4.093	1.525
50	5	15	22	16.116	38	415	5.476	2.093
50	5	20	31	11.414	27	389	4.777	1.863
50	30	20	31	10.975	122	283	2.736	1.484
100	5	15	92	13.306	389	104	1.917	0.731
100	3	15	92	13.250	242	154	2.667	1.049

[a] des. = Desamido-insulin.

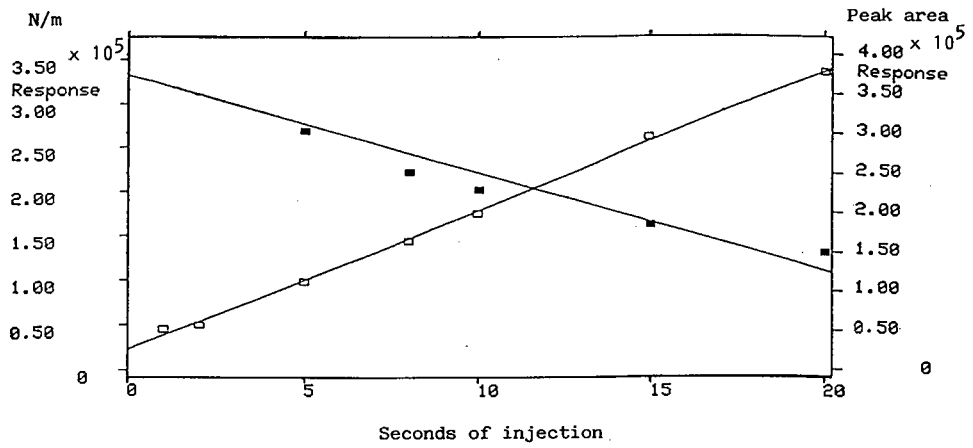

Fig. 7. Correlation between time of injection of HI in a standard solution and (■) efficiency (plate count per meter) and (□) peak area.

The above results concerning quantitative aspects were tested using standard solutions of HI and acidic desamido-insulin. The precision of the method was confirmed during tests with samples. Three lots of formulation products were tested on five different days with two replicates per day (except for day 7 with one replicate). The results obtained from analysing the three samples are presented in Table VI. Acidic desamido-insulin was not detected in any of the lots. The R.S.D. of the area percentage of neutral desamido-insulin increases with decreasing content of this compound, owing to the values approaching the detection limit.

In order to cover all the quantitative aspects the accuracy of the method was also tested on three different samples of formulation products. In the samples amounts corresponding to 4.5% of acidic desamido-insulin were added on four different days of analysis. As shown in Table VII, the results are satisfactory when the uncertainty of the weighing and the volume of addition of acidic desamido-insulin are taken into account.

Comparison of CZE, IEC and RP-HPLC

A formulation product of HI, which had been stored for at least 15 months at 15°C, was analysed

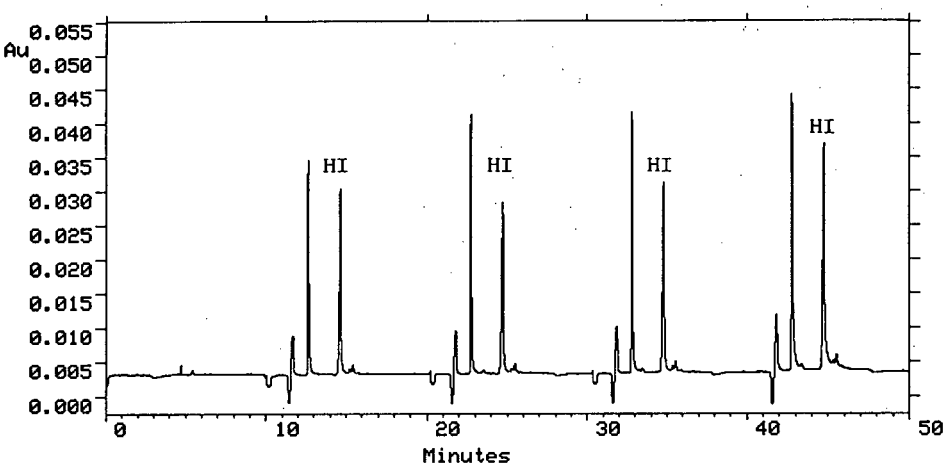

Fig. 8. Formulation product of HI introduced into the capillary at intervals of 10 min. Running buffer: 50 m*M* NaAc–0.85 *M* CHES–10% CH_3CN (pH 7.78) (15 kV, 48 μA).

TABLE VI

PERCENTAGE OF MAIN COMPONENT AND NEUTRAL DESAMIDO-INSULIN IN THREE DIFFERENT LOTS OF FORMULATION PRODUCTS

Lot No.	Day	Main component					Neutral desamido-insulin				
		Area %		Mean area %	S.D. (abs.) area %	R.S.D. (%)	Area %		Mean area %	S.D. (abs.) area %	R.S.D. (%)
1	1	91.36	91.16				7.40	7.55			
	2	90.64	90.59				8.36	8.39			
	3	90.60	90.00	90.68	0.39	0.4	8.15	8.61	8.06	0.43	5.3
	4	90.51	90.59				8.19	8.26			
	5	90.67	–				7.61	–			
2	1	98.73	98.65				1.27	1.35			
	2	98.51	98.49				1.10	1.00			
	3	98.60	98.70	98.63	0.17	0.2	1.40	1.30	1.27	0.20	15.7
	4	98.74	98.89				1.26	1.11			
	5	98.32	–				1.68	–			
3	1	98.97	99.21				1.03	0.79			
	2	–	–				–	–			
	3	99.17	99.35	98.79	0.58	0.6	0.83	0.65	0.99	0.24	24.1
	4	97.98	98.07				1.32	1.15			
	5	98.85	–				1.15	–			

by RP-HPLC, IEC and CZE. The patterns of the elution curves obtained with the three techniques are depicted in Fig. 9.

Comparing the electropherogram and the chromatogram obtained from IEC several observations can be made. The elution order of acidic and neutral desamido-insulin is reversed. Second, the resolution of neutral desamido-insulin and the efficiency are improved when using CZE. Further, the analysis period is reduced from 60 min using IEC (including gradient and equilibration to the starting composition) to a maximum of 20 min using CZE. The preservative in this particular sample migrates together with the EOF front in the electropherogram and elutes with the solvent front in the chromatogram from IEC. As mentioned earlier, only the acidic desamido-insulin is isolated from HI by RP-HPLC, while the neutral desamido-insulin co-elutes with HI. The peak at 10 min is the preservative in the sample.

TABLE VII

ACCURACY OF DETERMINATION OF ACIDIC DESAMIDO-INSULIN ADDED TO THREE SAMPLES OF FORMULATION PRODUCTS

Lot No.	Day	Acidic desamido-insulin added (%)	Found (%)	Recovery (%)
1	1	4.5	3.86	86
	2	4.5	4.01	89
	3	4.5	4.30	96
	4	4.5	4.33	96
2	1	4.5	4.05	90
	2	4.5	3.69	82
	3	4.5	3.55	79
	4	4.5	3.65	81
3	1	4.4	4.03	92
	2	4.4	4.39	100
	3	4.4	4.14	94
	4	4.4	4.39	100

Comparative data obtained by CZE, IEC and RP-HPLC of two different samples are presented in Table VIII. The qualitative determination of the two deamidation products showed a close resemblance between CZE and IEC. In order to obtain comparative results for the purity of HI, the integration of the chromatogram from RP-HPLC does not include the peak of the preservative.

A more thorough investigation of the relationship between results achieved by CZE and IEC was made. Eight samples were analysed for neutral and acidic desamido-insulin by CZE and IEC using dual

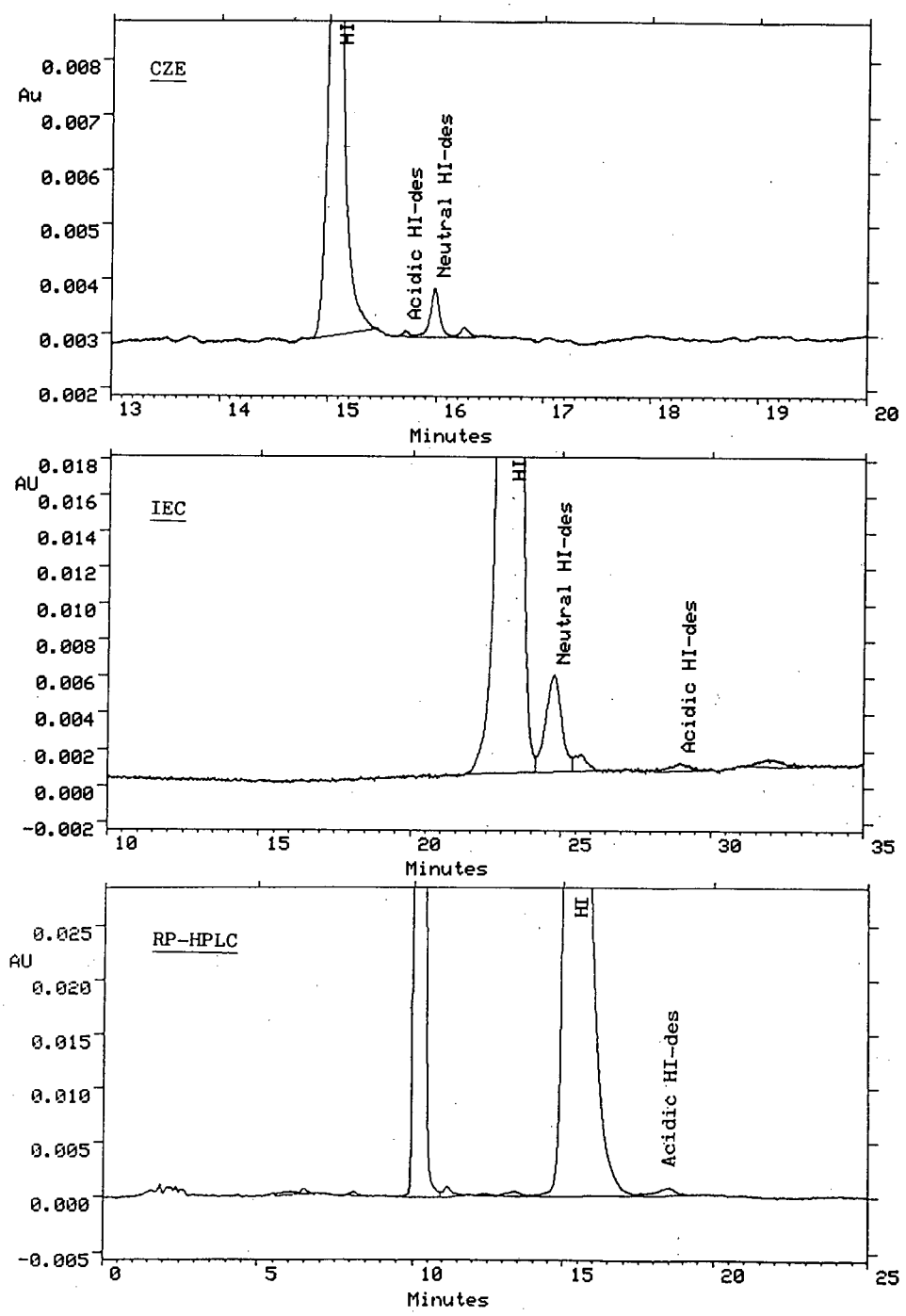

Fig. 9. Formulation product of HI stored at 15°C. Comparison of electropherogram and chromatograms obtained using CZE, IEC and RP-HPLC. Analytical conditions as described in the procedures for CZE, IEC and RP-HPLC under Experimental.

TABLE VIII

COMPARISON OF QUALITATIVE RESULTS OBTAINED USING CZE, IEC AND RP-HPLC

Technique	Sample No.	Area %		
		HI	Acidic desamido-insulin	Neutral desamido-insulin
CZE	1	98.41	0.24	1.35
	2	95.53	0.29	3.69
IEC	1	97.90	0.25	1.82
	2	95.36	0.30	3.65
RP-HPLC	1	99.89[a]	0.11	–
	2	99.84[a]	0.16	–

[a] Integration starting from the main peak.

determination. The comparative results are shown in Table IX. The determination of neutral desamido-insulin showed a good agreement between the results obtained by CZE and IEC. In most of the samples the content of acidic desamido-insulin was close to or below the detection limit using both CZE and IEC. The low content of acidic desamido-insulin explains the poor correlation between CZE and IEC. It should also be mentioned that during analysis by IEC the samples were stored at 5°C in the autosampler, whereas the CZE apparatus still does not have the capability to keep the samples cooled. The formation of deamidation products increases at higher temperatures.

TABLE IX

COMPARATIVE RESULTS OF SAMPLES ANALYSED BY CZE AND IEC

Sample No.	Desamido-insulin	CZE			IEC			$Mean_{CZE}$:$Mean_{IEC}$[a]
		Area %		$Mean_{CZE}$ (area%)	Area %		$Mean_{IEC}$ (area%)	
1	Neutral	0.96	0.96	0.96	0.78	0.78	0.78	1.21
	Acidic	0.07	0.15	0.11	0.11	0.11	0.11	1.00
2	Neutral	0.26	0.32	0.29	0.27	0.28	0.28	1.04
	Acidic	0.12	0.08	0.10	0.10	0.12	0.11	0.91
3	Neutral	10.20	9.86	10.08	10.21	10.30	10.26	0.98
	Acidic	0.48	0.12	0.30	0.16	0.17	0.17	1.76
4	Neutral	7.85	7.97	7.91	8.65	8.56	8.61	0.92
	Acidic	0.74	0.55	0.65	0.24	0.23	0.24	2.71
5	Neutral	0.68	0.68	0.68	0.66	0.62	0.64	1.06
	Acidic	0.38	0.51	0.45	0.18	0.21	0.20	2.25
6	Neutral	3.11	2.77	2.94	2.89	2.99	2.94	1.00
	Acidic	0	0	0	0.09	0.11	0.10	–
7	Neutral	16.11	15.23	15.67	15.59	15.48	15.54	1.01
	Acidic	0	0	–	0.07	0.07	–	–
8	Neutral	4.69	4.89	4.79	4.42	4.44	4.43	1.08
	Acidic	0	0	0	0.08	0.09	0.09	–

[a] Neutral desamido-insulin: mean ($mean_{CZE}$:$mean_{IEC}$) = 1.04, S = 0.09–8.3% (n = 8). Acidic desamido-insulin: mean ($mean_{CZE}$:$mean_{IEC}$) = 1.73, S = 0.78–45.2% (n = 5).

It is important to note that among the eight samples were formulation products consisting of three different species of insulin. The main component in the different samples was either HI, porcine insulin or bovine insulin. Because of the small differences in charge between the three species of insulin, they all have the same retention time in IEC and the same migration time in CZE. Likewise, there is no separation between the desamido products of the three species of insulin in either CZE or IEC. However, human, procine and bovine insulin and their desamido products are easily separated by the RP-HPLC method described.

CONCLUSIONS

This work has shown that CZE is a complementary technique which may facilitate discrimination between the main protein component and closely related impurities or degradation products.

A method for the determination of acidic and neutral desamido-insulin in HI was developed. The method is reproducible even without a base wash between each run and without controlling the outer temperature of the capillary. Under these conditions the R.S.D. of the migration times is excellent (below 1%). The detection limit is 80 pg for acidic desamido-insulin and the calibration graph for HI is linear up to 84 ng (correlation coefficient 0.999 based on peak-area evaluation).

An excellent correlation was observed between CZE and IEC. Although the desamido components can be separated by IEC, CZE gives a better resolution in a shorter analysis time. The excellent separation efficiencies obtained indicate that CZE is complementary to RP-HPLC and IEC in the analysis of insulin. CZE adds another dimension to chromatographic separation techniques and therefore enhances the confidence level in the analytical results. The high speed and impressive separation power make this technique very valuable.

ACKNOWLEDGEMENT

The author thanks Ramcon (Beckman Instruments, Denmark) for kindly providing the P/ACE 2050 capillary electrophoresis system for parts of this study.

REFERENCES

1 J. Brange, S. Skelbæk-Pedersen, L. Langkjær, U. Damgaard, H. Ege, S. Havelund, L. G. Heding, K. H. Jørgensen, J. Lykkeberg, J. Markussen, M. Pingel and E. Rasmussen, in M. Berger (Editor), *Subcutaneous Insulin Therapy*, Springer, Berlin, Ch. 3, p. 2.
2 L. M. Atkins, D. J. Miner, G. S. Sittampalam and C. D. Wentling, *J. Assoc. Off. Anal. Chem.*, 70 (1987) 610–617.
3 B. S. Welinder, *Acta Chem. Scand.* 25 (1971) 3737–3742.
4 J. Markussen, P. Hougaard, U. Ribel, A. R. Sørensen and E. Sørensen, *Protein Eng.*, 1 (1987) 205–213.
5 D. S. H. W. Nicol and L. F. Smith, *Nature (London)*, 187 (1960) 483–485.
6 J. Markussen, *Human Insulin*, MTP Press, Lancaster, 1987, p. 14.
7 J. Brange, L. Langkjær, S. Havelund and E. Sørensen, *Diabetologia*, 25 (1983) 193.
8 M. M. Bushey and J. W. Jorgenson, *J. Chromatogr.*, 480 (1989) 301–310.
9 M. Merion, B. Bell-Alden, E. Grover, U. Neue and J. Peterson, poster presented at the *3rd International Symposium on High-Performance Capillary Electrophoresis, San Diego, CA, February 3–6, 1991.*
10 R. G. Nielsen, G. S. Sittampalam and E. C. Rickard, *Anal. Biochem.*, 177 (1989) 20–26.
11 P. D. Grossmann, J. C. Colburn, H. H. Lauer, R. G. Nielsen, G. S. Sittampalam and E. C. Rickard, *Anal. Chem.*, 61 (1989) 1186–1194.
12 M. Lookabaugh, M. Biswas and I. S. Krull, *J. Chromatogr.*, 549 (1991) 357–366.
13 I. Z. Atamna, C. J. Metral, G. M. Muschik and H. J. Issaq, *J. Liq. Chromatogr.*, 13 (1990) 2517–2527.
14 I. Z. Atamna, C. J. Metral, G. M. Muschik and H. J. Issaq, *J. Liq. Chromatogr.*, 13 (1990) 3201–3210.
15 D. S. Burgi, K. Salomon and R. Chien, *J. Liq. Chromatogr.*, 14 (1991) 847–867.
16 K. Lee and G. S. Heo, *J. Chromatogr.*, 559 (1991) 317–324.
17 A. Vinther, *Capillary Electrophoresis*, Vol. 1, Novo Nordisk Denmark, 1990, p. 3.9.

Journal of Chromatography, 604 (1992) 282–284
Elsevier Science Publishers B.V., Amsterdam

CHROM. 24 219

Short Communication

Application of ion chromatography to the determination of selectivity coefficients

Ü. Haldna

Institute of Chemistry, Estonian Academy of Sciences, Akadeemia tee 15, Tallinn 200108 (Estonia)

(First received October 21st, 1991; revised manuscript received March 30th, 1992)

ABSTRACT

Ion chromatography was applied to calculate the selectivity coefficients between Cl^-, NO_3^-, HPO_4^{2-} and SO_4^{2-} ions on HIKS-1 resin containing $-CH_2N^+(CH_3)_3$ groups. For each combination of ions, 25 different eluents were applied.

INTRODUCTION

Ion chromatography is based on the assumption that the retention times (t_R) of the ions present in the sample are virtually independent of their concentration [1,2]. On the other hand, retention times depend on several factors, including the type of resin in the separation column [3]. Provided that an ion chromatogram has been obtained isocratically, the selectivity coefficients between the sample ions on the resin used can be determined. Further, by changing the eluent in the next run it is possible to examine the influence of eluents on the selectivity coefficients obtained. Selectivity coefficients may be considered to be dependent on the resin used as a whole. Nevertheless, it is to be expected that selectivity coefficients will depend greatly on the type of functional groups of the resin.

Correspondence to: Dr. Ü. Haldna, Institute of Chemistry, Estonian Academy of Sciences, Akadeemia tee 15, Tallinn 200108, Estonia.

THEORETICAL

The ion-exchange equilibrium for the binding of two solute anions, A^{x-} and B^{y-}, to a stationary phase in a separation column is given by

$$yA_m^{x-} + xB_r^{y-} \rightleftharpoons yA_r^{x-} + xB_m^{y-} \quad (1)$$

where the subscripts m and r refer to the mobile and stationary phase, respectively. Neglecting the activity coefficients, the selectivity coefficient for the system is given by [4]

$$K_{A,B} = \frac{[A_r^{x-}]^y[B_m^{y-}]^x}{[A_m^{x-}]^y[B_r^{y-}]^x} = \frac{D_A^y}{D_B^x} \quad (2)$$

The distribution coefficients $D_A = [A_r^{x-}]/[A_m^{x-}]$ and $D_B = [B_r^{y-}]/[B_m^{y-}]$ are related to the retention times $t_{R,A}$ and $t_{R,B}$ respectively. In general [5,6],

$$D = (t_R - t_0)/pt_0 \quad (3)$$

where p is the phase ratio ($p = V_r/V_m$; V_r and V_m are the volumes of resin and mobile phase in the separation column) and t_0 is the void time [7] of the separation column. If a chemical suppressor is used, the retention time t_R also includes the retention time

0021-9673/92/$05.00

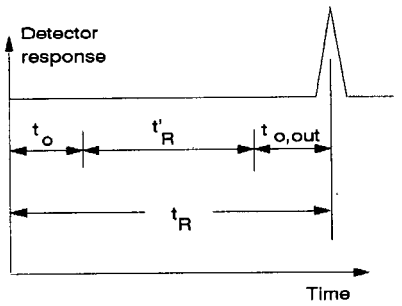

Fig. 1. Parameters for defining retention: t_R = retention time measured for the whole system; t'_R = reduced retention time for the separation column; t_0 = void time for the separation column; $t_{0,out}$ = the time due to the mobile phase outside the separation column.

$t_{0,out}$ due to the mobile phase outside the separation column (in the tubing used to interconnect the chromatographic components, in the suppressor device, etc.). The parameters t_0, t_R and $t_{0,out}$ are illustrated in Fig. 1. In a good chromatographic system $t_{0,out} \ll t_0$. However, if a classical suppression column is involved, $t_{0,out}$ and t_0 may be of the same order of magnitude. In this respect the use of single-column ion chromatography [8] is to be preferred, because usually in this instance $t_{0,out} \ll t_0$. Taking the time $t_{0,out}$ also into account, eqn. 3 can be rewritten as

$$D = (t_R - t_{0,out} - t_0)/pt_0 \quad (4)$$

Provided that the retention times $t_{R,A}$ and $t_{R,B}$ used in eqn. 4 for calculating D_A and D_B, respectively, were obtained from the same chromatogram, $t_{0,out}$ is the same for both the ions A^{x-} and B^{y-}. Substitution of D_A and D_B (eqn. 4) into eqn. 2 gives

$$K_{A,B} = \frac{(t_{R,A} - t_{0,out} - t_0)^y}{(t_{R,B} - t_{0,out} - t_0)^x}(pt_0)^{x-y} \quad (5)$$

If the two solutes, A^{x-} and B^{y-} have equal charge numbers, $x = y = 1$, then eqn. 5 reduces to

$$K_{A,B} = (t_{R,A} - t_{0,out} - t_0)/(t_{R,B} - t_{0,out} - t_0) \quad (6)$$

EXPERIMENTAL

We calculated the selectivity coefficients (eqn. 5) between Cl^-, NO_3^-, HPO_4^{2-} and SO_4^{2-} ions by making use of the corresponding retention times (t_R) given in ref. 9, where values are available for 25 different carbonate eluents for each ion considered. The retention times in ref. 9 were measured on a Model IVK-1 ion chromatograph (Design Office of the Estonian Academy of Sciences, Tallinn, Estonia) equipped with a JD-1 conductimetric detector. The separation column (200 × 3 mm I.D.) was packed with HIKS-1 resin (Himifil Co, Tallinn, Estonia) and the suppression column (250 × 4 mm I.D.) with KU-2 resin (Sojuzkhimreaktiv, Moscow, Russia). Ion exchange on the HIKS-1 resin occurred on the $-CH_2\overset{+}{N}(CH_3)_3$ groups. The capacity of the HIKS-1 resin was 0.022 mequiv./cm^3.

The sum $t_0 + t_{0,out}$ was measured by injecting doubly distilled water instead of a sample containing the ions studied, and $t_{0,out}$ was measured in the same way on the same equipment but with the suppression column only (*i.e.*, with the separation column removed). The void time t_0 was calculated as the difference $(t_0 + t_{0,out}) - t_{0,out}$. We obtained t_0 = 43 s and $t_{0,out}$ = 55 s by applying the eluent flow-rate used in ref. 9 (1.50 ml/min).

The phase ratio $P = V_r/V_m$ was obtained by taking V_r = 1.41 cm^3 for the separation column and V_m equal to the weight of water (grams) present in the packed separation column. The latter quantity was determined as the difference between the weight of the wet resin, pressed out from the separation column used, and the weight of the same amount of the resin after drying at 110°C. The phase ratio in the separation column was 1.10.

RESULTS

Using the t_R values from ref. 9, t_0 = 43 s and $t_{0,out}$ = 55 s, the selectivity coefficients $K_{A,B}$ (eqn. 5) were calculated (see Table I). Each selectivity coeffi-

TABLE I

SELECTIVITY COEFFICIENTS, $K_{A,B}$

$K_{A,B}$	Obtained with eqn. 5, ±S.D. (n = 25)	Calculated from $K_{A,CO_3^{2-}}$ and $K_{B,CO_3^{2-}}$
K_{Cl^-,NO_3^-}	0.39 ± 0.06	0.33
$K_{Cl^-,HPO_4^{2-}}$	0.44 ± 0.13	0.29
$K_{Cl^-,SO_4^{2-}}$	0.21 ± 0.07	0.17
$K_{NO_3^-,HPO_4^{2-}}$	2.88 ± 0.77	2.65
$K_{NO_3^-,SO_4^{2-}}$	1.38 ± 0.41	1.56
$K_{HPO_4^{2-},SO_4^{2-}}$	0.25 ± 0.10	0.35

cient value given is the mean of 25 values obtained for different carbonate eluents [9]. The root mean square errors given in Table I are those with 24 degrees of freedom. The relatively large root mean square errors are probably due mainly to random experimental errors in $t_{R,A}$ and $t_{R,B}$, because no clear dependence of $K_{A,B}$ values on the eluent composition has been found. It should also be noted that eqn. 5, containing the squares of differences if $y = 2$, is sensitive to errors in $t_{R,A}$ and $t_{R,B}$. The $K_{A,B}$ values (eqn. 5) may be compared with those obtained as the ratio of $K_{A,CO_3^{2-}}$ to $K_{B,CO_3^{2-}}$ published elsewhere [10]. The $K_{A,B}$ values obtained in this way are close to those calculated with eqn. 5 (see Table I). It should be pointed out that the $K_{A,CO_3^{2-}}$ and $K_{B,CO_3^{2-}}$ values used were obtained by non-linear regression analysis [10]. The closeness of the $K_{A,B}$ values obtained in this work (with eqn. 5) and by the non-linear regression may be considered mutually to verify the two methods applied.

REFERENCES

1 H. Small, T. S. Stevens and W. D. Bauman, *Anal. Chem.*, 47 (1975) 1801.
2 J. S. Fritz, D. T. Gjerde and C. Pohlandt, *Ion Chromatography*, Hüthig, Heidelberg, 1982, p. 216.
3 R. E. Barron and J. S. Fritz, *J. Chromatogr.*, 284 (1984) 13.
4 P. R. Haddad and P. E. Jackson, *Ion Chromatography*, Elsevier, Amsterdam, 1990, p. 133.
5 J. H. Knox, *High-Performance Liquid Chromatography*, Edinburgh University Press, Edinburgh, 1978, p. 5.
6 V. D. Shatz and O. V. Sakhartova, *Vysokoeffektivnaja Zhidkostnaja Chromatografia (High-Performance Liquid Chromatography*, Zinatne Press, Riga, 1988, p. 27.
7 P. R. Haddad and P. E. Jackson, *Ion Chromatography*, Elsevier, Amsterdam, 1990, p. 4.
8 F. C. Smith and R. C. Chang, *The Practice of Ion Chromatography*, Wiley, New York, 1983, p. 213.
9 Ü. Haldna, I. Jakovleva, R. Palvadre and R. Juga, *Proc. Est. Acad. Sci.*, 39 (1990) 44.
10 Ü. Haldna, *J. Chromatogr.*, 589 (1992) 197.

Journal of Chromatography, 604 (1992) 285–289
Elsevier Science Publishers B.V., Amsterdam

CHROM. 24 191

Short Communication

Optimization of high-performance liquid chromatographic conditions for the determination of cyclosporins A, B and C in fermentation samples

Nisha George, M. Kuppusamy and K. Balaraman

Vector Control Research Centre, Indian Council of Medical Research, Pondicherry 605006 (India)

(First received November 7th, 1991; revised manuscript received March 17th, 1992)

ABSTRACT

Variations in the retention behaviour of cyclosporins A, B and C, which have very similar structures, were studied with respect to mobile phase composition, temperature, stationary phase and UV detection wavelength. Cyclosporins A, B and C were well separated with a Supelco C_8 column (7.5 cm × 4.6 mm I.D.) at 60°C using acetonitrile–water (50:50) containing 0.01% of orthophosphoric acid at a flow-rate of 1 ml/min with UV detection at 202 nm. Cyclosporins A, B and C obtained from an indigenous isolate of *Tolypocladium* sp. were determined and it was found that the major component was cyclosporin A followed by C and B. The advantage of this method is that the interference of closely eluting peaks can be avoided as there is a good separation between the peaks and the analysis can be carried out economically as the solvent consumption is low.

INTRODUCTION

Cyclosporins represent a group of cyclic peptides composed of eleven amino acids. They are produced by fungi of the genus *Tolypocladium* in submerged culture [1]. Cyclosporins A, B and C differ in their structures only at the second amino acid. They are neutral and hydrophobic in nature [2]. Cyclosporin A is a promising immunosuppressive drug which is being used extensively in organ transplantation and the treatment of autoimmune diseases [3].

Various methods have been reported for the determination of cyclosporin A [4–9]. Owing to the close similarity of their structures, the determination of the cyclosporins A, B and C in fermentation samples is complicated. However, their resolution is of the utmost importance for the identification and determination of cyclosporin A. The optimization of the analytical conditions for a high-performance liquid chromatographic (HPLC) procedure for the separation of cyclosporin A, B and C obtained from an indigenous isolate of *Tolypocladium* sp. [10] is presented here.

EXPERIMENTAL

A Shimadzu (Tokyo, Japan) Model LC-3A high-performance liquid chromatograph equipped with a Model SPD-2A variable-wavelength UV detector, a Model CTO-6A column oven and a Model C-R3A data processor was used. All sample injections were

Correspondence to: Dr. K. Balaraman, Vector Control Research Centre, Indian Council of Medical Research, Pondicherry 605006, India.

0021-9673/92/$05.00

made with a Rheodyne (Cotati, CA, USA) Model 7125 injector using a Hamilton (Reno, NV, USA) microsyringe.

Standard samples of cyclosporin A, B and C used for determining retention indices were kindly supplied by SPIC Pharmaceuticals (Madras, India). Methanol and acetonitrile were of HPLC grade (S.D. Fine-Chem, Boisar, India). Analytical-reagent grade orthophosphoric acid was obtained from Ranbaxy (Punjab, India). HPLC-grade water was obtained with a Milli-Q water-purification system (Millipore, Bedford, MA, USA).

Standard samples were prepared by dissolving pure cyclosporins A, B and C in acetonitrile (0.3 mg/ml). The fermentation samples were prepared by extracting the mycelial biomass obtained after 21 days of static fermentation of the fungus *Tolypocladium* sp. [10] with methanol (1:2, w/v) and filtering through a 0.2-μm filter unit (Millex-FGS; Millipore).

The optimization of the analytical conditions was carried out with respect to mobile phase composition, pH, temperature, analytical column and UV detection wavelength.

Mobile phases were prepared with different proportions of acetonitrile and water and containing three different orthophosphoric acid concentrations (0.001, 0.01 and 0.1%), leading to variations in pH in the range 2.2–3.5. Experiments were conducted at three different temperatures (40, 60 and 70°C) and also using different columns differing in their packing materials and dimensions, *viz.*, Resolve C_{18}, 5 μm (15 cm × 3.9 mm I.D.) (Waters–Millipore, Milford, MA, USA) and Supelco C_8, 3 μm (7.5 cm × 4.6 mm I.D.) (Supelco, Gland, Switzerland). Analyses were carried out at different wavelengths from 202 to 214 nm at 0.01 a.u.f.s. The capacity factor, k' [$k' = (t_R - t_0)/t_0$, where t_R is the retention time of the solute and t_0 is the retention time of an unretained compound] [11] and the selectivity factor, α ($\alpha = k'_2/k'_1$), were calculated. All analyses were carried out at a flow-rate of 1 ml/min.

RESULTS AND DISCUSSION

The effects of the mobile phase composition and the nature of the stationary phase on the retention of cyclosporins A, B and C at three column temperatures are shown in Figs. 1 and 2.

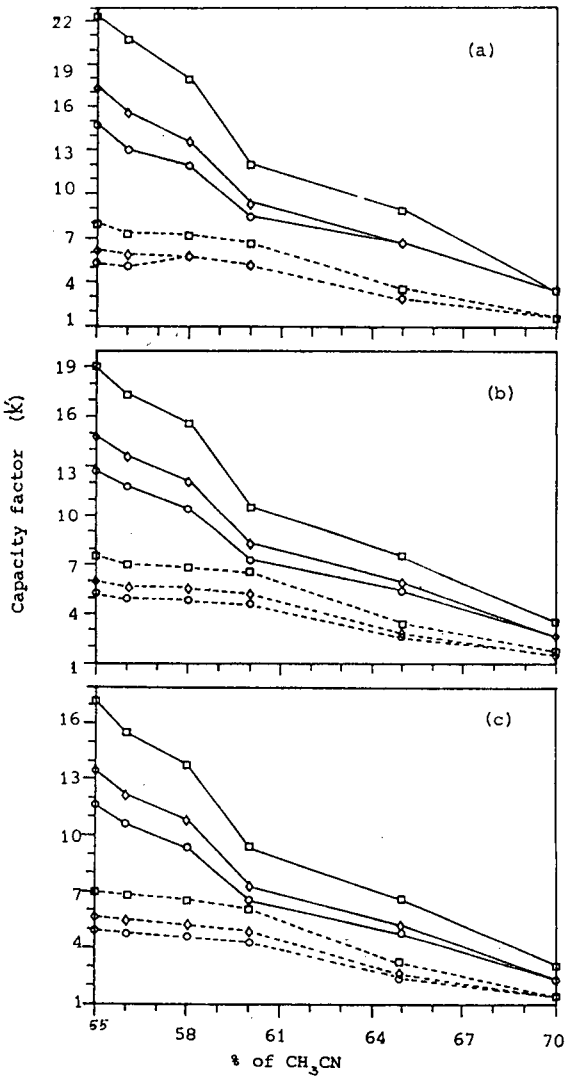

Fig. 1. Variation in k' for cyclosporins A, B and C at (a) 40°C, (b) 60°C and (c) 70°C with respect to acetonitrile concentration in the mobile phase containing 0.01% of H_3PO_4 and the type of column used. Solid lines, Resolve C_{18} column; dashed lines, Supelco C_8 column. Cyclosporins: □ = A; ◇ = B; ○ = C.

The variation of the capacity factor at three levels of orthophosphoric acid concentration and column temperature with respect to two columns (C_{18} and C_8) and different percentages of acetonitrile in water (70, 65, 60, 58, 56 and 55%) as mobile phase was studied. At a column temperature of 40°C with 70% acetonitrile, the cyclosporins were eluted together with $\alpha = 1$. As the percentage of acetonitrile was

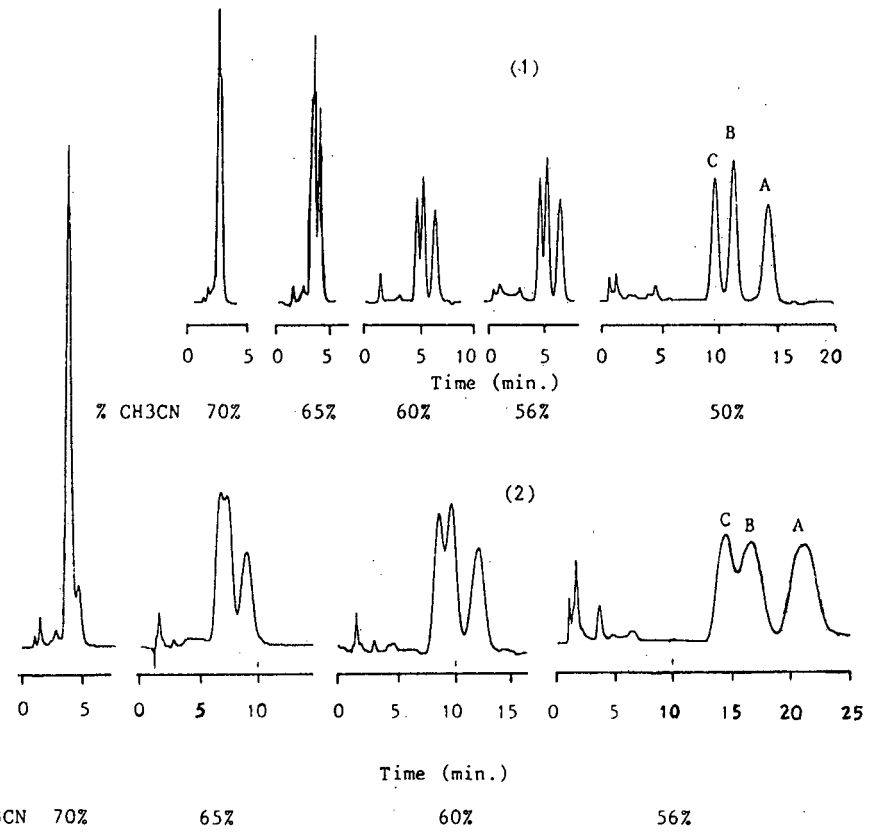

Fig. 2. HPLC profiles of a mixture of cyclosporins A, B and C (0.3 μg per injection) with various percentages acetonitrile in the mobile phase using (1) the Supelco C_8 column and (2) the Resolve C_{18} column at 60°C.

decreased the retention times of the cyclosporins became longer and the separation improved. The separation was very poor and peak broadening was observed at 40°C (Fig. 1) compared with the results obtained at the column temperatures of 60°C (Fig. 1b) and 70°C (Fig. 1c), which showed a reduction in retention time and better separation. However, the changes in selectivity were insignificant in most instances.

Even though the results of the analysis with the Resolve C_{18} column showed a good resolution, the higher values of the capacity factors indicate the need for a longer time of analysis or higher flow-rates with low percentages of acetonitrile. Compared with the Resolve C_{18} column, the Supelco C_8 column with a shorter length gave shorter retention times with very good peak separation and narrower peaks (Fig. 2). The analysis time is shorter with good separation and low solvent consumption. Subsequent experiments were therefore performed using only the Supelco C_8 column with 52% and 50% of acetonitrile in the mobile phase containing 0.01% of H_3PO_4 at 60°C in order to effect further improvements in the separation. With acetonitrile–water (50:50) at a flow-rate of 1 ml/min a very good separation was obtained for cyclosporins A, B and C using this column whereas a higher flow-rate has to be used with the C_{18} column to avoid longer retention times. With respect to the acid concentration, better results were observed with concentrations of 0.01% and 0.1% than 0.001%. The analyses at 60 and 70°C gave good results but considering the column lifetime, 60°C and 0.01% of orthophosphoric acid were selected as the optimum temperature and acid concentration for the determination of cyclosporins.

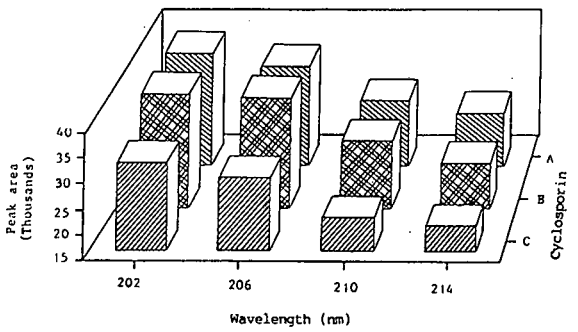

Fig. 3. Detection of cyclosporins A, B and C (0.15 μg per injection) at different UV wavelengths.

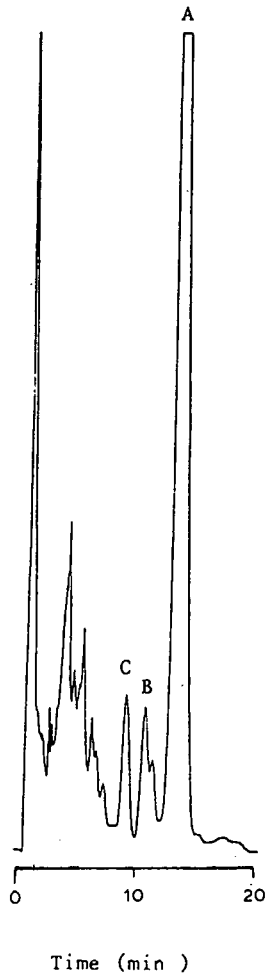

Fig. 4. HPLC profile of a crude fermentation sample showing the presence of cyclosporins A, B and C.

In order to establish the optimum detection wavelength, analyses were carried out at 202, 206, 210 and 214 nm and the corresponding peak areas were compared for the same sample amount (0.15 μg). Maximum peak areas were observed for cyclosporins A, B and C at 202 nm; the peak areas were reduced at higher wavelengths more for cyclosporin C than B and A (Fig. 3).

After optimizing the chromatographic conditions for the determination of cyclosporins A, B and C as acetonitrile–water (50:50) containing 0.01% of orthophosphoric acid as mobile phase and using a Supelco C_8 column at 60°C, fermentation samples were analysed. The chromatogram in Fig. 4 shows that the major component of the fermentation samples was cyclosporin A, followed by cyclosporin C and B.

The advantage of this method is that in quantitative analysis the interference of closely eluting peaks can be avoided as there is a good separation between the peaks. Analyses can be carried out economically as the solvent consumption is low.

ACKNOWLEDGEMENTS

The authors are highly indebted to Dr. V. Dhanda, Director, and Dr. P. K. Rajagopalan, former Director, VCRC, Pondicherry, for provinding the necessary facilities. They are grateful to Dr. M. Kalyanasundram, Assistant Director, for valuable suggestions. Technical assistance provided by Mr. D. Jayakumar and S. Venugopal is gratefully acknowledged.

REFERENCES

1 M. Dreyfuss, E. Harri, H. Hofmann, H. Kobel, W. Pache and H. Tscherter, *Eur. J. Appl. Microbiol. Biotechnol.*, 3 (1976) 125.
2 R. Wenger, in B. D. Kahan (Editor), *Cyclosporin Biological Activity and Clinical Applications*, Grune & Stratton, Orlando, FL, 1984, p. 14.
3 R. M. Merion, D. J. G. White, S. Thiru, D. B. Evans and R. Y. Calne, *N. Engl. J. Med.*, 310 (1984) 148.
4 W. Niederberger, P. Schaub and T. Beveridge, *J. Chromatogr.*, 182 (1980) 454.
5 F. Kreuzig, *J. Chromatogr.*, 290 (1984) 181.
6 L. D. Bowers and J. Singh, *J. Liq. Chromatogr.*, 10 (1987) 411.
7 W. M. Awni and J. A. Maloney, *J. Chromatogr.*, 425 (1988) 233.

8 D. J. Gmur, P. Meier and G. C. Yee, *J. Chromatogr.*, 425 (1988) 343.
9 *United States Pharmacopeia XXII, National Formulary XVII*, US Pharmacopeial Convention, Rockville, MD, 1990, p. 372.
10 K. Balaraman, M. Kuppusamy, Nisha George, K. Anandkumar and C. Sekar, *Indian J. Med. Res. (B)*, 94 (1991) 304.
11 C. K. Lim (Editor), *HPLC of Small Molecules, A Practical Approach*, IRL Press, Washington, DC, 1986, p. 1.

Journal of Chromatography, 604 (1992) 290–293
Elsevier Science Publishers B.V., Amsterdam

CHROM. 24 232

Short Communication

Determination of alkali-soluble phenolic monomers in grasses after separation by thin-layer chromatography

P. L. Escott-Watson and J. P. Marais

Cedara Agricultural Research Station, Private Bag X9059, Pietermaritzburg 3200 (South Africa)

(First received February 25th, 1992; revised manuscript received April 2nd, 1992)

ABSTRACT

A solvent system is described for the complete separation of ferulic acid, *p*-coumaric acid and vanillin on silica gel 60A K6F thin-layer plates. A spray reagent which distinguishes between these substances on a colour basis is also described. After separating the alkali-labile phenolic monomers in grass cell wall material on thin-layer plates, these substances were quantitatively eluted and assayed by means of a spectrophotometric procedure.

INTRODUCTION

In plant tissue, lignin is cross-linked to cellulose by means of low-molecular-weight phenolic acids [1,2]. During rumen digestion these links are broken and the phenolic monomers are released. Ferulic acid and *p*-coumaric acid seem to be the major components released from grasses [3].

At present, alkali-soluble phenolic monomers are receiving much attention from animal nutritionists as these compounds have been implicated in the poor digestibility of forage crops [4,5]. They have been shown to inhibit the growth of rumen bacteria and fungi [6,7] and decrease the digestion of structural carbohydrates [8–10]. A highly significant correlation was found between the digestibility of the cell walls from perennial ryegrass and the ferulic acid to *p*-coumaric acid ratio [5]. Alkali-labile phenolic monomers such as *p*-coumaric acid, ferulic acid and vanillin are usually separated by means of gas chromatography [11] or high-performance liquid chromatography [12].

Separation of these substances by means of thin-layer chromatography on silica gel plates is generally poor [13,14], thus making their quantitative analysis after thin-layer separation difficult. This prompted the authors to develop a solvent that would separate these compounds on silica gel plates. A spray reagent that could distinguish between compounds on a colour basis is also described. After separation, the individual phenolic acids could be eluted and accurately determined. The method was applied to the determination of alkali-labile phenolic monomers from the cell walls of several pasture grasses.

EXPERIMENTAL

Materials and reagents

All chemicals were of analytical-reagent grade. Standard solutions of vanillin (4-hydroxy-3-meth-

Correspondence to: P. L. Escott-Watson, Cedara Agricultural Research Station, Private Bag X9059, Pietermaritzburg 3200, South Africa.

0021-9673/92/$05.00

oxybenzaldehyde), ferulic acid (4-hydroxy-3-methoxycinnamic acid) and *p*-coumaric acid (4-hydroxycinnamic acid) were prepared by dissolving each compound (0.781 g) in ethanol (25 ml).

Cell wall material was isolated from kikuyu grass *(Pennisetum clandestinum)*, Italian ryegrass *(Lolium multiflorum)* and fescue *(Festuca arundinacea)* by the procedure of Van Soest and Wine [15].

A chromatographic solvent for the complete separation of vanillin, ferulic acid and *p*-coumaric acid on precoated silica gel 60A K6F (200 × 50 mm) plates was developed and consisted of hexane–ethyl acetate–isobutyl alcohol–2-propanol–acetic acid (21:2:1:1:0.1).

Phenolic substances on the chromatoplate were revealed by spraying with a reagent prepared as follows. Solution A was tin(IV) oxide (0.2 g) and iron(III) chloride (2 g) dissolved in 0.8 *M* hydrochloric acid (100 ml) and solution B was 2,4-dinitrophenylhydrazine (1 g) dissolved in 3 *M* hydrochloric acid (500 ml). Just before use, one part of solution A was mixed with three parts of solution B.

Extraction of phenolic monomers

Throughout the extraction process, care was taken to keep the samples away from sunlight. Grass cell wall material (0.5 g) was shaken in 1 *M* sodium hydroxide solution (20 ml) for 24 h at 20°C. The sample was vacuum filtered through a sintered-glass crucible and washed with distilled water (20 ml). The filtrate was acidified to pH 2.5 with hydrochloric acid and saturated with solid sodium chloride. The phenolic monomers were extracted with petroleum spirit (b.p. 80–100°C) (3 × 60 ml) using a separating funnel. The volume of the petroleum spirit extract was reduced to *ca.* 2 ml and then made up to 25 ml with ethanol.

Thin-layer separation

An aliquot (80 μg) of phenolic acid standard or phenolic monomer extract (0.4 ml) was applied as a band to an activated silica gel plate. The plate was developed with the proposed solvent in a chromatographic chamber (55 × 75 × 245 mm) for 40 min and subsequently dried at ambient temperature (21°C).

Identification

For qualitative identification of phenolic monomers, the plate was sprayed with the proposed spray reagent and heated (120°C, 10 min) to reveal the compounds. For quantitative analysis, the bands on the chromatogram were located by brief scanning under UV light.

Quantitative analysis

Each band was scraped off the plate into a centrifuge tube and the phenolic acid was dissolved in ethanol (2 ml). After centrifugation to remove the silica gel from the suspension, the phenolic acid

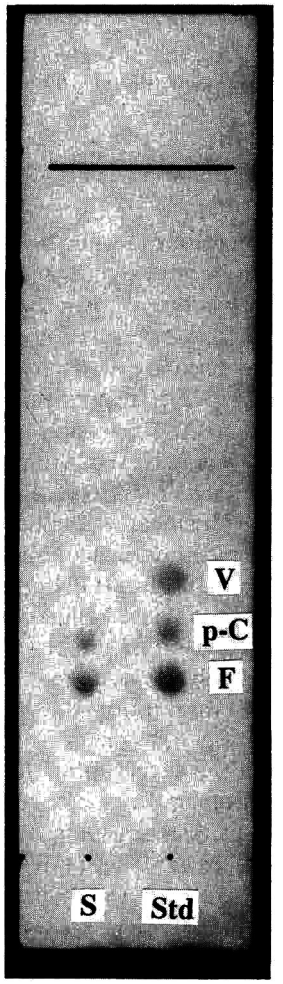

Fig. 1. Thin-layer chromatogram of phenolic monomers separated on a silica gel 60A K6F plate as described in the text. S = Phenolic compounds isolated from kikuyu *(Pennisetum clandestinum)* stem cell walls; Std = standard solution containing 10 μg each of ferulic acid (F), *p*-coumaric acid (p-C) and vanillin (V).

TABLE I

PHENOLIC MONOMER CONTENT OF GRASS CELL WALLS

Phenolic monomers were released from cell wall (CW) material, separated and determined as described in the text. Reported values represent the means of six analyses and the standard error of the mean.

Grass	Phenolic acid content (g/kg CW)		
	Ferulic acid	*p*-Coumaric acid	Total
Pennisetum clandestinum	6.2 ± 0.1	6.5 ± 0.3	12.7 ± 0.5
Lolium multiflorum	3.9 ± 0.3	12.1 ± 0.2	16.1 ± 0.3
Festuca arundinacea	3.7 ± 0.1	12.6 ± 0.1	16.3 ± 0.1

content in an aliquot (0.4 ml) of the supernatant solution was determined spectrophotometrically by the Folin–Denis procedure [16].

RESULTS AND DISCUSSION

The separation and determination of ferulic acid and *p*-coumaric acid are of considerable significance to ruminant nutritionists, as it has been shown that high *p*-coumaric acid concentrations and a low ferulic acid to *p*-coumaric acid ratio are associated with low forage digestibility [5]. The results presented in Fig. 1 show that complete separation of these substances and vanillin was achieved within 40 min using the proposed solvent system. No trailing of spots was observed. The mean R_F values (six replicates) of ferulic acid, *p*-coumaric acid and vanillin were 0.20 ± 0.02, 0.36 ± 0.01 and 0.46 ± 0.01, respectively. The R_F values varied slightly according to the degree of saturation of the chromatographic chamber. The chamber was therefore saturated with solvent for 30 min prior to the introduction of the plates.

The proposed spray reagent for revealing the positions of the phenolic monomers on the chromatoplate has the advantage of distinguishing between substances on a colour basis. The vanillin appeared as an orange spot directly after spraying, while *p*-coumaric acid and ferulic acid developed as light brown and dark mauve-brown spots, respectively, on heating the plate at 120°C. The detection limit of the spray reagent is *ca.* 0.2 μg.

The chromatoplate appears to lend itself to direct quantification of spots by fluorescence scanning. However, very satisfactory results were obtained by the spectrophotometric analysis of phenolic monomers after elution from the chromatoplates. The recoveries of ferulic acid, *p*-coumaric acid and vanillin were 100.2 ± 0.7%, 99.0 ± 0.7% and 100.1 ± 0.6% respectively (means of six recoveries).

The results in Table I show that reproducible results were obtained when the method was applied to plant cell wall material. It was further shown that the grasses analysed contained only ferulic acid and *p*-coumaric acid in significant amounts.

The new chromatographic solvent and spray reagent provide a rapid method for separating and identifying plant cell wall phenolic acids. These procedures, in conjunction with a spectrophotometric method for determining phenolic substances, offer an accurate technique for the determination of alkali-soluble phenolic monomers in plant cell wall material.

REFERENCES

1 R. D. Hartley, *Phytochemistry*, 12 (1973) 661.
2 H. G. Jung, G. C. Fahey and N. R. Merchen, *Br. J. Nutr.*, 50 (1983) 637.
3 R. D. Hartley, *J. Sci. Food Agric.*, 23 (1972) 1347.
4 D. E. Akin, N. Ames-Gottfred, R. D. Hartley, R. G. Fulcher and L. L. Rigsby, *Crop Sci.*, 30 (1990) 396.
5 B. C. Gabrielson, K. P. Vogel, B. E. Anderson and J. K. Ward, *Crop Sci.*, 30 (1990) 1313.
6 D. E. Akin and L. L. Rigsby, *Agron. J.*, 77 (1985) 180.
7 W. S. Borneman, D. E. Akin and W. P. Van Eseltine, *Appl. Environ. Microbiol.*, 52 (1986) 1331.
8 A. Chesson, C. S. Stewart and R. J. Wallace, *Appl. Environ. Microbiol.*, 44 (1982) 597.
9 H. G. Jung, *J. Sci. Food Agric.*, 36 (1985) 74.
10 V. H. Varel and H. G. Jung, *Appl. Environ. Microbiol.*, 52 (1986) 275.
11 R. D. Hartley, *J. Chromatogr.*, 54 (1971) 335.

12 J. H. Cherney, K. S. Aniliker, K. A. Albrecht and K. V. Wood, *J. Agric. Food Chem.*, 37 (1989) 345.
13 M. Vanhaelen and R. Vanhaelen-Fastré, *J. Chromatogr.*, 187 (1980) 255.
14 K. Egger, in E. Stahl (Editor), *Thin-Layer Chromatography*, Springer, Berlin, 1969, p. 687.
15 P. J. van Soest and R. H. Wine, *J. Assoc. Off. Agric. Chem.*, 50 (1967) 50.
16 R. Swain and W. E. Hillis, *J. Sci. Food Agric.*, 10 (1959) 63.

Author Index

Erratum

J. Chromatogr., 541 (1991) 131–183

Page 146, Fig. 3a middle frame for the PnCDFs on DB-5 column: the elution order for the fourth last peak in retention time should read: 23478/12679/12369 and for the third last peak in retention time 23478/12489 *i.e.* isomer 12489 coelutes with 23467 and not with 23478 etc. as in the original figure. These changes are shown on the corrected part of Fig. 3a with the isomer change underlined:

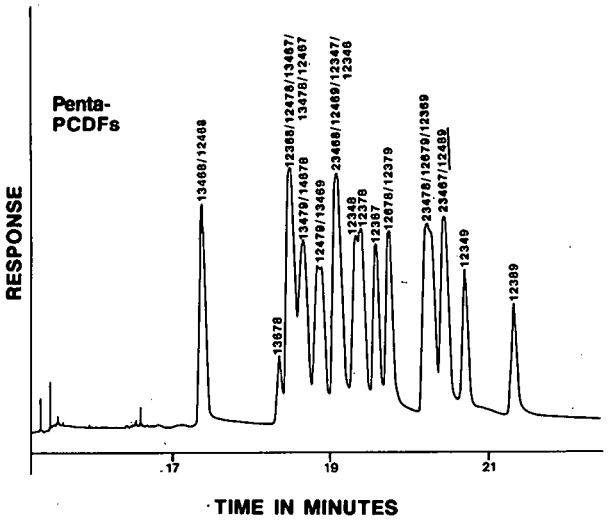

Fig. 3a.

PUBLICATION SCHEDULE FOR 1992

Journal of Chromatography and *Journal of Chromatography, Biomedical Applications*

MONTH	O 1991–F 1992	M	A	M	J	J	
Journal of Chromatography	Vols. 585–593	594/1 + 2 595/1 + 2	596/1 596/2 597/1 + 2	598/1 598/2 599/1 + 2 600/1 600/2	602/1 + 2 603/1 + 2 604/1	604/2 605/1 605/2 606/1	The publication schedule for further issues will be published later.
Cumulative Indexes, Vols. 551–600					[a]		
Bibliography Section		610/1			610/2		
Biomedical Applications	Vols. 573 and 574	575/1 575/2	576/1	576/2 577/1	577/2	578/1 578/2	

[a] Cumulative Indexes will be Vol. 601, to appear early 1993.

INFORMATION FOR AUTHORS

(Detailed *Instructions to Authors* were published in Vol. 558, pp. 469–472. A free reprint can be obtained by application to the publisher, Elsevier Science Publishers B.V., P.O. Box 330, 1000 AH Amsterdam, The Netherlands.)

Types of Contributions. The following types of papers are published in the *Journal of Chromatography* and the section on *Biomedical Applications:* Regular research papers (Full-length papers), Review articles and Short Communications. Short Communications are usually descriptions of short investigations, or they can report minor technical improvements of previously published procedures; they reflect the same quality of research as Full-length papers, but should preferably not exceed five printed pages. For Review articles, see inside front cover under Submission of Papers.

Submission. Every paper must be accompanied by a letter from the senior author, stating that he/she is submitting the paper for publication in the *Journal of Chromatography*.

Manuscripts. Manuscripts should be typed in double spacing on consecutively numbered pages of uniform size. The manuscript should be preceded by a sheet of manuscript paper carrying the title of the paper and the name and full postal address of the person to whom the proofs are to be sent. As a rule, papers should be divided into sections, headed by a caption (*e.g.*, Abstract, Introduction, Experimental, Results, Discussion, etc.). All illustrations, photographs, tables, etc., should be on separate sheets.

Introduction. Every paper must have a concise introduction mentioning what has been done before on the topic described, and stating clearly what is new in the paper now submitted.

Abstract. All articles should have an abstract of 50–100 words which clearly and briefly indicates what is new, different and significant.

Illustrations. The figures should be submitted in a form suitable for reproduction, drawn in Indian ink on drawing or tracing paper. Each illustration should have a legend, all the *legends* being typed (with double spacing) together on a *separate sheet*. If structures are given in the text, the original drawings should be supplied. Coloured illustrations are reproduced at the author's expense, the cost being determined by the number of pages and by the number of colours needed. The written permission of the author and publisher must be obtained for the use of any figure already published. Its source must be indicated in the legend.

References. References should be numbered in the order in which they are cited in the text, and listed in numerical sequence on a separate sheet at the end of the article. Please check a recent issue for the layout of the reference list. Abbreviations for the titles of journals should follow the system used by *Chemical Abstracts*. Articles not yet published should be given as "in press" (journal should be specified), "submitted for publication" (journal should be specified), "in preparation" or "personal communication".

Dispatch. Before sending the manuscript to the Editor please check that the envelope contains four copies of the paper complete with references, legends and figures. One of the sets of figures must be the originals suitable for direct reproduction. Please also ensure that permission to publish has been obtained from your institute.

Proofs. One set of proofs will be sent to the author to be carefully checked for printer's errors. Corrections must be restricted to instances in which the proof is at variance with the manuscript. "Extra corrections" will be inserted at the author's expense.

Reprints. Fifty reprints of Full-length papers and Short Communications will be supplied free of charge. Additional reprints can be ordered by the authors. An order form containing price quotations will be sent to the authors together with the proofs of their article.

Advertisements. The Editors of the journal accept no responsibility for the contents of the advertisements. Advertisement rates are available on request. Advertising orders and enquiries can be sent to the Advertising Manager, Elsevier Science Publishers B.V., Advertising Department, P.O. Box 211, 1000 AE Amsterdam, Netherlands; courier shipments to: Van de Sande Bakhuyzenstraat 4, 1061 AG Amsterdam, Netherlands; Tel. (+31-20) 515 3220/515 3222, Telefax (+31-20) 6833 041, Telex 16479 els vi nl. *UK*: T. G. Scott & Son Ltd., Tim Blake, Portland House, 21 Narborough Road, Cosby, Leics. LE9 5TA, UK; Tel. (+44-533) 753 333, Telefax (+44-533) 750 522. *USA and Canada*: Weston Media Associates, Daniel S. Lipner, P.O. Box 1110, Greens Farms, CT 06436-1110, USA; Tel. (+1-203) 261 2500, Telefax (+1-203) 261 0101.

For Superior Chiral Separation

From Analytical to Semi-preparative column

HPLC column output is directly proportional to cross section

● Analytical column
0.46cmϕ×25cm

● Semi-preparative column
2cmϕ×25cm

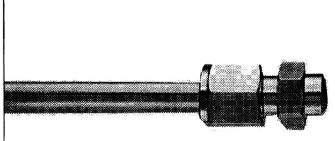

$$A\ mg \times \left(\frac{1^2 \times 3.14}{(0.23)^2 \times 3.14}\right) \fallingdotseq A\ mg \times 20$$

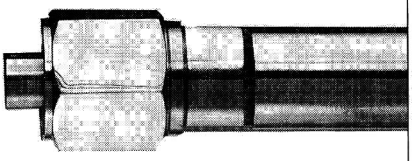

A=maximum sample amount of Analytical column

Analytical column

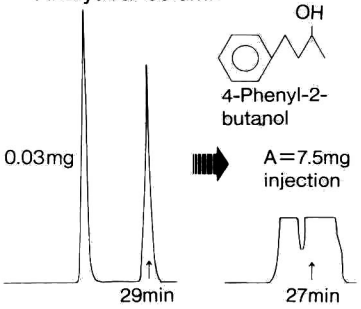

CHIRALCEL OD	column	CHIRALCEL OD
0.46cmϕ×25cm	column size	2cmϕ×25cm
10μm	Particle size	10μm
Hexane/IPA (9:1)	eluent	Hexane/IPA (9:1)
0.3ml/min.	flow rate	6ml/min.
UV 254nm	detection	UV 254nm
max 0.03mg→7.5mg	injection amount	7.5mg×20=150mg

Semi-preparative column

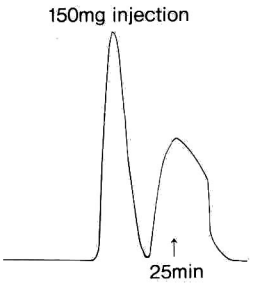

● Standard Available Column

● CHIRALPAK® /CHIRALCEL® (Particle size 10μm)

	I. D. Length
Analytical column	0.46cmϕ×25cm
Pre-column	0.46cmϕ× 5cm
Semi-preparative column	1cmϕ×25cm
	2cmϕ×25cm

● CROWNPAK™ (Particle size 5μm)

	I. D. Length
Analytical column	0.4cmϕ×15cm
Pre-column	0.4cmϕ× 1cm

CHIRAL TECHNOLOGIES, INC.
730 SPRINGDALE DRIVE
DRAWER I
EXTON, PA 19341
Phone: 215-594-2100
Fax: 215-594-2325

DAICEL (EUROPA) GmbH
Oststr. 22
4000 Düsseldorf 1, Germany
Phone: 49/211/369848
Telex: (41) 8588042 DCEL D
Fax: 49/211/364429

DAICEL CHEMICAL INDUSTRIES, LTD.
8-1, Kasumigaseki 3-chome, Chiyoda-ku, Tokyo 100, Japan
Phone: 81-3-3507-3151 Fax: 81-3-3507-3193